

DEVELOPING A GNSS SUITE FOR GEODETIC APPLICATIONS

By

SAMUEL OSAH, BSc (Hons) Geomatic Engineering

A THESIS

SUBMITTED TO THE DEPARTMENT OF GEOMATIC ENGINEERING

KWAME NKRUMAH UNIVERSITY OF SCIENCE AND TECHNOLOGY

IN PARTIAL FULFILLMENT OF THE REQUIREMENTS FOR THE DEGREE

OF



MASTER OF SCIENCE

DEPARTMENT OF GEOMATIC ENGINEERING

COLLEGE OF ENGINEERING

OCTOBER, 2013

ACKNOWLEDGEMENT

I am highly indebted to the Lord God Almighty, whose grace and mercies, strength, knowledge and understanding in all ways has brought me this far throughout my course. I wish to express profound gratitude and sincere appreciation to Dr.-Ing. Collins Fosu whose untiring exertions and forbearance as my supervisor greatly contributed towards the completion of this study. His immense support and boundless encouragement inspired me a lot for which I am most grateful. Much gratitude also goes to Mr. Afrifa Acheampong for his encouragement, numerous supports and valuable suggestions on this research. Sincere thanks also go to the staff members of the Geomatic Engineering Department, KNUST, for the kind support they offered me throughout this research work.

Last but not least, I would like to extend my deepest thanks to my family, all my friends especially Mr. Osman and my Msc. colleagues for their love, friendship, support, patience and encouragement in times of need and all who contributed one way or the other towards the successful completion of this study. God richly bless you all.



ABSTRACT

Global Navigation Satellite System (GNSS) is one of the most innovative and practical technology developed today. Since its inception it has grown to provide not only world-wide, all-weather navigation, but precise position determination capabilities to all manner of users especially for surveying and geodetic applications. In surveying and mapping, this represents a revolutionary departure from conventional surveying procedures, which rely on observed angles and distances, for determining point positions. The scope of GNSS is enormous: from data acquisitions and processing, to detailed Computational algorithm in position estimations.

Many processing software or applications both scientific and commercial have been developed for GNSS post-processing. These software are developed for general applications or standards and might not meet a country's mapping specifications particularly Africa. This means, that the inherent accuracy of a GNSS receiver can be enhanced or degraded depending on which software is used to do the post-processing. Besides, these software tend to be limited to the institutions that wrote them and use of them can require a considerable investment in time to understand the software and how best to use it under various circumstances. Expert training is often recommended by the distributors.

In the light of these setbacks and limitations, a GNSS suite, 'GeoSuite' for geodetic applications such as, GNSS data post-processing, Datum transformation and Direct and Inverse geodetic computations for Ghana, has been developed. The suite is a standalone window base application with a user-friendly interface written in Matlab. The GNSS data post-processing application of the Suite is based on both code and phase observables, and on double differences between simultaneous observations using Rinex file as an input GNSS raw data. In addition, the Datum transformation application of the Suite is also centered on the WGS 84 and War Office ellipsoids using the 3, 5, 7 and 10 transformation parameters, published by the Survey and Mapping Division of Ghana as default transformation parameters or user-defined transformation and ellipsoid parameters. The suite was tested on field measurements and existing coordinates, and from the results obtained it was concluded that, GPS data can be successfully processed using the developed suite for survey work in Ghana and can perform any form of transformation on the WGS 84 and the War Office ellipsoids or user-defined ellipsoid. The Suite can easily be adapted for other countries particularly within the Africa continent.

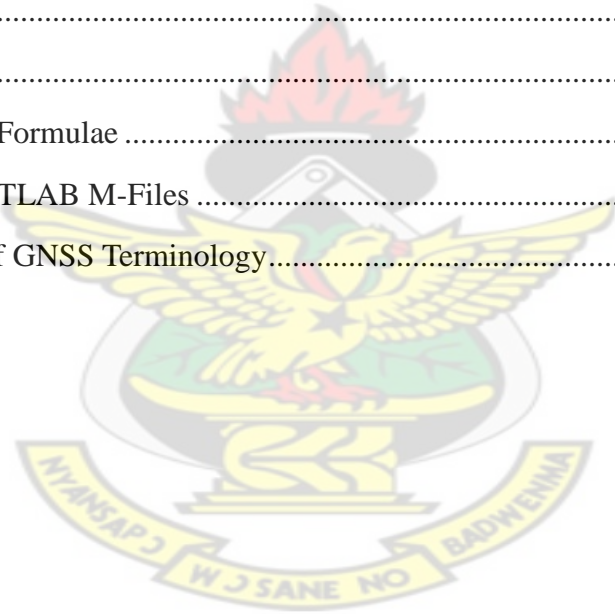
TABLE OF CONTENTS

DECLARATION.....	i
ACKNOWLEDGEMENT	ii
ABSTRACT.....	iii
TABLE OF CONTENTS	iv
LIST OF TABLES	viii
CHAPTER ONE - INTRODUCTION.....	1
1.1 Background	1
1.2 Problem Statement	3
1.3 Research Significance	3
1.4 Aim and Objectives	4
1.5 Scope of Project	4
1.6 Thesis Outline	5
CHAPTER TWO - GLOBAL NAVIGATION SATELLITE SYSTEM (GNSS)	7
2.0 INTRODUCTION.....	7
2.1 Satellite Orbits.....	8
2.1.1 Keplerian Elements.....	9
2.1.2 Keplerian Motion in Orbital and ECEF Coordinate Systems.....	11
2.1.3 Perturbed satellite motion.....	14
2.1.4 GPS broadcast ephemeris.....	15
2.1.5 RINEX File.....	18
2.1.5.1 RINEX Navigation Files (N-file).....	18
2.1.5.2 RINEX Observation Files (O-file).....	18
2.2 Time Scales	19
2.2.1. Coordinated Universal Time (UTC).....	19
2.2.2. GPS Time.....	20
2.2.3 Julian Date	20
2.3 GPS Signal Components, Structure, and Characteristics.....	21

2.3.1 Two L-band Carrier Waves	21
2.3.2 Ranging Codes	21
2.3.3 Navigation Message	22
2.3.3.1 Subframe Contents	23
2.4 Error Sources in GNSS Positioning.....	24
2.3.7 Fundamental GNSS Measurements.....	24
2.3.7.1 Pseudorange Measurements.....	25
2.3.7.2 Carrier Phase Measurement	26
2.3.8 GNSS Positioning Methods.....	27
2.3.8.1 Single Point Positioning (SPP)	27
2.3.8.1.1 Pseudorange-based point positioning.....	28
2.3.8.1.2 Carrier Phase-based Point Positioning	34
2.3.8.2 Relative or Differential Position	35
2.3.8.2.1 Single Difference Observables.....	36
2.3.8.2.2 Double Difference Observables	37
2.3.8.2.3 Pseudorange Differential Corrections	38
2.4 Coordinate Systems.....	39
2.4.1 World Geodetic System 1984 (WGS 84).....	39
2.4.2 ECEF Cartesian Coordinate System.....	42
2.4.2 ECEF Geographical Coordinate System	42
2.4.4 Coordinate Conversion	43
2.4.4.1 ECEF Cartesian coordinates to Geodetic coordinates	43
2.4.4.2 Geodetic coordinates to ECEF Cartesian coordinates	44
2.4.5 Datum Transformations	44
2.4.6 Projected Coordinates.....	47
CHAPTER THREE - GNSS TECHNIQUE AND ALGORITHM.....	48
3.1 Materials.....	48
3.2 Converting Universal Time to GPS Time	48

3.3 Calculation of Satellite Position in ECEF Systems.....	49
3.4 Receiver Position Computation in ECEF Coordinate System	52
3.5 Baseline Estimation and Separation of Ambiguities	56
3.6 Transformation of Receiver Position.....	63
3.6.1 Parameter Transformation from WGS 84 – War Office	64
3.6.7 Geographic Coordinates to National Grid on War Office ellipsoid.....	65
CHAPTER FOUR - SOFTWARE DEVELOPMENT AND TESTING.....	66
4.1 Software Development.....	66
4.1.1 Materials Used	66
4.2 Software Testing of GPS Data Processing.....	70
4.2.1 Data Collection.....	70
4.2 Data Processing.....	72
4.2.1 Data Processing using SSS v3.2.....	72
4.2.2 Data Processing using TOPCON Software	73
4.2.2 Data Processing using GNSS Suite Developed.....	73
4.3 Software Testing of Datum Transformation.....	75
4.4 Software Testing of Geodetic Computations.....	78
CHAPTER FIVE - RESULT AND ANALYSIS.....	79
5.1 RESULTS	79
5.1.1 Data Processing	79
5.1.2 Datum Transformation.....	81
5.2 ANALYSIS.....	82
5.2.1 Data Processing Results.....	82
5.2.1 Positions over Time	82
5.2.2 Comparison of Processed Results.....	83
5.2.2.1 GNSS Suite vs. Spectrum Survey.....	83
5.2.2.2 GNSS Suite vs. TOPCON Software.....	84
5.2.2.3 SSS vs. TOPCON Software.....	85

5.2.2.4 GNSS Suite vs. Original Coordinates.....	86
5.2.2.5 SSS vs. Original Coordinates	87
5.2.2.6 TOPCON Software vs. Original Coordinates.....	88
5.2.1 Datum Transformation Results.....	90
5.2.1.1 Transformed vs. Existing War Office Geographic Coordinates (ϕ, λ).....	90
5.2.1.2 Transformed vs. existing National Grid Coordinates (N, E)	91
5.2.1.2 Projected vs. existing National Grid Coordinates (N, E).....	91
CHAPTER SIX-CONCLUSIONS AND RECOMMENDATION	93
6.1 Conclusions	93
6.2 Recommendations	94
REFERENCES	96
APPENDICES	99
Appendix A: Projection Formulae	99
Appendix B: List of MATLAB M-Files	103
Appendix C: Glossary of GNSS Terminology.....	104



LIST OF TABLES

Table 2. 1: Summary of the various GNSS (Courtesy: Gyamfi, 2011)	8
Table 2. 2: Keplerian elements	10
Table 2. 3: Orbital Perturbation Parameters	15
Table 2.4: Content of GPS Broadcast ephemeris (Courtesy: Abidin, 2003).....	16
Table 2.5: Sample Broadcast Ephemeris message for satellite PRN26.	17
Table 2.6: Rinex File Types	18
Table 2.7: GPS Observation file: Data Section (Courtesy: Wing-ye, 2006).....	19
Table 2.8: DOP values.....	33
Table 2.9: The published transformation parameters of Ghana	46
Table 2 10: Projection Parameters	47
Table 4.1: Occupational Times	72
Table 4.2: Test point coordinates on WGS84	76
Table 4.3: Test point coordinates on Ghana War office ellipsoid.....	76
Table 4.4: Projected Northings and Eastings for test points on Ghana TM.....	76
Table 5.1: baseline results from SSS processing	79
Table 5.2: baseline results from TOPCON processing.....	80
Table 5.3: baseline results from developed GNSS suite processing	80
Table 5.4: Baseline results in TM Mapping System (SSS vs. Suite)	80
Table 5.5: Baseline results in TM Mapping System (TOPCON vs. Suite).....	81
Table 5.6: Baseline results in TM Mapping System (SSS vs. TOPCON).....	81
Table 5.7: Transformed coordinates on Ghana War office ellipsoid	82
Table 5.8: Transformed National Grid Coordinates	82
Table 5.9: Projected National Grid Coordinates	82
Table 5.10: Comparison of GNSS suite Processed Coordinates & Original coordinates.	87
Table 5.11: Comparison of Spectrum Processed Coordinates & Original coordinates.....	88
Table 5.12: Comparison of TOPCON Processed Coordinates & Original coordinates.	89
Table 5.13 Geographic coordinate difference	91
Table 5.14: Transformed and existing National Grid Coordinates.....	91
Table 5.15: Projected and existing National Grid Coordinates.....	92

LIST OF FIGURES

Figure 2.1: Keplerian orbit (courtesy: Hofmann-Wellenhof et al 2008).....	11
Figure 2.2: Broadcast Ephemeris Orbital representation (Courtesy: Abidin, 2003)	17
Figure 2.3: GPS satellite signal components (Courtesy: Rizos, 1997)	22
Figure 2.4: The structure of the Navigation Message (Courtesy: Zogg, 2002)	23
Figure 2.5: GNSS Error Sources (Courtesy: Afrifa, 2008).....	24
Figure 2.6: Carrier-phase measurements (Courtesy: Abidin, 2003).	27
Figure 2.7: Principle of GNSS point positioning (Courtesy: Thao, 2007)	28
Figure 2.8: Single differencing geometry	36
Figure 2.9: Double differencing geometry.....	37
Figure 2.10: The WGS 84 Coordinate System Definition.....	41
Figure 2.11: ECEF coordinate system.....	43
Figure 2.12: Datum Transformations (Courtesy: Ayer et al, 2008)	45
Figure 4.1: Interface for the creation of GUI in MATLAB	67
Figure 4.2: MATLAB M-file Editor	67
Figure 4.3: GPSweek M-file	68
Figure 4.4: Flow Chart Diagram for Designing Suite.....	70
Figure 4.5: Diagram of Survey showing Baselines	71
Figure 4.6: Project Settings.....	74
Figure 4.7: Import Rinex Option	74
Figure 4.8: Import Rinex.....	75
Figure 4.9: Flow chart for the testing procedure.....	76
Figure 4.10: Datum Transformation	77
Figure 4.11: Direct & Inverse Geodetic Computations	78
Figure 5.1: Positions of Pillars over Time.....	83
Figure 5.2: Plot Showing the Coordinates (N, E) & Differences (ΔN , ΔE) -Suite vs. SSS.....	84
Figure 5.3: Plot Showing the Coordinates (N, E) & Differences (ΔN , ΔE)-Suite vs. Topcon	85
Figure 5.4: Plot Showing the Coordinates (N, E) & Differences (ΔN , ΔE): SSS vs. Topcon	86
Figure 5.5: Plot Showing the Original & Suite processed Coordinates (N, E) & Differences (ΔN , ΔE)	87

Figure 5.6: Plot Showing the Original & Spectrum processed Coordinates (N, E) & Differences (ΔN , ΔE)..... 88

Figure 5.7: Plot Showing the Original & TOPCON processed Coordinates (N, E) & Differences (ΔN , ΔE)..... 89

KNUST



LIST OF ACRONYMS

ECEF	Earth-Centered Earth Fixed
KNUST	Kwame Nkrumah University of Science and Technology
UTM	Universal Transverse Mercator
TM	Transverse Mercator
WGS 84	World Geodetic Service 84
MATLAB	Matrix Laboratory
M-file	Matlab Function file
2D	Two dimension
GNSS	Global Navigation Satellite System
GLONASS	Global Orbiting Navigation Satellite System
GPS	Global Positioning System
RINEX	Receiver Independent Exchange Format
C/A code	Coarse Acquisition code
P-Code	Precise Code

CHAPTER ONE - INTRODUCTION

1.1 Background

Global Navigation Satellite System (GNSS) is one of the most innovative and practical technology developed today (Chan, 2008). Since its inception it has grown to provide not only world-wide, all-weather navigation, but precise position determination capabilities to all manner of users especially for surveying and geodetic applications (Carl, 1997; Satirapod, 2002). The scope of GNSS is enormous: from data acquisitions and processing, to detailed Computational algorithm in position estimations (Chan, 2008).

GNSS measurements are affected by a number of biases and errors. Their combined magnitude will affect the accuracy of the position determination. Among these biases and errors are Satellite Orbit Errors, Satellite Clock Errors, Receiver Clock Error, Tropospheric Delay, Ionospheric Delay and Multipath. The impact of these errors can be cancelled or significantly reduced by the method of Differential GNSS (DGNSS) (Petrovskyy et al, 2007). DGNSS employs two receivers, one that is stationary with a known location that has been previously surveyed (called the Base Station) and another that is roving around making position measurements (called the Rover). The base receiver collects data from all visible satellites and computes predicted satellite ranges which are compared with actual ranges. The difference is the satellite range error which is common to it and the roving receiver. This is then converted to correction signals or standard format and then relays the information to the roving receiver. The roving receiver is thus able to make appropriate corrections. The roving receiver position is computed either in real time or non-real time depending on the accuracy desired. In real time applications datalink is used to send the corrections and positions are computed. For post processing applications the measurements are stored in the receiver or on suitable media and processed at a later time. This is done by using a GNSS processing software.

There are many GNSS processing software available, these include Spectrum Survey, Trimble Business Office, GNSS Solutions, and Survey Project Manager for commercial applications. In addition, there are also software for scientific applications, notably Bernese software, Gipsy/OASIS II suite, GAMIT and the GPS Toolkit (GPSTk). These software are developed for general applications or standards and might not meet a country's accuracy specifications,

especially Ghana. This means that the inherent accuracy of a GNSS receiver can be enhanced or degraded depending on which software is used to do the post-processing (Borre et al, 1997). This therefore makes it imperatively important to custom design one that will ensure that the accuracy specifications needed for processing in this country are used.

Moreover, these software tend to be limited to the institutions that wrote them and use of them can require a considerable investment in time to understand the software and how best to use it under various circumstances. Expert training is often recommended by the distributors (Blewitt, 1997). Furthermore, Ghana has adapted the War Office ellipsoid for datum transformation and all transformation parameters needed to convert GNSS data to local mapping are based on the War Office ellipsoid. In order to use data obtained from GNSS measurements correctly and effectively in Ghana, we need to use appropriate transformation parameters that relate our Ghana National Survey Mapping coordinate system to that used for the GNSS (Ayer and Fosu, 2008). In most of the processing software, the War Office ellipsoid is not incorporated in their software for datum selection to enhance proper and effective transformation between the GNSS ellipsoid (WGS84) and the War Office ellipsoid.

In the light of these setbacks was this project designed to meet the country's mapping specifications as well as the implementation of the transformation parameters based on the War Office ellipsoid for accurate transformation between the GNSS ellipsoid (WGS84) and the War Office ellipsoid during post-processing. Also, an interactive user friendly interface with less program settings or parameterization for processing and displaying is implemented to aid in the effective use of the application. The application further allows the user to select or user-defined the type of transformation parameters (3, 5, 7 and 10) to be used for the processing. Finally, a stand-alone datum transformation and geodetic computations (direct and inverse) applications have also been developed.

1.2 Problem Statement

GNSS applications are continually being developed. There are many areas of application that require up to cm-level positional accuracy, such as surveying and mapping.

Though GNSS measurement biases and errors affect the accuracy of the position determination, processing the GNSS data with a software that does not meet a country's mapping accuracy specifications may also degrade the positional accuracy. These available software have been developed to suite general accuracy specifications.

Furthermore, the issue of datum transformation is also another problem with the commercial software. Ghana adapting the War Office ellipsoid means that all datum transformation between the Ghana datum and the GNSS datum should be based on the War Office ellipsoid. Most of the commercial Software do not have the War Office ellipsoid and its parameters in their system. In addition, these software tend to be limited to the institutions that wrote them and use of them can require a considerable investment in time to understand the software and how best to use it under various circumstances. Expert training is often recommended by the distributors (Blewitt, 1997).

There is therefore the need to custom design a GNSS suite for Ghana that will meet the country's mapping accuracy standards and specifications based on the War Office ellipsoid and the transformation parameters based on it.

1.3 Research Significance

- ✓ This research provides an open source GNSS suite written in MATLAB programming language that provides a number of models and algorithms found in GPS textbook for satellite and receiver positions computation.
- ✓ The research has also provided a wide array of functions that solves processing problems associated with GNSS.
- ✓ Furthermore, the issue of datum transformation between the WGS84 and War Office ellipsoids is also dealt with in this research.

- ✓ Last but not least, the source codes in this research are systematically and chronologically written which will enhance easy reading and understanding. Researchers in the GNSS community in Ghana can easily access the source codes to develop new processing applications.

1.4 Aim and Objectives

The main objective of this study is to develop a GNSS suite for geodetic applications that will

- provide an open source library and suite of applications custom design to meet the country's mapping specifications for processing GNSS data using RINEX files to the GNSS community in Ghana
- Provide a license free source codes to be written in Matlab Programming Language which can be modified and redistributed.
- Perform coordinate transformation using the existing published transformation parameters from Survey and Mapping Division of Ghana or user-defined transformation parameters.

1.5 Scope of Project

The study was much of research work with some assisted tutorials. In order to achieve the defined objectives. The following approach was adopted:

- Literature review on existing suite/packages
- Investigation of GPS processing algorithms (i.e. mathematical computations, Keplerian motion etc)
- Study of the structure of GPS observables and RINEX (**R**eceiver **I**ndependent **E**xchange) formats.
- Writing subroutines in Matlab programing language to load and read Rinex Observation and Navigation files.
- Writing M-file codes for GPS time conversion (GPS week, GPS day of week, GPS seconds of week, etc.).

- Writing M-file codes in Matlab to compute satellite positions using Navigation message as well as receiver positions using Broadcast ephemeris for both GNSS Code and Carrier Phase measurements.
- Writing M-file codes for other geodetic computations (coordinate transformation, inverse geodetic computations, etc.)
- Designing a flexible Graphic User Interface (GUI) under MATLAB Environment to integrate all the M-file codes.
- Field Measurements
- Testing suite by processing field data gathered.
- Processing of field data using commercial software
- Comparing suite processed results with commercial software results for analysis.

1.6 Thesis Outline

This thesis is organized in six chapters. Chapter One outlines the Background on the GNSS suite developed, problem statement, aim and objectives of this study, scope of project and the outline of the thesis. Chapter Two reviews the concept of satellite orbits and position determination in the ECEF frame, Rinex files, various time scales for GPS positioning, concept of GNSS and their error sources, GPS signal components, structure and characteristics. Coordinate systems, coordinate or datum transformation between the WGS84 and War Office ellipsoids are also outlined in this chapter.

Chapter Three provides the algorithms, procedures and steps for computing GPS time, Calculation of Satellite Position in ECEF Systems, Calculation of Receiver Position ECEF Systems, Baseline Estimation and Separation of Ambiguities between a base or reference receiver and rover receiver, performs the various coordinate or datum transformation.

In Chapter Four the development of the software or suite for GNSS data processing, datum transformation and geodetic computations is highlighted. Finally in this chapter, the developed software is tested on field data observations. In addition, the Sokkia Spectrum Survey (SSS) and

the TOPCON software are also used to process the same field data for the purpose of comparison or validation.

Chapter Five presents the results obtained from the developed software, Sokkia Spectrum Survey and the TOPCON software. Analysis and discussions of results and findings through statistical comparisons and graphical displays are also packaged in this chapter.

Chapter Six summarises the thesis with conclusions, and makes recommendations for future works.

KNUST



CHAPTER TWO - GLOBAL NAVIGATION SATELLITE SYSTEM (GNSS)

2.0 INTRODUCTION

Global Navigation Satellite Systems (GNSS) is a term used to describe all forms of space based navigation systems and encompasses all space-based radio-navigation systems that provide global coverage and signals that provide navigation, positioning, surveillance and timing information for ground, marine, aviation and space applications (Afrifa, 2008).

Two GNSS systems are currently in operation: the United States' Global Positioning System (GPS) and the Russian Federation's Global Orbiting Navigation Satellite System (GLONASS). A third, European Global Satellite Navigation System – Galileo, which is slated to reach full operational capacity in 2020. Each of the GNSS systems employs a constellation of orbiting satellites working in conjunction with a network of ground stations and consists mainly of three segments: (a) space segment, (b) control segment and (c) user segment. These segments are almost similar in the three satellite technologies.

GNSS positioning is based on the reception of signals transmitted by satellites, hence their performances are related to signal quality and operational development and hence variation in precision (Angrisano et al, 2011). The working principles of GNSS are based on the principle of trilateration: the position of unknown point is determined by measuring ranges to four or more known points. In this particular case, the known points are the position of the satellites moving in nearly circular orbits in space and the unknown point is the position of the receiver. Each satellite transmits a unique radio signal code which is received passively by the receiver, and the time is measured that it takes the signal to travel from the satellite to the receiver. The distance is basically the product of the transit time and the velocity of the radio signal (Petrovskyy, et al, 2007). Therefore subject to receiver type and tracked signals, GNSS has the ability to provide an autonomous three-dimensional position, velocity and time information (Afrifa, 2008; Angrisano et al, 2011; Chao, 1998). Table 2.1 below summarises the various GNSSs

Table 2. 1: Summary of the various GNSS (Courtesy: Gyamfi, 2011)

	US GPS	Russian GLONASS	European GALILEO	Chinese BEIDUO 2
No of Satellites	24	24	30	5 GEO & 30 MEO
Orbital Planes	6	3	3	n/a
Orbit Mean Altitude	20,200km	19,100 km	23,222 km	21,150 km
Orbital Periods	11-hrs 58-mins	11 hrs 15 mins	14 hrs 4 mins	n/a
Orbital Planes Inclination	55 degrees	64.8 degrees	56 degrees	55.5 degrees
Clocks	atomic clocks – caesium, rubidium or hydrogen maser			
System Frequencies	three L-band - L1, L2 & L5	two L-band - L1 & L2	E2-L1-E1, E5A-E5B and E6	four bands: E1, E2, E5B, and E6
Transmission Modes	Open access & Restricted	Open access & Restricted	Open access & Restricted	Open access & Restricted
Coordinates System	WGS84	Parametry Zemli 1990 (PZ90)	n/a	n/a
No SVs	30	27(21)	1	9

2.1 Satellite Orbits

The positions of the GPS satellites play the vital role in the receiver's position determination. The orbital error affects the accuracy of the measurements. Hence, the ability to predict the precise position of the satellite is crucial for the positioning. By Kepler's laws of planetary motion, ideal elliptical orbits of the GPS satellites can be described (Petrovskyy et al, 2007). The position of a satellite at a given time instant can be calculated from the ephemeris information included in the navigation message. Orbit epoch and orbital elements are used to accurately describe the orbit of a satellite in space and time. Orbit epoch is the time at which the establish orbital elements are true. Many different types of orbital elements may be used to describe the shape and size of an orbit and the location of the satellite. There is a standard type of orbital elements called the Keplerian elements. The Keplerian orbital elements define an orbital ellipse around the earth, orient it three dimensionally and place the satellite along the ellipse in time.

2.1.1 Keplerian Elements

The motion of a satellite around the Earth may be described mathematically by three scalar second-order differential equations (Hofmann-Wellenhof et al, 2008). The integration of these equations of motion yield six constants of integration. It is these constants of integration that are known as the orbital elements. The Keplerian orbital elements are often referred to as classical or conventional element and are the simplest and easiest to use.

There are six set of orbital elements which can be divided into two groups: the dimensional elements and the orientation elements (Petrovskyy et al, 2007). The dimensional elements specify size and shape of the orbit and relate the position in the orbit to time (Fig. 2.12). They are as follows:

- a = semi-major axis of the ellipse, the distance from the centre of the orbit ellipse to satellite's apogee or perigee point which specifies defining the size of the orbit.
- e = eccentricity of the ellipse, describing the shape of the orbit
- τ = epoch or time of perigee passage, which relates position in orbit to time (τ is often replaced by v , the true anomaly which is the angle between the perigee and the satellite position at a specified epoch measured in the orbital plane).

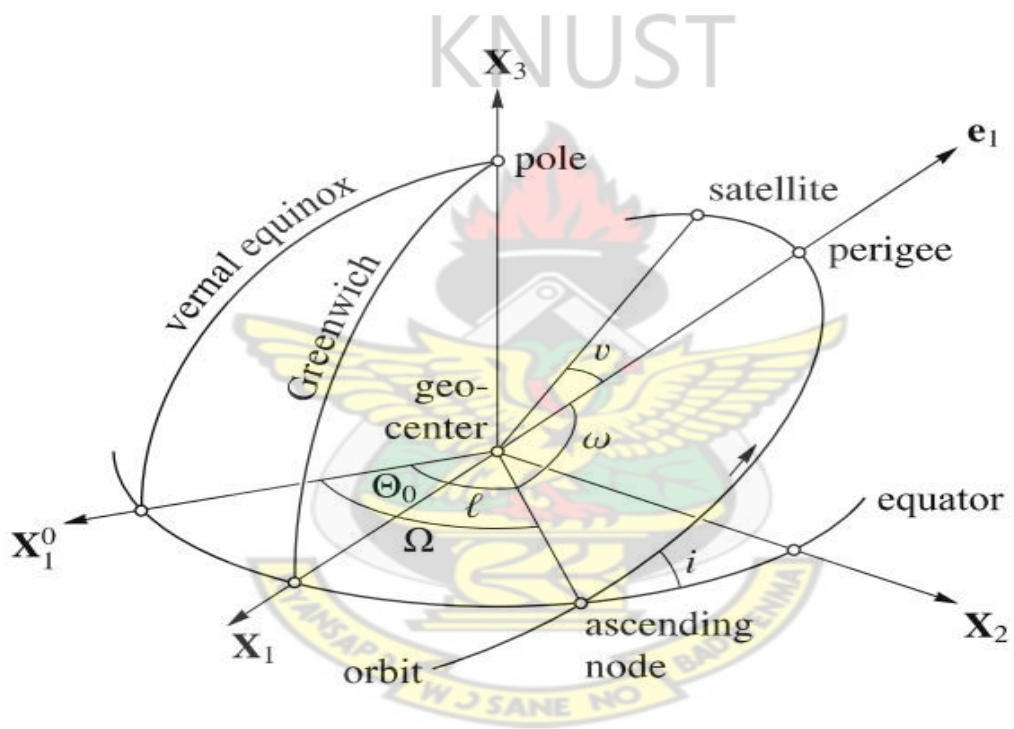
The orientation elements specify the orientation of the orbit in space (Fig. 2.12). They are as follows:

- i = inclination of the orbit plane with respect to the reference plane, which is taken to be the Earth's equator plane for satellites orbit. Inclination is the angle between the Earth's equatorial plane and the orbital plane ($0^\circ \leq i \leq 180^\circ$).
- Ω = right ascension of the ascending node, the angle measured at the centre of the earth from the vernal equinox to the ascending node ($0^\circ \leq \Omega \leq 360^\circ$).
- ω = argument of perigee, the angle in the plane of the orbit between the ascending node and the perigee ($0^\circ \leq \omega \leq 360^\circ$).

The angles i and Ω specify the orientation of the orbit plane in space. The angle ω then specifies the orientation of the orbit in its plane. Table 2.2 summarizes the six Keplerian elements

Table 2. 2: Keplerian elements

a	Semi-major axis	Size and shape of orbit
e	Eccentricity	
i	Inclination	Orientation of the orbital plane in the Inertial system
Ω	Right ascension of ascending node	
ω	Argument of perigee	
v	True anomaly	Position of the satellite in the orbital plane



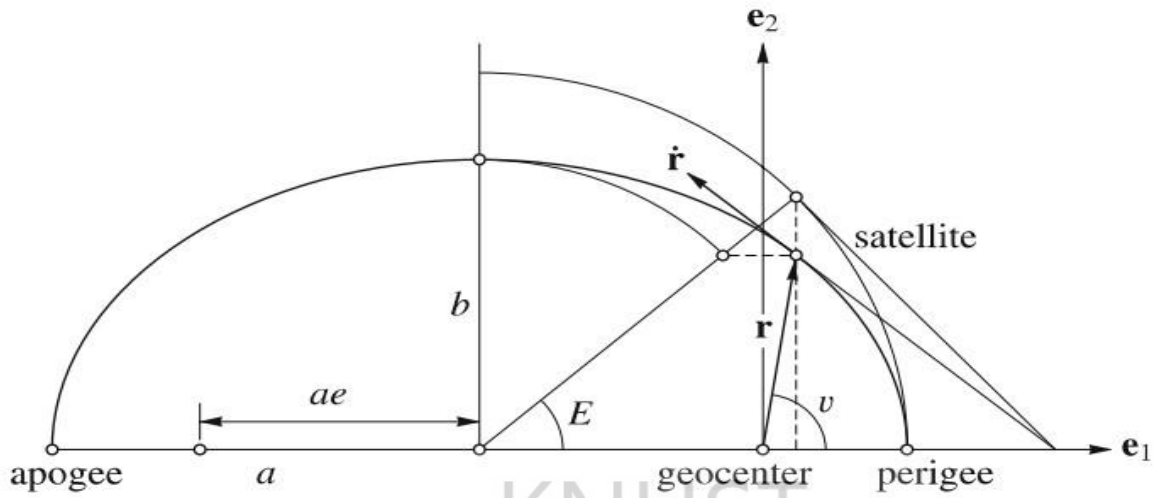


Figure 2.1: Keplerian orbit (courtesy: Hofmann-Wellenhof et al 2008)

2.1.2 Keplerian Motion in Orbital and ECEF Coordinate Systems

In order to determine the location of the satellite in the orbital plane the orbital coordinate system is needed (Figure 2.1). (Petrovskyy et al, 2007). The coordinate system used to describe a satellite can be considered as the satellite orbit frame because the center of the earth and the satellite are all in the same orbital plane. (TSUI, 2005). Figure 2.1 shows such a frame, and the x-axis or the e_1 -axis is along the direction of the perigee and the z-axis or the e_3 -axis is perpendicular to the orbital plane. The y-axis or the e_2 -axis is perpendicular to the x (e_1) and z (e_3) axes to form a right-hand coordinate system. The distance r from the satellite to the center of the earth is given as (Hofmann-Wellenhof et al, 2008; Calais, 2008):

$$r = a(1 - e \cos E) = \frac{a(1 - e^2)}{1 + e \cos v} \quad (2.10)$$

Where 'a' is the semi-major axis of the satellite orbit, e is the eccentricity of the satellite orbit, v is the true anomaly. The mean angular satellite velocity n (also known as the mean motion) with revolution period P follows from Kepler's third law given by

$$n = \frac{2\pi}{P} = \sqrt{\frac{\mu}{a^3}} = \sqrt{\frac{GM_E}{a^3}} \quad (2.11)$$

Where μ is the Earth's gravitational constant, M_E =Earth's mass, $GM_E = \mu = 3,986,005 \times 10^8 \text{ m}^3 \text{ s}^{-2}$

The instantaneous position of a satellite within its orbit is described by angular quantities known as anomalies. The mean anomaly $M(t)$ is a mathematical abstraction relating to mean angular motion, while both the eccentric anomaly $E(t)$ and the true anomaly $\nu(t)$ are geometrically producible (Fig. 2.1). The three anomalies are related by the formulas:

$$M(t) = n(t - T_0) \quad (2.12)$$

$$E(t) = M(t) + e \sin E(t) \quad (2.13)$$

$$\nu(t) = \tan^{-1} \left[\frac{\sqrt{1-e^2} \sin E(t)}{(\cos E(t) - e)} \right] \quad (2.14)$$

where n = mean motion = number of orbits in 24 hours, T_0 = time of perigee. Equation (2.13) is known as Kepler's equation. Navigation message transmitted by the GPS satellites contains the mean anomaly. In finding the position of the satellite, the true anomaly is needed. There is no straightforward way to obtain the true anomaly from the mean anomaly. Therefore, the eccentric anomaly should be introduced first. This equation can be solved iteratively.

The coordinate system e_1, e_2 defining the orbital plane is shown in Fig. 2.1. The position vector \mathbf{r} and the velocity vector $\dot{\mathbf{r}} = d\mathbf{r}/dt$ of the satellite can be represented by means of the eccentric as well as the true anomaly:

$$e_1 = r \cos \nu = a \cos E - ae = a(\cos E - e) \quad (2.15)$$

$$e_2 = r \sin \nu = \left(\frac{b}{a}\right)a \sin E = b \sin E = a(\sqrt{1-e^2} \sin E) \quad (2.16)$$

$$e_3 = 0 \quad (2.17)$$

$$\mathbf{r} = \begin{bmatrix} e_1 \\ e_2 \\ e_3 \end{bmatrix} = r \begin{bmatrix} \cos \nu \\ \sin \nu \\ 0 \end{bmatrix} = a \begin{bmatrix} \cos E - e \\ \sqrt{1-e^2} \sin E \\ 0 \end{bmatrix} \quad (2.18)$$

where the magnitude r is computed as

$$r = a(1 - e \cos E) = \frac{a(1 - e^2)}{1 + e \cos v}$$

In order to find the user position on the globe the satellite coordinates have to be transformed to the Earth-Centered-Earth-Fixed (ECEF) coordinate system. (Petrovskyy et al, 2007). From Figure 2.1, it can be seen that the transformation of the Cartesian components of a satellite position vector \mathbf{r} from the orbital plane coordinate system to the ECEF system may be carried out by three rotations by means of direction cosine matrices in the following order:

- a first rotation by the argument of the perigee ω ;
- a second rotation by the angle of inclination i ; and
- finally a rotation by the angle of the longitude of ascending node Ω . (Zhang et al, 2006).

$$R(\omega) = \begin{bmatrix} \cos \omega & -\sin \omega & 0 \\ \sin \omega & \cos \omega & 0 \\ 0 & 0 & 1 \end{bmatrix} \quad R(i) = \begin{bmatrix} 0 & 0 & 0 \\ 0 & \cos i & -\sin i \\ 0 & \sin i & \cos i \end{bmatrix} \quad R(l) = \begin{bmatrix} \cos l & -\sin l & 0 \\ \sin l & \cos l & 0 \\ 0 & 0 & 1 \end{bmatrix} \quad (2.21)$$

The transformation of \mathbf{r} into the equatorial system \mathbf{X}_i^0 (X_1^0, X_2^0, X_3^0) is performed by a rotation matrix \mathbf{R} and results in vector denoted by P . The transformation is defined by

$$P = R \times r \quad (2.22)$$

Where the matrix \mathbf{R} is composed of the three successive rotation matrices and is given by

$$R = R_3(-\Omega)R_1(-i)R_3(-\omega) \quad (2.23)$$

$$R = \begin{bmatrix} \cos \Omega \cos \omega - \sin \Omega \sin \omega \cos i & -\cos \Omega \sin \omega - \sin \Omega \cos \omega \cos i & \sin \Omega \sin i \\ \sin \Omega \cos \omega + \cos \Omega \sin \omega \cos i & -\sin \Omega \sin \omega + \cos \Omega \cos \omega \cos i & -\cos \Omega \sin i \\ \sin \omega \sin i & \cos \omega \cos i & \cos i \end{bmatrix} \quad (2.24)$$

$$= [e_1 \quad e_2 \quad e_3] \quad (2.25)$$

In order to rotate the system \mathbf{X}_i^0 into the terrestrial or Earth fixed system \mathbf{X}_i (X_1, X_2, X_3), an additional rotation through the angle Θ_0 , the Greenwich sidereal time which can be expressed in terms of earth rotation rate ω_e and time t_s elapsed since the Greenwich meridian crossed the

vernal equinox, is required. (Hofmann-Wellenhof et al, 2008). The transformation matrix, therefore, becomes

$$P = R' \times r$$

$$R' = R_3(\Theta_o)R = R_3(\Theta_o)R_3(-\Omega)R_1(-i)R_3(-\omega) \quad (2.26)$$

The product $R_3(\Theta_o)R_3(-\Omega)$ can be expressed by a single matrix $R_3(-l)$, where

$l = \Omega - \Theta_o$ is the longitude of the ascending node. Hence, Eq. (3.12) can be written in the form

$$\mathbf{R}' = \mathbf{R}_3(-l) \mathbf{R}_1(-i) \mathbf{R}_3(-\omega) \quad (2.27)$$

$$\Theta_o = \omega_e t_s \quad (2.28)$$

and the matrix \mathbf{R}' corresponds to the matrix \mathbf{R} if in Eq. (3.6) the parameter Ω is replaced by l .

$$R' = \begin{bmatrix} \cos l \cos \omega - \sin l \sin \omega \cos i & -\cos l \sin \omega - \sin l \cos \omega \cos i & \sin l \sin i \\ \sin l \cos \omega + \cos l \sin \omega \cos i & -\sin l \sin \omega + \cos l \cos \omega \cos i & -\cos l \sin i \\ \sin \omega \sin i & \cos \omega \cos i & \cos i \end{bmatrix} \quad (2.29)$$

The resulting position of satellite in ECEF coordinates is calculated as:

$$\begin{bmatrix} e_1 \\ e_2 \\ e_3 \end{bmatrix} = \begin{bmatrix} X \\ Y \\ Z \end{bmatrix} = R(\Omega)R(i)R(\omega) \begin{bmatrix} r \cos \nu \\ r \sin \nu \\ 0 \end{bmatrix} \quad (2.30)$$

2.1.3 Perturbed satellite motion

A satellite orbiting the Earth follows Keplerian laws. However, due to the Earth's non-central gravity field, forces of gravitational and non-gravitational origin that perturb the motion of the GPS satellites, causing the orbits to deviate from a Keplerian ellipse in an inertial space (see Figure 2.1 above). These forces include the gravitational effects of the sun and the moon, solar radiation pressure, albedo (reflection of solar light from the surface of the earth back into space), effects of earth and ocean tides, radiation from space, atmospheric drag etc. (Jensen ,2008. Curiel, 2000, Leick, 1995). The effect on the Kepler elements, describing the size, shape and location of the satellite orbit, is rather large and must be considered when dealing with real

satellite positions. The effect is larger for satellites located in orbits close to the surface of the earth, the Low Earth Orbiting (LEO) satellites. Although the Keplerian representation has physical meaning, additional parameters are required to model the perturbations about the Keplerian orbit. The Orbital Perturbation Parameters are contained in table 2.3 below.

Table 2. 3: Orbital Perturbation Parameters

	Orbital Perturbation Parameters
Δn	Mean motion difference from computed value(semicircles/s)
$\dot{\Omega}$	Rate of change of right ascension (semicircles/s)
\dot{i}	Rate of change of inclination (semicircles/s)
C_{us} and C_{uc}	Amplitude of the sine and cosine harmonic correction terms to the argument of latitude(rad)
C_{is} and C_{ic}	Amplitude of the sine and cosine harmonic correction terms to the inclination angle(m)
C_{rs} and C_{rc}	Amplitude of the sine and cosine harmonic correction terms to the orbit radius(m)

2.1.4 GPS broadcast ephemeris

For GPS positioning, the GPS receiver needs information on the satellite positions at the point in time where the satellite signals were transmitted from the satellites. This information is called broadcast ephemeris and is transmitted from the satellites to the receiver in the navigation message (Jensen, 2008). The broadcast ephemerides are forecasted, predicted, extrapolated or produced by the GPS Control Segment that uses the Kalman filter to estimate satellite position, velocity, solar radiation, pressure coefficient, clock bias, clock drift and clock drift rate. (Warren et al, 2003). The estimated parameters are used to propagate the satellite orbit and clock correction in the future. The propagated values are converted into a set of Keplerian elements

and uploaded into the navigation message and distributed in ASCII format in Receiver Independent Exchange format (RINEX). Information contained broadcast ephemeris is:

- Keplerian elements with periodic terms added to account for solar radiation and gravity perturbations
- Periodic terms are added for argument of perigee, geocentric distance and inclination.

The content of broadcast ephemeris are given in table 2.4 below (Abidin, 2003)

Table 2.4: Content of GPS Broadcast ephemeris (Courtesy: Abidin, 2003)

Time Parameters	
• t_{oc}	Reference time for the ephemeris parameters (s)
• t_{oc}	Reference time for the clock parameters (s)
• a_0, a_1, a_2	Polynomial coefficients for satellite clock correction, i.e. representing the bias (s), drift (s/s), and drift-rate (s/s ²) components.
• IOD	Issue of Data (arbitrary identification number)
Satellite Orbit Parameters	
• \sqrt{a}	Square root of the semi-major axis (m ^{1/2})
• e	Eccentricity of the orbit (dimensionless)
• i_0	Inclination of the orbit at t_{oc} (semicircles)
• Ω_0	Longitude of the ascending node at t_{oc} (semicircles)
• ω	Argument of perigee (semicircles)
• M_0	Mean anomaly at t_{oc} (semicircles)
Orbital Perturbation Parameters	
• Δn	Mean motion difference from computed value (semicircles/s)
• $\dot{\Omega}$	Rate of change of right ascension (semicircles/s)
• \dot{i}	Rate of change of inclination (semicircles/s)
• C_{us} and C_{uc}	Amplitude of the sine and cosine harmonic correction terms to the argument of latitude (rad)
• C_{is} and C_{ic}	Amplitude of the sine and cosine harmonic correction terms to the inclination angle (m)
• C_{rs} and C_{rc}	Amplitude of the sine and cosine harmonic correction terms to the orbit radius (m)

Hasanuddin Z. Abidin, 2003

The broadcast ephemerides are uploaded once daily and are valid for two hours, the accuracies of which are 160 cm for the orbit and 7 ns for the satellite clock (International GNSS Service). While it is difficult to judge the accuracy of the broadcast ephemerides, the procedures are undergoing continual improvement, and the average is expected to be better than 10m. Figure 2.2

below shows a representation of the broadcast ephemerides based on *Keplerian elements plus perturbations*.

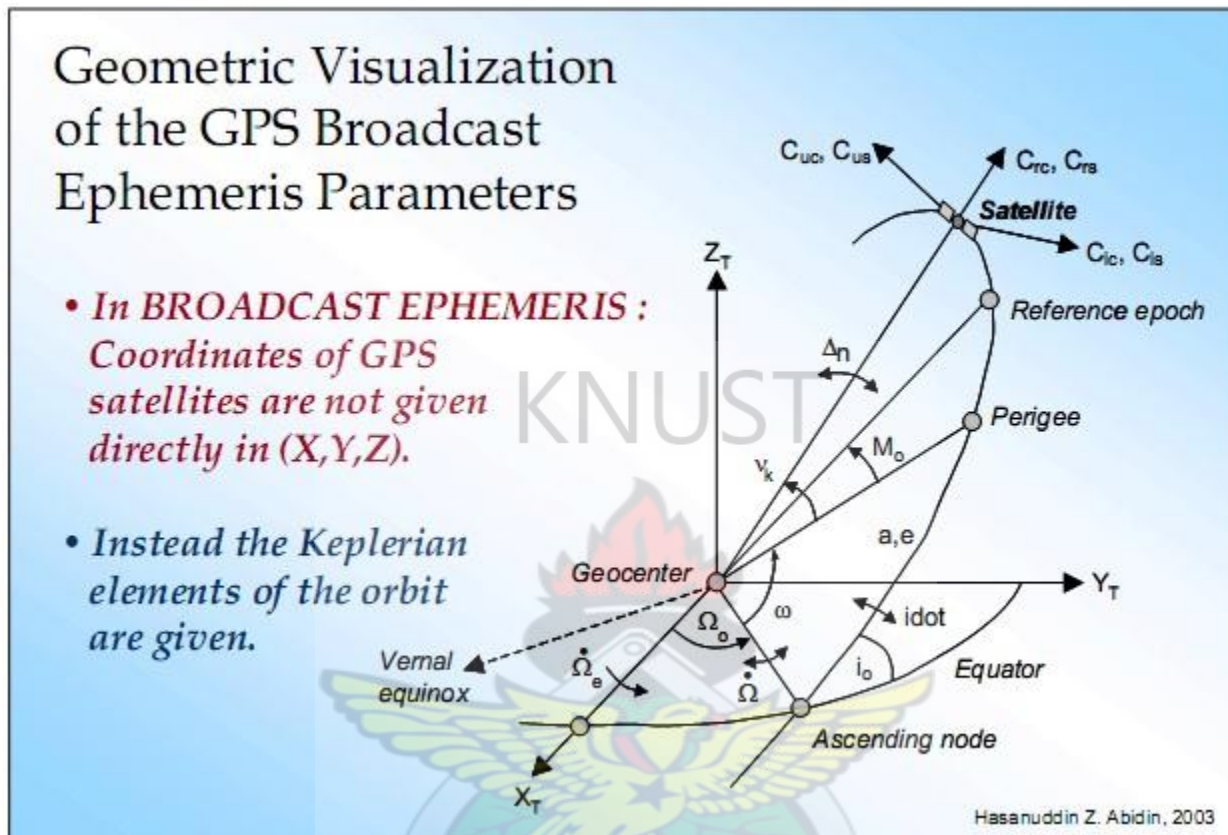


Figure 2.2: Broadcast Ephemeris Orbital representation (Courtesy: Abidin, 2003).

A sample of the broadcast Navigation Message for one satellite is presented in Table 2.5 below.

Table 2.5: Sample Broadcast Ephemeris message for satellite PRN26.

PRN	Date/time of clock toc	a0 (msec)	a1 (msec/day)	a2 (msec/day ²)
26	92 07 26 08 51 44.0	1.635868102312D-06	-3.410605131648D-13	0.000000000000D+00
	Age of ephemeris (sec)	Crs (m)	Dn (rad/sec)	Mo (rads)
	2.170000000000D+02	1.128125000000D+01	4.738768932810D-09	5.863412966114D-02
	Cuc (rads)	e	Cus (rads)	
	4.898756742477D-07	8.141674217768D-03	9.039416909218D-06	5.153610269547D+03
	toe (secs in GPS wk)	Cic (rads)	Wo (rads)	Cis (rads)
	3.190400000000D+04	-7.636845111847D-08	-1.371976967685D+00	-4.470348358154D-08
	io (rads)	Crc (m)	w (rads)	
	9.603279283700D-01	2.067812500000D+02	-1.491259472097D+00	-8.059264366977D-09
		GPS week number		
		-4.760912775126D-10	1.000000000000D+00	6.550000000000D+02
				0.000000000000D+00

2.1.5 RINEX File

RINEX is an acronym which stands for Receiver Independent Exchange Format, developed by the Astronomical Institute of the University of Berne for the easy exchange of the GPS data collected for processing in various software. Consists of three ASCII file types (see table 2.6):

Table 2.6: Rinex File Types

File Type	Containing Information
Observation Data File (O-file)	GPS Measurements
GPS Navigation Message File (N-file)	Ephemeris (Orbit information)
Meteorological Data File	Pressure, Temperature, Relative Humidity, etc

Each file type consists of a header section and a data section. The header section contains global information for the entire file and is placed at the beginning of the file, and the data section contains the actual data (Gurtner et al, 2008, Hofmann-Wellenhof et al, 2008).

2.1.5.1 RINEX Navigation Files (N-file)

The data section of the Rinex navigation file contains the ephemeris for satellite position computation. One block of data per satellite and each block of data contains: PRN, year, month, day, hour, minutes, seconds, satellite clock correction and the orbit parameters (See Table 2.5). The Navigation Message File from one receiver may be used by other receivers.

2.1.5.2 RINEX Observation Files (O-file)

Observation file contains data from one site and one session. There are 3 fundamental observables:

- ✓ TIME – the time of measurement in seconds
- ✓ PSEUDORANGE (on both L1 and L2 codes) – stored in meters, includes all offsets and biases and are indicated as C1, C2, P1, P2
- ✓ PHASE (on both L1 and L2 codes) – carrier phase measurements in whole cycles (no systematic drifts from receiver).

Where

C1 and C2 - Pseudorange using C/A code on L1 and L2 frequencies

P1 and P2 - Pseudorange using P-Code on L1 and L2 frequencies

L1 and L2 - Phase measurements on L1 and L2 frequencies

Observation block consists of observation time and observation set for each satellite. Table 2.7 illustrates GPS observation file data section.

Table 2.7: GPS Observation file: Data Section (Courtesy: Wing-ye, 2006)

4	C1	Number of Satellites										# / TYPES OF OBSERV
2006	5.0000	0	0.000000	0	0.000000	INTERVAL						
2006		59	55.000000	0	0.000000	TIME OF FIRST OBS						
14				0	0.000000	TIME OF LAST OBS						
							LEAP SECONDS					
							END OF HEAD					
06	6	5	3	0	0.000000	0	100 2G 6G 7G 8G 9G10G18G21G26G29					
23288740.069	122383102.613	7	23288741.198	95363442.36846								
21880080.633	114980606.034	8	21880082.183	89595291.87246								
25444792.816	133713291.799	5	25444797.337	104192196.61943								
25044883.981	131611749.406	5	25044886.790	102554615.56243								
23132107.018	121560054.186	8	23132109.516	94722138.03345								

4	C1	L1	P2	L2	# / TYPES OF OBSERV
2006	6	5	3	0	0.000000
2006	6	5	3	59	55.000000
14					0.000000
06	6	5	3	0	0.000000
23288740.069	122383102.613	7	23288741.198	95363442.36846	
21880080.633	114980606.034	8	21880082.183	89595291.87246	
25444792.816	133713291.799	5	25444797.337	104192196.61943	
25044883.981	131611749.406	5	25044886.790	102554615.56243	

2.2 Time Scales

There are many time scales used to describe or predict the occurrences of events. But for the purpose of this study only Coordinated Universal Time (UTC) and GPS Time are considered since within GPS calculations, 'time' is expressed as either Coordinated Universal Time (UTC) or GPS Time. These are described in the following sub-sections. (Chan, 2008).

2.2.1. Coordinated Universal Time (UTC)

UTC is based on a combination of solar and atomic times. Its second is the second of atomic time, the basis of civil time. Civil time is obtained from an atomic clock adjusted in epoch to

remain close to UT1 (within 0.9 second of mean solar time) (Bâki İz, 2010). Universal Time is expressed in Year, Month, Day, Hour, Minute and Second. This is the type of time format recorded in a Receiver Independent Exchange (RINEX) format observation file (Chan, 2008).

2.2.2. GPS Time

GPS Time is a continuous measurement of time or a uniformly counting time scale from an epoch started at January 6, 1980 at midnight (0 hours 0 minutes 0 seconds) Universal Time Coordinated (UTC). GPS Time is derived from the onboard atomic clocks of the GPS satellites. (Dana, 1997; Clynch, 2006; Bâki İz, 2010). GPS Time counts in weeks and seconds of a week from this instant. The weeks begin at the Saturday/Sunday transition. The days of the week are numbered, with Sunday being 0, 1 Monday, etc. GPS week 0 began at the beginning of the GPS Time Scale. Within each week the time is usually denoted as the second of the week. This is a number between 0 and 604,800 ($60 \times 60 \times 24 \times 7$). Sometimes the second-of-week (SOW) is split into a day of week (DOW) between 0 and 6 and a second of day (SOD) between 0 and 86400. The GPS time may differ from UTC because GPS time is a continuous time scale and does not introduce leap seconds, while UTC is corrected periodically with an integer number of leap seconds. The GPS time scale is maintained to be within one μs of UTC (modulo of one second). This means the two times can be different by an integer number of seconds. (Clynch, 2006; TSUI, 2005). When carrying out any GPS calculations, the parameter 'time' must be expressed in GPS time. (Chan, 2008).

2.2.3 Julian Date

In everyday life we use month, day and year to denote a date. However adding and subtracting dates is complicated. Astronomers use a time scale that counts uniformly in days they call the Julian Date (JD). This count does not have any leap years. (Or even any years as it counts days.) They set the origin of this date system far back in time, at January 0, 4713 BC at noon. This scale is counted in days and fractions of a day. January 1, 2000 at noon is $\text{JD} = 2,451,545.0$. Days used to be started at noon, hence the use of noon as the reference time. (Clynch, 2006).

The Julian date (JD) therefore, defines the number of mean solar days elapsed since January 1st, 4713 B.C., 12:00 (midday). (Hofmann-Wellenhof et al, 2008; Calais, 2008).

2.3 GPS Signal Components, Structure, and Characteristics

Each satellite transmits a unique navigational signal centered on two L-band frequencies of the electromagnetic spectrum. These frequencies are derived from the fundamental frequency of 10.23 MHz generated by the atomic clock onboard oscillators and have stability in the range of 10^{-13} over one day (Spilker, et al 1978; Satirapod, 2002; Petrovskyy, et al, 2007). The satellite signal consists of the following components: the two L-band carrier waves, the ranging codes and the navigation message. These are discussed below.

2.3.1 Two L-band Carrier Waves

The two L-band carrier waves are L1 at 1575.42 MHz and L2 at 1227.60 MHz. They are generated by multiplying the fundamental frequency (10.23 MHz) by 154 and 120, respectively. These carrier waves provide the means by which the ranging codes and the navigation message are transmitted to the receiver. The L1 has a wavelength of 19.03 cm and is used to carry the navigation message and for providing the Standard Positioning Service (SPS) code signals. The L2 has a wavelength of 24.45 cm and is used to measure ionospheric delay and also for providing the Precise Positioning Service (PPS) code signals (Bâki İz, 2010).

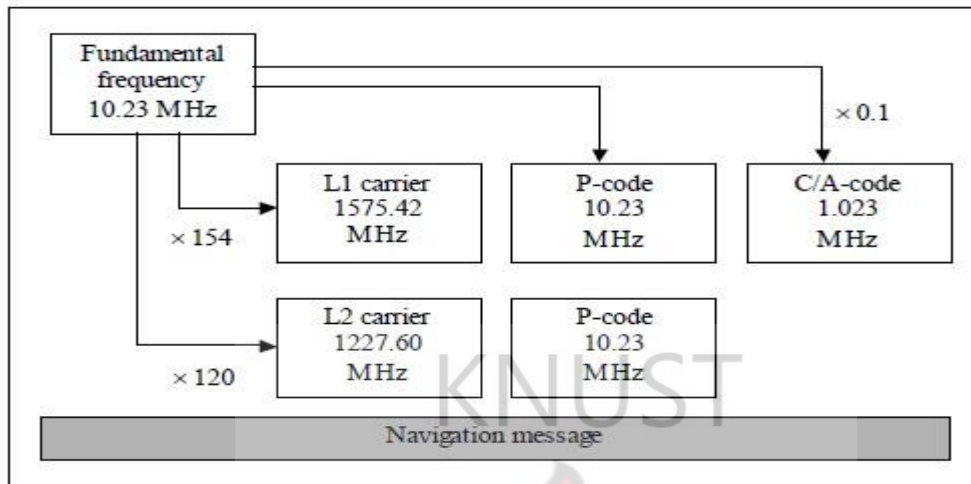
2.3.2 Ranging Codes

GPS codes consist of a sequence with the states +1 or -1, corresponding to the binary values 0 or 1. The two basic codes are modulated on the carrier frequencies as so-called *pseudo random noise* (PRN) sequences (Seeber, 2003). They are the Precise Code (P-Code) and the Coarse Acquisition Code (C/A Code). The Coarse Acquisition code (C/A-code) is modulated only on the L1 carrier and is generated at 1.023MHz (i.e. one-tenth of the fundamental frequency). Each satellite broadcasts a completely unique C/A Code modulated on only the L1 frequency and it is repeated every millisecond. The Precise code (P-code) is modulated on both the L1 and L2 carriers and is generated at the fundamental frequency (i.e. 10.23 MHz) (Satirapod, 2002). Each satellite repeats its portion of the P-Code every seven days, and the entire code is renewed every 37 weeks.

Generally, there are two levels of service in Single Point Positioning (SPP) mode. The first one is called Standard Positioning Service (SPS) and the second one is called Precise Positioning Service (PPS) (Seeber, 1993; Satirapod, 2002). The SPS is intended for civilian use and uses

only the C/A-code. Unlike the SPS, the PPS accesses both codes (C/A-code and P-code), but is generally reserved for U.S. military use.

Figure 2 3: GPS satellite signal components (Courtesy: Rizos, 1997)



2.3.3 Navigation Message

The navigation message is a continuous stream of data transmitted at 50 bits per second and modulated on both the L1 and L2 bands. (Zogg, 2002; Bâki İz, 2010). This message contains information such as (Abidin, 2003):

- Satellite almanac data,
- Satellite clock correction parameters,
- Satellite health and constellation status,
- Ionospheric model parameters for single-frequency users
- The offset between the GPS and Universal Time Coordinated (UTC).

The content of the navigation message is determined by the GPS Control Segment and broadcast to users by the GPS satellites. The navigation message is needed to calculate the current position of the satellites and to determine signal transit times. The data stream is modulated to the HF carrier wave of each individual satellite. Data is transmitted in logically grouped units known as frames or pages. (Zogg, 2002). A complete message consists of 25 frames, each containing 1500 bits long and takes 30 seconds to transmit. (Leick, 2004). Each frame is subdivided into 5 subframes transmitting different information. Each subframe is 300 bits long and takes 6 seconds to transmit. Each subframe is in turn divided into 10 words each containing 30 bits (Zogg, 2002). Each subframe begins with a telemetry word (TLM) and the handover word (HOW).

Transmission time for the entire almanac is therefore 12.5 minutes. (Zogg, 2002; Seeber, 2003). The structure of the navigation message is illustrated in figure 2.4 below.

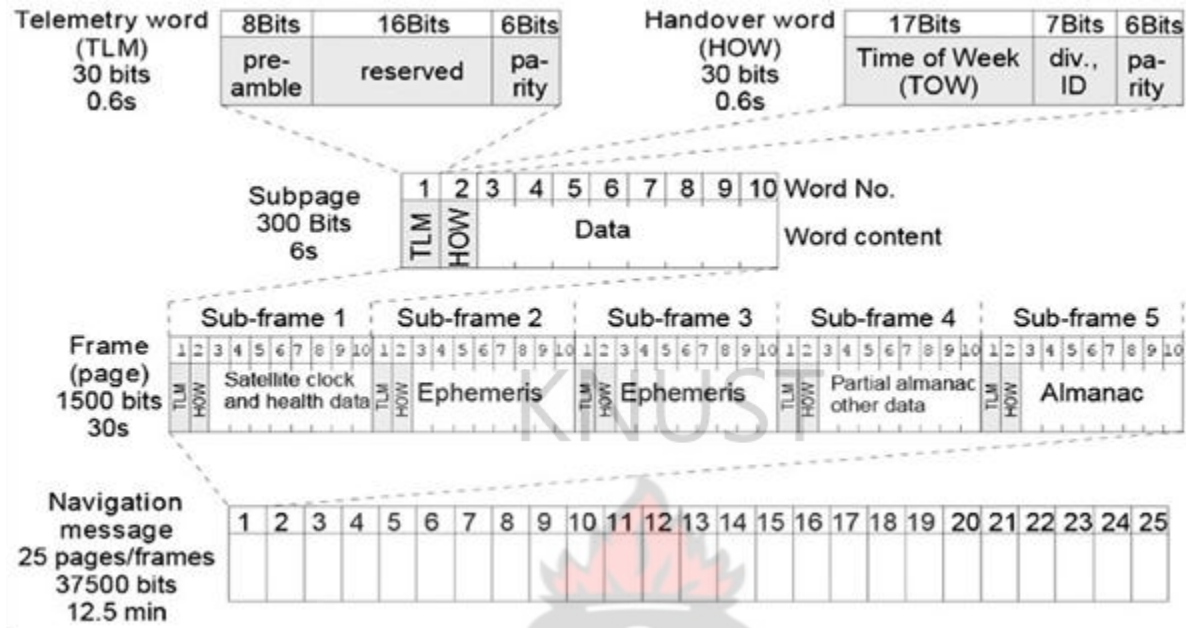


Figure 2.4: The structure of the Navigation Message (Courtesy: Zogg, 2002)

2.3.3.1 Subframe Contents

Subframe 1 contains the GPS week number, space vehicle accuracy and health status, satellite clock correction terms a_0 , a_1 , a_2 and the clock reference time t_{oc} , the differential group delay, T_{GD} , and the issue of date clock (IODC) term. Subframes 2 and 3 contain the ephemeris data or parameters of the transmitting satellite. The various elements are listed in table 2.4 (Leick, 2004, Zogg, 2002). Subframe 4 contains the almanac data on satellite numbers 25 to 32, ionospheric correction terms, coefficients to convert GPS time to Universal Time Coordinated (UTC) (Zogg, 2002; Leick, 2004; Seeber, 2003). For accurate computation of UTC from GPS time, the message provides a constant offset term, a linear polynomial term, reference time t_{oe} , and the current value of the leap second (Leick, 2004).

Subframe 5 contains the almanac data on satellite 1 to 24 as well as time and the number of the GPS week. All 25 pages are transmitted together with information on the health of satellite numbers 1 to 24 (Leick, 2004; Zogg, 2002; Seeber, 2003).

2.4 Error Sources in GNSS Positioning

GNSS measurements are affected by biases and errors. Their combined magnitude will affect the accuracy of the position determination (Petrovskyy et al, 2007).

In general, the errors or biases related to GNSS positioning can be conveniently categorized into three classes, satellite-dependent biases, receiver-dependent biases and signal propagation biases (Satirapod, 2002). See figure 2.5. But these are expanded into:

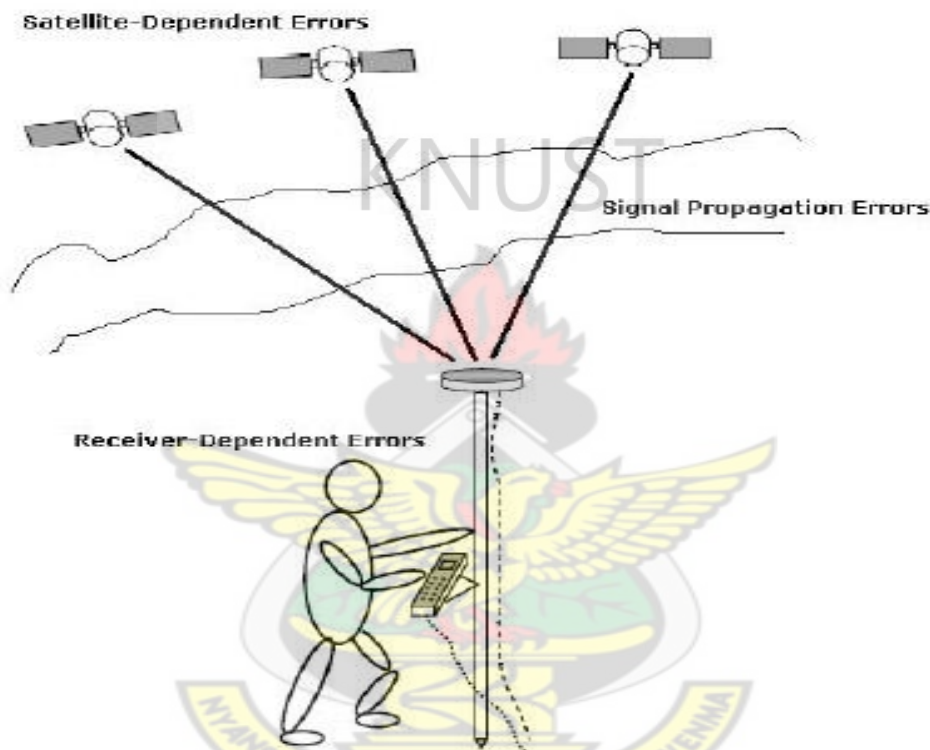


Figure 2.5: GNSS Error Sources (Courtesy: Afrifa, 2008)

- ✓ Satellite and receiver clock biases
- ✓ Ionospheric and tropospheric delays
- ✓ Satellite ephemeris errors (orbit errors)
- ✓ Multipath

Detail explanation of these biases can be read from many text books. See (Satirapod, 2002; Leick, 2004; Seeber, 1993 etc).

2.3.7 Fundamental GNSS Measurements

There are two types of fundamental measurements used in position determination, namely pseudorange measurements and carrier phase measurements (Satirapod, 2002).

2.3.7.1 Pseudorange Measurements

A pseudorange is a measure of the distance between the satellite and the receiver's antenna. The distance is measured through the measurement of the time shift between the code generated by a receiver and the code transmitted from a GNSS satellite. If the receiver and satellite clocks are synchronised with the GNSS time, the travel time of the satellite signal will be equal to the difference between the transmission time and the reception time (Satirapod, 2002). The range between the satellite and the receiver can be calculated by multiplying the travel time with the speed of light, c (Hofmann-Wellenhof et al., 2001; Leick, 2003; Satirapod, 2002).

$$R = c(t_i - t^k) = c\Delta t_i^k$$

However, the satellite and receiver clocks are not synchronised with the GPS Time and therefore, the two signals are affected by the clocks errors. Hence, the range measured is not true and it is called pseudorange. Moreover, apart from clocks errors, there are other errors or biases such as atmospheric delays and multipath that affect the signals when the satellite signal propagates from the satellite to the receiver. The pseudorange measurement between receiver i and satellite k can be expressed as (Xu, 2007; Borre et al, 1997):

$$R_i^k(t_i, t_k) = \rho_i^k(t_i, t_k) - (\delta t_i - \delta t_k)c + \delta_{ion} + \delta_{trop} + \delta_m + \varepsilon \quad (2.55)$$

Where $R_i^k, \rho_i^k, \delta_{ion}, \delta_{trop}, \delta_m, \delta t_i, \delta t_k$ are pseudorange, true range, ionospheric delay, tropospheric delay, multipath, receiver clock offset and satellite clock offset between satellite k and receiver i scaled to range units.

Neglecting ionospheric delay, tropospheric delay, multipath, Eq. (2.55) becomes:

$$R_i^k(t_i, t_k) = \rho_i^k(t_i, t_k) - (\delta t_i - \delta t_k)c \quad (2.49)$$

The geometric distance ρ_i^k between satellite k and receiver i is given by:

$$\rho_i^k(t_i, t_k) = \sqrt{(x^k - x_i)^2 + (y^k - y_i)^2 + (z^k - z_i)^2}$$

where

x^k, y^k, z^k = satellite position in an ECEF coordinate system

(x_i, y_i, z_i) = receiver position in an ECEF coordinate system

The pseudorange measurement is generally used in applications where the accuracy is not high (few metre level), as is typical for single-epoch navigation applications (Satirapod, 2002).

2.3.7.2 Carrier Phase Measurement

Carrier phase is the measurement of the phase difference between the carrier signal generated by a receiver's internal oscillator and the carrier signal transmitted from a satellite when a satellite is locked on (Satirapod, 2002; Hofmann-Wellenhof et al, 2001). This means that the phase shift in the signal that occurs from the instant or time that the signal is transmitted by the satellite, until it is received by the receiver, is observed (Nagi and Munzir, 2011). This process gives the fractional cycle of the signal from satellite to receiver (Nagi and Munzir, 2011). If the satellite signal is assumed to be continuously locked, the receiver will keep track of changes to the phase (Satirapod, 2002). However, this does not account for the number of full wavelengths or cycles that occurred as the signal traveled between the satellite and the receiver (Nagi and Munzir, 2011). It remains unknown, or ambiguous by a number of full cycles (Satirapod, 2002; Rabbany, 2002). This number is called the integer ambiguity (N) or simply ambiguity. To convert the carrier phase measurements to a range between the satellite and the receiver, or to be able to use the carrier phase as a measurement for positioning, this initially unknown number of cycles or the phase ambiguity must be resolved or accounted for (Satirapod, 2002). If the integer cycle ambiguity parameters are correctly resolved or estimated, very precise range measurements (at the few mm precision level) can be obtained, leading to precise or accurate position determination. The total distance can therefore be computed by the summation of the phase measurement, initial ambiguity at first observation, and number of full cycles counted by receiver (Nagi and Munzir, 2011).

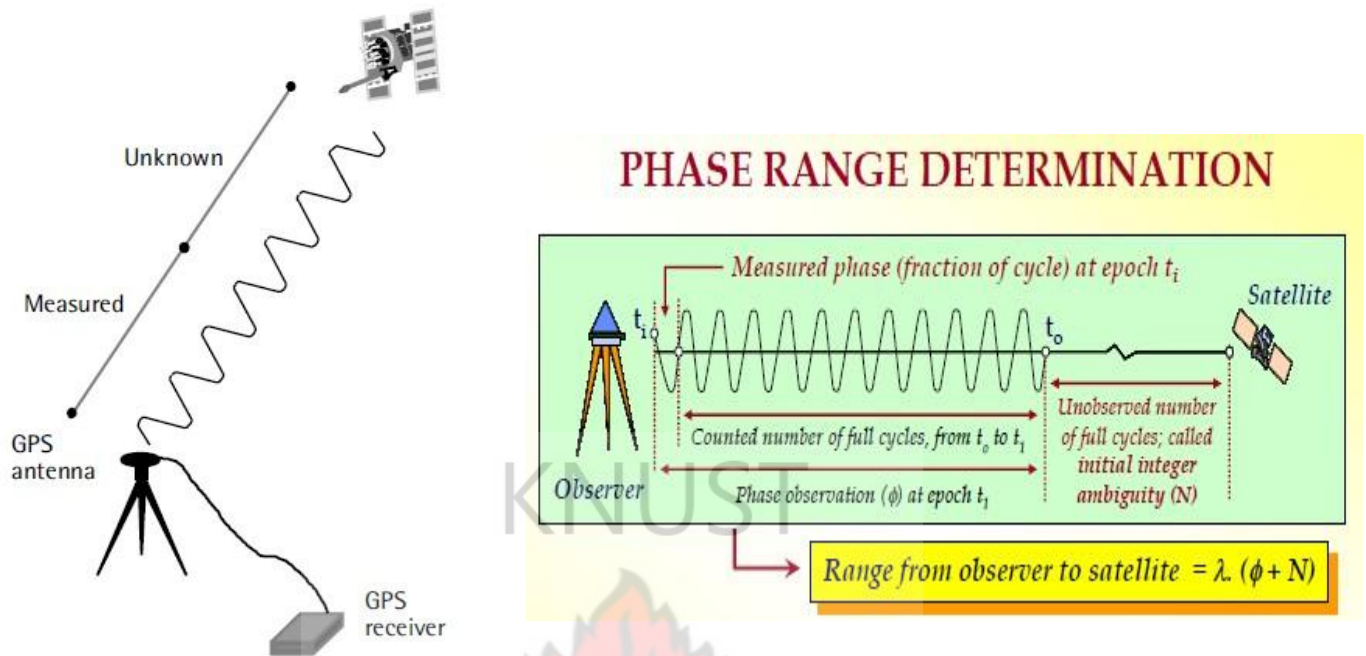


Figure 2.6: Carrier-phase measurements (Courtesy: Abidin, 2003).

The basic equation for the carrier phase measurement between receiver i and satellite k measured using the phase of carrier L1 is modeled as follows:

$$\Phi_i^k(t_i, t_k) = \rho_i^k(t_i, t_k) + (\delta t_k - \delta t_i)c + \lambda N_i^k - \delta_{ion} + \delta_{trop} + \delta_m + \varepsilon_i^k \quad (2.52)$$

Where Φ_i^k, λ, N carrier phase measurement in unit of metres, wavelength and phase ambiguity.

2.3.8 GNSS Positioning Methods

Based on the available measurements made on the GNSS signals, the determination of the receiver's position can be conveniently classified into two techniques, Single Point Positioning (SPP) or Absolute Positioning and Relative or Differential Positioning (Satirapod, 2002).

2.3.8.1 Single Point Positioning (SPP)

When GNSS observations made at only one particular station are used to independently derive the position coordinates of the point with respect to the reference frame WGS-84, the positioning technique is referred to as single point positioning (Afrifa, 2008). That is, one GNSS receiver simultaneously tracks four or more GNSS satellites to determine its own coordinates with respect

to the center of the reference frame WGS-84 (see figure 2.15). The accuracy of SPP is currently about 7 metres in the horizontal component and 12 metres in the vertical component (at the 95% confidence level) for civilian users (Satirapod, 2002). SPP technique can be divided into two classes depending on the measurements used, namely pseudorange-based point positioning and carrier phase-based point positioning.

2.3.8.1.1 Pseudorange-based point positioning

To determine the receiver's point position at any time, the satellite coordinates as well as a minimum of four ranges to four satellites is required (Ashtech Inc, 2001; Rabbany, 2002). The receiver gets the satellite coordinates through the navigation message, while the ranges are obtained from either the C/A-code or the P(Y)-code, depending on the receiver type (civilian or military) (Rabbany, 2002). As stated before, the measured pseudoranges are corrupted by both the satellite and receiver clock synchronization errors. Satellite clock correction terms in the

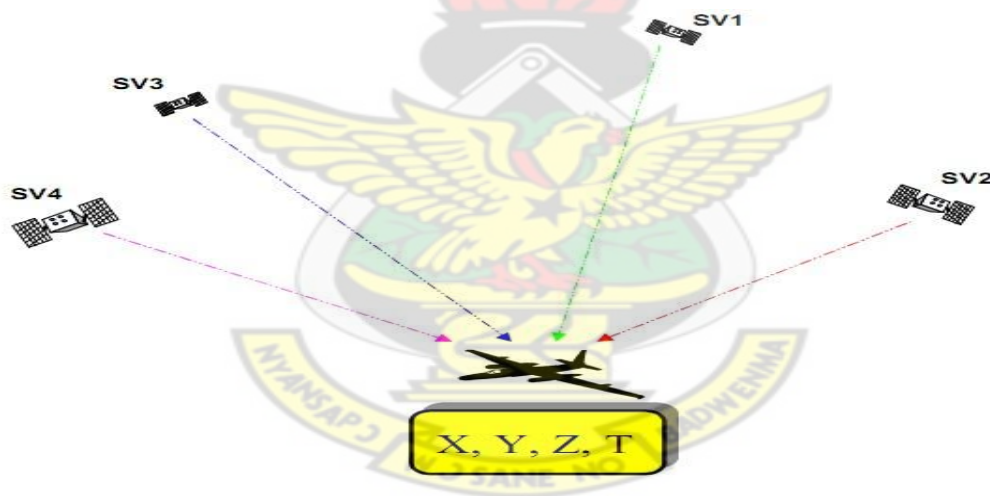


Figure 2.7: Principle of GNSS point positioning (Courtesy: Thao, 2007)

navigation message are used to correct the satellite clock errors. The receiver clock error is treated as an additional unknown parameter in the estimation process (Ashtech Inc, 2001). This brings the number of unknown parameters to four: three for the receiver coordinates and one for the receiver clock error. It should be noted that if more than four satellites are tracked, the so-called least-squares estimation or Kalman filtering technique is applied (Ashtech Inc, 2001, Rabbany, 2002). The basic principle of the single point positioning technique is to use simple resection by

distances or trilateration to determine the receiver's coordinates (Satirapod, 2002). The receiver position in the SPP mode is determined as follows (Calais, 2008):

The pseudorange measurements R_i^k from Eqn 3.5 and 3.6 can be modeled as:

$$R_i^k(t_i, t_k) = \rho_i^k(t_i, t_k) - (\delta t_i - \delta t_k)c + \delta_{ion} + \delta_{trop} + \delta_m + \varepsilon \quad (2.55)$$

Neglecting the propagation, multipath, and receiver errors

$$R_i^k(t_i, t_k) = \rho_i^k(t_i, t_k) - (\delta t_i - \delta t_k)c \quad (2.56)$$

The geometric distance between satellite k and receiver i from Eqn 3.7 is given by:

$$\rho_i^k(t_i, t_k) = \sqrt{(x^k - x_i)^2 + (y^k - y_i)^2 + (z^k - z_i)^2}$$

or

$$\rho_i^k(t_i, t_k) = f(x_i, y_i, z_i) \quad (2.57)$$

The Navigation message allows us to compute the satellite position (x^k, y^k, z^k) and the satellite clock bias δt_k . Therefore we are left with 4 unknowns, the receiver position

$$(x_i, y_i, z_i) \text{ and the receiver clock bias } \delta t_i \text{ i.e. the unknowns are } (x_i, y_i, z_i, \delta t_i)$$

Since the position of the user is not known, an estimate of the user position (x_0, y_0, z_0) is used to generate a set of estimated pseudoranges to each of the n satellites in view, where $n \geq 4$. The actual coordinates therefore equal the approximate coordinates plus a slight adjustment:

$$\begin{aligned} x_i &= x_0 + \Delta x_i \\ y_i &= y_0 + \Delta y_i \\ z_i &= z_0 + \Delta z_i \end{aligned} \quad (2.58)$$

With $\Delta x_i, \Delta y_i, \Delta z_i$ as new unknowns, we can write:

$$f(x_i, y_i, z_i) = f(x_0 + \Delta x_i, y_0 + \Delta y_i, z_0 + \Delta z_i) \quad (2.59)$$

Next, we apply Taylor's series, to expand about the model $f(x_0 + \Delta x_i, y_0 + \Delta y_i, z_0 + \Delta z_i)$ ignoring second and higher order terms.

$$f(x_i, y_i, z_i) = f(x_0, y_0, z_0) + \frac{\partial f(x_0, y_0, z_0)}{\partial x_0} \Delta x_i + \frac{\partial f(x_0, y_0, z_0)}{\partial y_0} \Delta y_i + \frac{\partial f(x_0, y_0, z_0)}{\partial z_0} \Delta z_i \quad (2.60)$$

Now Recall from Eq. (2.57)

$$f(x_0, y_0, z_0) = \sqrt{(x^k(t_k) - x_0)^2 + (y^k(t_k) - y_0)^2 + (z^k(t_k) - z_0)^2} = \rho_0^s(t_i, t_k) \quad (2.61)$$

Taking partial derivatives in Eq. (2.60)

$$\frac{\partial f(x_0, y_0, z_0)}{\partial x_0} = -\frac{x^k(t_k) - x_0}{\rho_{i0}^k(t_i, t_k)} \quad \frac{\partial f(x_0, y_0, z_0)}{\partial y_0} = -\frac{y^k(t_k) - y_0}{\rho_{i0}^k(t_i, t_k)} \quad \frac{\partial f(x_0, y_0, z_0)}{\partial z_0} = -\frac{z^k(t_k) - z_0}{\rho_{i0}^k(t_i, t_k)} \quad (2.62)$$

Now substituting Eq. (2.62) into Eq. (2.60) gives:

$$f(x_i, y_i, z_i) = f(x_0, y_0, z_0) - \frac{x^k(t_k) - x_0}{\rho_{i0}^k(t_i, t_k)} \Delta x_i - \frac{y^k(t_k) - y_0}{\rho_{i0}^k(t_i, t_k)} \Delta y_i - \frac{z^k(t_k) - z_0}{\rho_{i0}^k(t_i, t_k)} \Delta z_i \quad (2.63)$$

Rewrite Eq. (2.56) gives:

$$\begin{aligned} R_i^k(t_i, t_k) &= \rho_{i0}^k(t_i, t_k) - \frac{x^k(t_k) - x_0}{\rho_{i0}^k(t_i, t_k)} \Delta x_i - \frac{y^k(t_k) - y_0}{\rho_{i0}^k(t_i, t_k)} \Delta y_i - \frac{z^k(t_k) - z_0}{\rho_{i0}^k(t_i, t_k)} \Delta z_i - (\delta_i - \delta_k)c \\ &= \rho_{i0}^k(t_i, t_k) - \frac{x^k(t_k) - x_0}{\rho_{i0}^k(t_i, t_k)} \Delta x_i - \frac{y^k(t_k) - y_0}{\rho_{i0}^k(t_i, t_k)} \Delta y_i - \frac{z^k(t_k) - z_0}{\rho_{i0}^k(t_i, t_k)} \Delta z_i + c\delta_k - c\delta_i \end{aligned} \quad (2.63)$$

Rearranging Eq. (2.63) by separating the known and unknown terms of each side gives

$$\begin{aligned} R_i^k(t_i, t_k) - \rho_{i0}^k(t_i, t_k) - c\delta_k &= -\frac{x^k(t_k) - x_0}{\rho_{i0}^k(t_i, t_k)} \Delta x_i - \frac{y^k(t_k) - y_0}{\rho_{i0}^k(t_i, t_k)} \Delta y_i - \frac{z^k(t_k) - z_0}{\rho_{i0}^k(t_i, t_k)} \Delta z_i - c\delta_i \\ &= \frac{-1}{\rho_0^s(t_r, t_s)} \left((x^k(t_k) - x_0) (y^k(t_k) - y_0) (z^k(t_k) - z_0) \right) \begin{pmatrix} \Delta x_i \\ \Delta y_i \\ \Delta z_i \end{pmatrix} - c\delta_i \end{aligned} \quad (2.64)$$

Let

$$a_{xi}^k = -\frac{x^k(t_k) - x_0}{\rho_{i0}^k(t_i, t_k)} \quad a_{yi}^k = -\frac{y^k(t_k) - y_0}{\rho_{i0}^k(t_i, t_k)} \quad a_{zi}^k = -\frac{z^k(t_k) - z_0}{\rho_{i0}^k(t_i, t_k)} \Delta z_i \quad l^k = R_i^k(t_i, t_k) - \rho_{i0}^k(t_i, t_k) - c \delta t_k \quad (2.66)$$

$$\Rightarrow l^k = a_{xi}^k \Delta x_i + a_{yi}^k \Delta y_i + a_{zi}^k \Delta z_i$$

Where l^k is the so-called O – C (observed minus computed pseudorange)

For n number of satellites visible simultaneously where $n \geq 4$

$$A = \begin{bmatrix} a_{xi}^1 & a_{yi}^1 & a_{zi}^1 & -c \\ a_{xi}^2 & a_{yi}^2 & a_{zi}^2 & -c \\ a_{xi}^3 & a_{yi}^3 & a_{zi}^3 & -c \\ \vdots & \vdots & \vdots & \vdots \\ a_{xi}^n & a_{yi}^n & a_{zi}^n & -c \end{bmatrix}, \quad X = \begin{bmatrix} \Delta x_i \\ \Delta y_i \\ \Delta z_i \\ \delta t_i \end{bmatrix}, \quad L = \begin{bmatrix} l^1 \\ l^2 \\ l^3 \\ \vdots \\ l^n \end{bmatrix} \quad (2.67)$$

where

A = matrix of linear function of the unknowns (= design matrix)

L = matrix of absolute terms

X = vector of unknowns

The general least squares solution equation is often written using matrix symbols as:

$$L = Ax + v \quad (2.73)$$

The least squares solution to Eq. (2.72) is:

$$(A^T A)X = A^T L \quad (2.74)$$

Eq. (2.73) is called the system of “normal equations”. The solution to the normal equations is therefore:

$$X = (A^T A)^{-1} A^T L \quad (2.75)$$

$$X = (A^T P A)^{-1} A^T P L \quad (2.76)$$

P is the weight matrix, defined by:

$$P = \frac{1}{\sigma_0^2} \sum_L^{-1} \quad (2.78)$$

σ_0^2 = a priori variance
 Σ_L = covariance matrix of the observations.

Error Computation: By the law of propagation covariance, the covariance matrix for the estimated or unknown parameters can be written in terms of its components as:

$$C_x = \sigma^2 (A^T \Sigma_L^{-1} A)^{-1} \quad (2.79)$$

In the case of pseudoranges, the observations are independent and have equal variance σ_0^2 . Therefore Σ_L is the diagonal matrix:

$$\Sigma_L = \sigma_0^2 I \quad (2.80)$$

Where I = identity matrix.

$$\Rightarrow C_x = \sigma^2 (A^T A)^{-1}$$

The associated covariance matrix of the unknowns C_x is:

$$C_x = \sigma^2 (A^T A)^{-1} = \sigma^2 \begin{bmatrix} \sigma_x^2 & \sigma_{xy} & \sigma_{xz} & \sigma_{x\tau} \\ \sigma_{yx} & \sigma_y^2 & \sigma_{yz} & \sigma_{y\tau} \\ \sigma_{zx} & \sigma_{zy} & \sigma_z^2 & \sigma_{z\tau} \\ \sigma_{\tau x} & \sigma_{\tau y} & \sigma_{\tau z} & \sigma_\tau^2 \end{bmatrix} \quad (2.81)$$

C_x can be transformed from an ECEF frame to a local Topocentric frame using the law of propagation variances by:

$$C_T = R C_x R^T = \begin{bmatrix} \sigma_n^2 & \sigma_{ne} & \sigma_{nu} \\ \sigma_{en} & \sigma_e^2 & \sigma_{eu} \\ \sigma_{un} & \sigma_{ue} & \sigma_u^2 \end{bmatrix} \quad (2.82)$$

Where R is the rotation matrix given by:

$$R = \begin{bmatrix} -\sin \varphi \cos \lambda & -\sin \varphi \sin \lambda & \cos \varphi \\ -\sin \lambda & \cos \lambda & 0 \\ \cos \varphi \cos \lambda & \cos \varphi \sin \lambda & \sin \varphi \end{bmatrix} \quad (2.83)$$

Dilution of Precision: The various types of “dilution of precision” (DOP) can now be defined as a function of diagonal elements of the covariance matrix in the local Topocentric system:

$$\begin{aligned} VDOP &= \sigma_u \\ HDOP &= \sqrt{\sigma_n^2 + \sigma_e^2} \\ PDOP &= \sqrt{\sigma_n^2 + \sigma_e^2 + \sigma_u^2} = \sqrt{\sigma_x^2 + \sigma_y^2 + \sigma_z^2} \\ TDOP &= \sigma_\tau \\ GDOP &= \sqrt{\sigma_n^2 + \sigma_e^2 + \sigma_u^2 + \sigma_\tau^2} \end{aligned} \quad (2.84)$$

Where, for example, *VDOP* stands for “vertical dilution of precision,” H stands for horizontal, P for position, T for time, and G for geometric.

The distribution of satellites above the observer’s horizon has a direct effect on the accuracy of the position determination. A low DOP factor is good, a high DOP factor is bad. When satellites are in optimal configuration for a reliable GPS position, the DOP value is low; when they are not, the DOP value is high. If all satellites used for 3-dimensional positioning are crowded together in one part of the sky, the DOP will be high. Visible satellites, widely and evenly spaced in the sky, indicate good geometry and, therefore, low DOP. Table 2.8 summarizes DOP values. (Sickle, 2001).

Table 2.8: DOP values

Quality	Very Good	Good	Fair	Suspect/Bad
DOP	1-2	2-4	4-5	>5

Satellite Clock Correction

Single point positioning estimates only receiver clock errors, and requires a correction for the satellite clock error since this is needed to be able to compute the corrected pseudorange measurement. The corrected pseudorange is given by:

$$\rho_{corrected} = \rho + c\Delta t_{sv} \quad (2.85)$$

Where

$$\begin{aligned} \rho_{corrected} &= \text{pseudorange corrected for SVclock error} \\ \rho &= \text{raw pseudorange measurement} \\ \Delta t_{sv} &= \text{SV clock correction} = a_{f0} + a_{f1}(t - t_0) + a_{f2}(t - t_0)^2 + \Delta t_r \\ a_{f0}, a_{f1}, a_{f2}, t_0 &= \text{SV clock correction parameters from navigation message} \\ \Delta t_r &= \text{relativity correction} = Fe\sqrt{a} \sin(E_k) \\ F &= \text{const} \tan t = -4.442807633 \times 10^{-10} \text{ sec}/(\text{meter})^{1/2} \\ e &= \text{eccentricity from navigation message} \\ \sqrt{a} &= \text{square root of semi-major axis from navigation message} \\ E_k &= \text{Eccentricity anomaly (from SV position calculation)} \end{aligned}$$

2.3.8.1.2 Carrier Phase-based Point Positioning

GPS carrier phase can be modeled as (Xu, 2007):

$$\lambda\Phi_r^s(t_r, t_s) = \rho_r^s(t_r, t_s) - (\delta t_r - \delta t_s)c + \lambda N_r^s - \delta_{ion} + \delta_{trop} + \varepsilon \quad (2.86)$$

Where $\lambda\Phi$ is the observed phase in length, Φ is the phase in cycle, wave length is denoted as λ , and N_r^s is the ambiguity related to receiver r and satellite s, except for the ambiguity term and the sign difference of the term of ionospheric effect; other terms are the same as that of the pseudorange discussed. The computed value (denoted as C) of phase is given by:

$$C = \rho_r^s(t_r, t_s) + \delta t_s c + \lambda N_{r0}^s - \delta_{ion} + \delta_{trop} \quad (2.87)$$

Where N_{r0}^s is the initial ambiguity parameter related to the receiver r and satellite s. Scaling the ambiguity parameter in length and denoting

$$\Delta N_r^s = \lambda N_r^s - \lambda N_{r0}^s \quad (2.88)$$

The phase single point positioning equation is:

$$R_r^s(t_r, t_s) - \rho_0^s(t_r, t_s) - c\delta t_s = \frac{-1}{\rho_0^s(t_r, t_s)} \left((x_s(t_s) - x_0) \quad (y_s(t_s) - y_0) \quad (z_s(t_s) - z_0) \right) \begin{pmatrix} \Delta x_r \\ \Delta y_r \\ \Delta z_r \end{pmatrix} + \Delta N_r^s + v_s \quad (2.89)$$

$$\Rightarrow l^s = \frac{-1}{\rho_0^s(t_r, t_s)} \left((x_s(t_s) - x_0) \quad (y_s(t_s) - y_0) \quad (z_s(t_s) - z_0) \right) \begin{pmatrix} \Delta x_r \\ \Delta y_r \\ \Delta z_r \end{pmatrix} + \Delta N_r^s + v_s \quad (2.90)$$

Where

$$l^s = R_r^s(t_r, t_s) - \rho_0^s(t_r, t_s) - c\delta t_s$$

Putting all equations related to all observed satellites together, the single point positioning equation system has a general form of (Xu, 2007):

$$L = AX + EN + V, P \quad (2.91)$$

where L is called the observation vector, X is the unknown vector of coordinates and clock error, A is the X related coefficient matrix, E is an identity matrix of order S, S is the number of observed satellites, N is the unknown vector of ambiguity parameters ΔN_r^s , V is the residual vector, and P is the weight matrix. If S satellites are observed, then there are K ambiguity parameters, three coordinate parameters and one clock parameter.

2.3.8.2 Relative or Differential Position

The relative positioning technique, sometimes also called the differential positioning technique, requires the use of two receivers, one as a *reference station* and the other one as a *user station*, in order to determine the coordinates of the user with respect to the reference station. This technique is very effective if the measurements are simultaneously made at both receivers. Many biases (e.g. satellite orbit bias, satellite clock bias, ionospheric and tropospheric delays) can be largely reduced by forming the difference between the measurements made at both stations (Satirapod, 2002). The effectiveness of the relative positioning technique is largely dependent on the distance between the two receivers. If the distance between the receivers becomes large, the residual errors will become larger and consequently, the positioning results become degraded.

2.3.8.2.1 Single Difference Observables

Single difference (SD) is the difference formed by data observed at two stations on the same satellite as:

$$SD_{AB}^j(O) = O_A^j - O_B^j, \quad (2.92)$$

Where O is the original observable, and A and B are two id number of the stations.

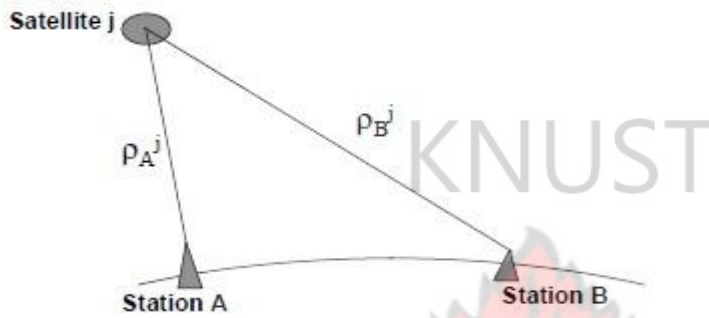


Figure 2.8: Single differencing geometry

Figure 2.8 shows the possible pseudorange measurements between two receivers (A, B) and the satellite j. If the pseudoranges from Figure 2.8 are differenced, then the satellite clock bias and satellite orbit errors will be removed. Any atmospheric errors will also be eliminated or reduced significantly with single differencing. Considering Eqs. (1 & 32), the basic mathematical model for single difference pseudorange and phase observations between A and B respectively are as follows (Xu, 2007):

$$\begin{aligned} SD_{A,B}^j(R(i)) &= \rho_B^j - \rho_A^j - c\delta t_A + c\delta t_B + d\delta_{ion}(i) + d\delta_{trop} + d\varepsilon_C \\ &= \Delta\rho_{AB}^j + c\Delta\delta t_{AB} + d\delta_{ion}(i) + d\delta_{trop} + d\varepsilon \end{aligned} \quad (2.93)$$

$$\begin{aligned} SD_{A,B}^j(\Phi(i)) &= \rho_B^j - \rho_A^j - c\delta t_B + c\delta t_A + \lambda_i N_B^j(i) - \lambda_i N_A^j(i) - d\delta_{ion}(i) + d\delta_{trop} + d\varepsilon_P \\ &= \Delta\rho_{AB}^j + c\Delta\delta t_{AB} + \lambda_i \Delta N_{AB}^j(i) - d\delta_{ion}(i) + d\delta_{trop} + d\varepsilon_P \end{aligned} \quad (2.94)$$

Where i ($i = 1, 2, 5$) is the index of frequency f , $d\delta_{ion}(i)$ and $d\delta_{trop}$ are the differenced ionospheric and tropospheric effects at the two stations related to the satellite j , respectively.

2.3.8.2.2 Double Difference Observables

Double differences are formed between two single differences related to two observed satellites as

$$DD_{AB}^{j,k}(O) = SD_{A,B}^k(O) - SD_{A,B}^j(O) \quad (2.95)$$

Where j and k are the two id numbers of the satellites.

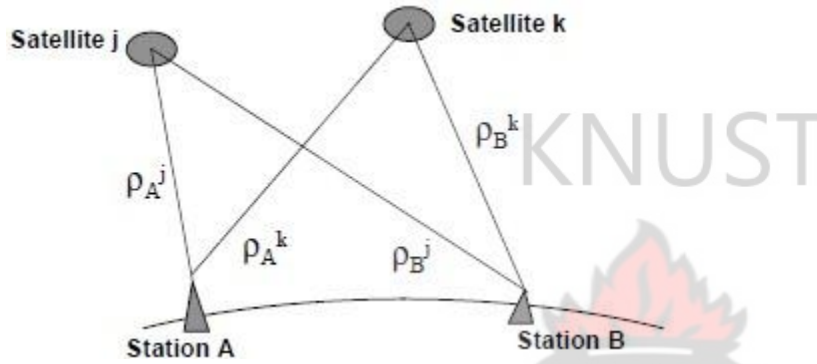


Figure 2.9: Double differencing geometry.

Again, considering Eqs. (1,32,39 & 40), the basic mathematical model for double difference pseudorange and phase observations between A and B respectively are as follows (Xu, 2007):

$$\begin{aligned} DD_{A,B}^{j,k}(R(i)) &= \rho_B^k - \rho_A^k - \rho_B^j + \rho_A^j + dd\delta_{ion}(i) + dd\delta_{trop} + dd\varepsilon_C \\ &= \Delta\rho_{AB}^{j,k} + dd\delta_{ion}(i) + dd\delta_{trop} + dd\varepsilon_C \end{aligned} \quad (2.96)$$

$$\begin{aligned} DD_{A,B}^{j,k}(\Phi(i)) &= \rho_B^k - \rho_A^k - \rho_B^j + \rho_A^j + \lambda_i(N_B^k(i) - N_A^k(i) - N_B^j(i) + N_A^j(i)) - dd\delta_{ion}(i) + dd\delta_{trop} + dd\varepsilon_p \\ &= \Delta\rho_{AB}^{j,k} + \lambda_i(\Delta N_{AB}^{j,k}(i)) - dd\delta_{ion}(i) + dd\delta_{trop} + dd\varepsilon_p \end{aligned} \quad (2.97)$$

Where $dd\delta_{ion}(i)$ and $dd\delta_{trop}$ are the differenced ionospheric and tropospheric effects at the two stations related to the two satellites, respectively. The advantage of the double differences is that receivers' clock offsets are completely eliminated. Ionospheric and tropospheric effects are also reduced greatly through difference forming, especially for those stations that are not very far away from each other (Xu, 2007). This method also allows to optimally exploit the integer nature of carrier phase ambiguity (Hamid, 2000).

2.3.8.2.3 Pseudorange Differential Corrections

To be able to determine the user receiver (B) position accurately with respect to the, the position of the reference station (A) in ECEF coordinates must be accurately known (Kaplan et al, 2006). Given that the position of the i^{th} satellite is (x_i, y_i, z_i) and the position of the reference station is known through a survey to be at position (x_A, y_A, z_A) , the computed geometric distance, ρ_A^i from the reference station to the satellite is (Kaplan et al, 2006):

$$\rho_A^i = \sqrt{(x_i - x_A)^2 + (y_i - y_A)^2 + (z_i - z_A)^2} \quad (2.971)$$

The reference receiver is then able to generate a pseudorange measurement to the i^{th} satellite as

$$R_A^i = \rho_A^i + c\delta t_A + \varepsilon_A \quad (2.972)$$

Where ε_A are the pseudorange errors and $c\delta t_A$ represents the reference station clock offset from GPS time. The reference receiver simply resolves the difference between the generated pseudorange to the i^{th} satellite, R_A^i and its geometric range, ρ_A^i , to create the differential correction

$$\Delta R_A^i = \rho_A^i - R_A^i = -c\delta t_A - \varepsilon_A \quad (2.973)$$

This correction is broadcast to the user receiver, where it is added to the user receiver's pseudorange measurement to the same satellite

$$R_B^i + \Delta R_A^i = \rho_B^i + c\delta t_B + \varepsilon_B + (-c\delta t_A - \varepsilon_A) \quad (2.974)$$

If the user's receiver is located relatively nearby the reference receiver, the user's receiver pseudorange equation error components will be nearly identical to those of the reference receiver with the exception of errors that are not common to both receivers, i.e. multipath and receiver noise. Therefore, the corrected user pseudorange can be expressed as

$$R_{B,corrected}^i = \rho_B^i + \varepsilon_{BA} + c\delta t_{BA} \quad (2.975)$$

Where $\varepsilon_{BA} = \varepsilon_B - \varepsilon_A$ represents residual pseudorange errors and δt_{BA} is the difference in user and reference station clock offsets, $\delta t_B - \delta t_A$.

In Cartesian coordinates (8.6) becomes

$$R_{B,corrected}^i = \sqrt{(x_i - x_B)^2 + (y_i - y_B)^2 + (z_i - z_B)^2} + \varepsilon_{BA} + c\delta_{BA} \quad (2.976)$$

Because pseudorange errors vary with time, the transmitted pseudorange correction,

$$\Delta R_A^i(t_A) = \rho_A^i(t_A) - R_A^i(t_A) \quad (2.977)$$

Which is an estimate of the pseudorange error with the sign inverted, is most accurate at the instant of time t_A , for which the correction was calculated. To facilitate the user receiver to compensate for pseudorange error rate, the station may also transmit a pseudorange rate correction, $\Delta \dot{R}_A^i(t_A)$. The user receiver then adjusts the pseudorange correction to correspond to the time of its own pseudorange measurement, t , as follows:

$$\Delta R_A^i(t) = \Delta R_A^i(t_A) + \Delta \dot{R}_A^i(t_A)(t - t_A) \quad (2.978)$$

The corrected user receiver pseudorange, $R_{B,corrected}^i(t)$ for time t is then calculated from

$$R_{B,corrected}^i(t) = R_B^i(t) + \Delta R_A^i(t) \quad (2.979)$$

2.4 Coordinate Systems

Within the GNSS calculations, the position of a point in space can be expressed in different coordinate system for suiting different types of GNSS calculations. Within the context of this project, three types of coordinate systems are considered. Namely the World Geodetic System 1984 (WGS 84), Earth-Centered-Earth-Fixed (ECEF) Cartesian and ECEF Geographical systems. These three main coordinate systems are described in detail in the following sub-sections. Coordinate conversions, datum transformations and map projections are also considered briefly in this section.

2.4.1 World Geodetic System 1984 (WGS 84)

The WGS 84 Coordinate System is a Conventional Terrestrial Reference System (CTRS) or an earth-fixed Cartesian coordinate system. The definitions of this coordinate system are as follows (McCarthy, 1996):

- It is geocentric, the center of mass being defined for the whole Earth including oceans and atmosphere.
 - Its scale is that of the local Earth frame, in the meaning of a relativistic theory of gravitation.
 - Its orientation was initially given by the Bureau International de l'Heure (BIH) orientation of 1984.0.
 - Its time evolution in orientation will create no residual global rotation with regard to the crust.
- The WGS 84 Coordinate System is a three-dimensional Cartesian right-handed, Earth-fixed orthogonal coordinate system, and is graphically depicted in Figure 2.10 with:
- Its origin at the earth's centre of mass, the geocentre (for two reasons: the geocentre is the physical point about which the satellite orbits; and it is preferable to any local geodetic datum).
 - Its Z-axis is aligned parallel to the direction of the Conventional Terrestrial Pole (CTP) for polar motion, as originally defined by the Bureau International de l'Heure (BIH), and since 1989 by the International Earth Rotation Service (IERS).
 - Its X-axis is the intersection of the WGS84 Reference Meridian Plane and the plane of the CTP Equator (the Reference Meridian being parallel to the Zero Meridian defined by BIH/IERS).
 - Its Y-axis completes a right-handed, earth-centred, earth-fixed (ECEF) orthogonal coordinate system, measured in the plane of the CTP Equator, 90 east of the x-axis.

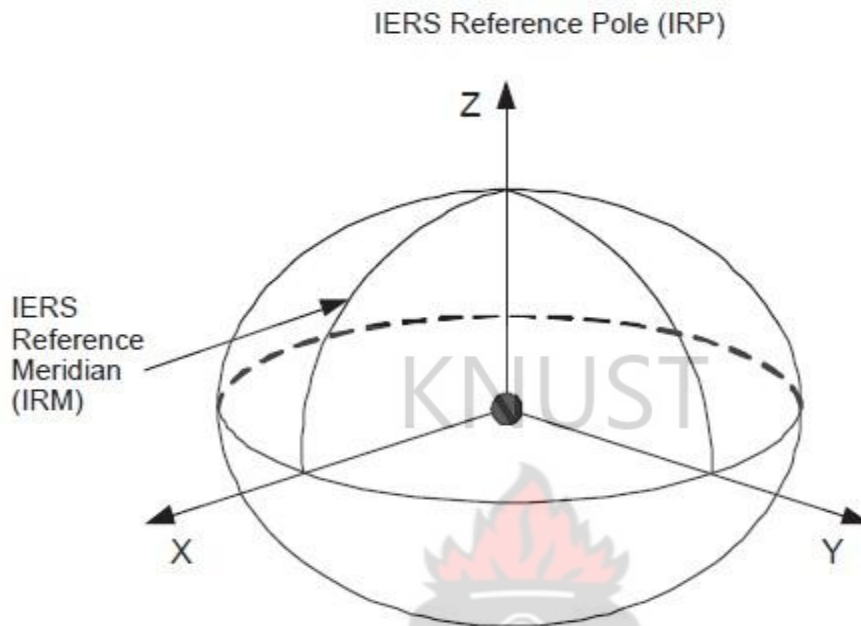


Figure 2.10: The WGS 84 Coordinate System Definition

The four defining parameters of the WGS84 ellipsoid with specified standard deviations are (Borre et al, 1997):

- Semi-major axis (a) = 6378137m ($\sigma_a = 2$ m).
- Ellipsoid flattening (f) = 1/298.257223563 (derived from the value of the normalised second degree zonal harmonic coefficient of the gravitational field: $-484.16685 \times 10^{-6}$).
- The Earth's rotational rate or Angular velocity of the earth (ω_e) :

$$\omega_e = 7292115.1467 \times 10^{-11} \text{ rad/sec}; \sigma_{\omega_e} = 15 \times 10^{-11} \text{ rad/s}$$

The Speed of Light in vacuum c

$$c = 299792458 \text{ m/s}; \sigma_c = 1.2 \text{ m/s}.$$

- The Earth's gravitational constant (including the mass of the Earth's atmosphere) (GM) = $3986005 \times 10^8 \text{ m}^3/\text{sec}^2$ ($\sigma_{GM} = 0.6 \times 10^8 \text{ m}^3/\text{s}^3$).

In order to maintain consistency with GPS calculations within this project, it is re-emphasized that only WGS 84 parameters are used. The WGS 84 Coordinate System origin also serves as the geometric center of the WGS 84 Ellipsoid and the Z-axis serves as the rotational axis of this ellipsoid.

2.4.2 ECEF Cartesian Coordinate System

For the purpose of computing the position of a GPS receiver, it is more convenient to use a coordinate system that rotates with the Earth, known as an Earth-Centered Earth-Fixed (ECEF) system. In such a coordinate system, it is easier to compute the latitude, longitude, and height parameters that the receiver displays (Kaplan et al, 2006).

The ECEF coordinate system is defined by three right-handed orthogonal Cartesian system (x, y, z). the Earth spinning axis 'z-axis', the axis that cuts both the equatorial plane and Greenwich Meridian 'x-axis', and the axis that is perpendicular to the other two axes 'y-axis' (Chan, 2008). The position of a point (which can be either satellite or receiver) in ECEF Cartesian coordinate system is expressed as follow (Chan, 2008):

$$X_{ECEF} = [x_{ECEF} \quad y_{ECEF} \quad z_{ECEF}]^T$$

2.4.2 ECEF Geographical Coordinate System

The ECEF coordinate system can also be represented by an ellipsoidal or geodetic coordinate system. It is defined in terms of Latitude ' ϕ ', Longitude ' λ ' and Ellipsoidal Height ' h ' (perpendicular to ellipsoidal surface). The position of a point (which can be either satellite or receiver) in ECEF Geographical coordinate system is expressed as follow (Chan, 2008):

$$X_{ECEF,geo} = [\phi \quad \lambda \quad h]^T$$

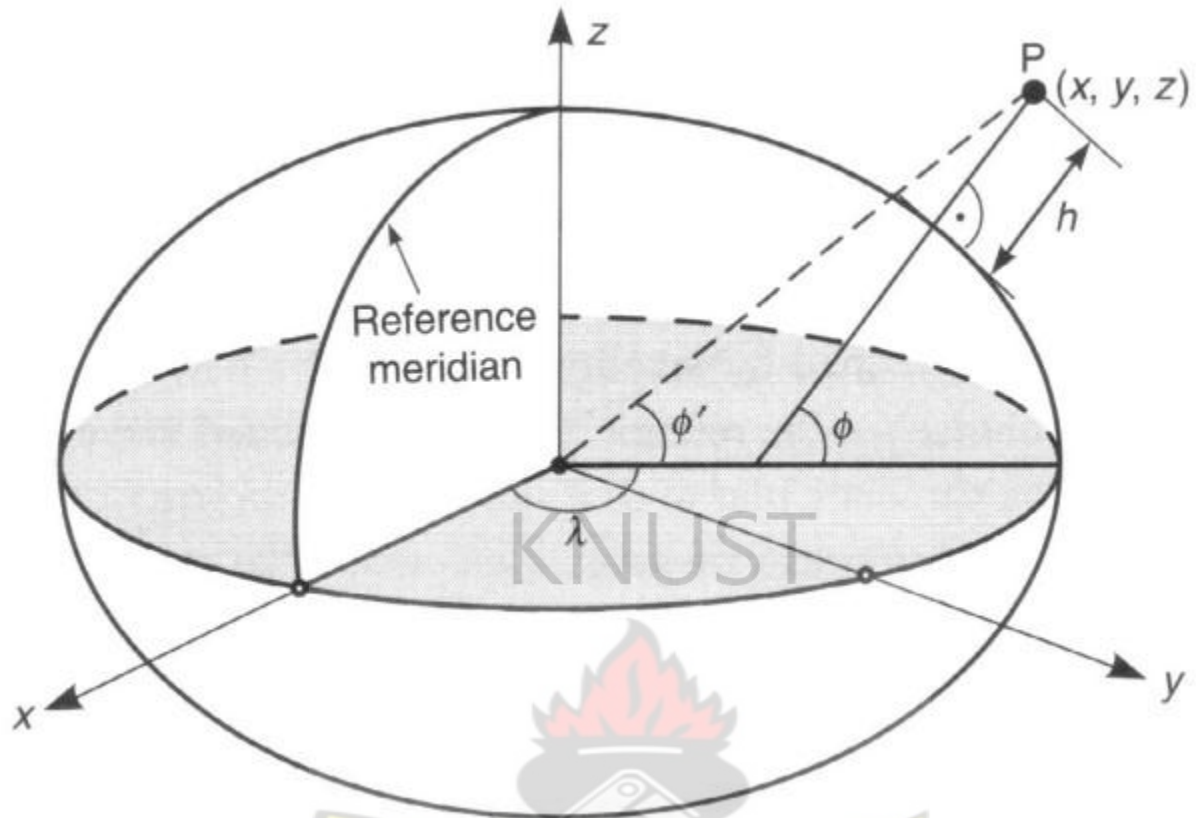


Figure 2.11: ECEF coordinate system

2.4.4 Coordinate Conversion

Cartesian and Geodetic coordinates can be converted from one representation to the other. Details of the conversions are given below.

2.4.4.1 ECEF Cartesian coordinates to Geodetic coordinates

For GNSS applications, the conversion of Cartesian coordinates to geodetic coordinates is more important since the Cartesian coordinates are given and the geodetic coordinates sought. Thus, given a user receiver's position (X, Y, Z) in the ECEF system, we can compute the geodetic coordinates (ϕ, λ, h) from the Cartesian coordinates (X, Y, Z) (Hofmann-Wellenhof et al, 2008; Kaplan et al, 2006). The non-iterative reverse transformation from Cartesian coordinates (X, Y, Z) to geodetic coordinates (ϕ, λ, h) is used given by Bowring (1985), (Ayer and Fosu, 2008) as:

$$\varphi = \tan^{-1}\left(\frac{Z + e'^2 b \sin^3 \theta}{p - e^2 a \cos^3 \theta}\right); \quad \lambda = \tan^{-1}\left(\frac{Y}{X}\right); \quad h = \frac{P}{\cos \varphi} - N(\varphi) \quad (2.980)$$

Where

$$p = \sqrt{X^2 + Y^2} \quad ; \quad \theta = \tan^{-1}\left(\frac{Za}{pb}\right); \quad e'^2 = \frac{a^2 - b^2}{b^2} \quad (2.981)$$

$$f = \frac{a - b}{a} = \textit{flattening} \quad ; \quad e^2 = 2f - f^2 = \textit{eccentricity squared} \quad (2.982)$$

a = semi – major axis

b = semi – minor axis

θ = parametric latitude

e^2 = the second eccentricity squared

KNUST

2.4.4.2 Geodetic coordinates to ECEF Cartesian coordinates

Given the ellipsoidal coordinates (φ, λ, h) of a point, the point can also be expressed by the ECEF Cartesian (XYZ) coordinates. The forward transformation from geodetic coordinates (φ, λ, h) to an ECEF Cartesian coordinates (X,Y,Z) is given in Seeber (2003: p. 44) as:

$$X = (N + h) \cos \varphi \cos \lambda \quad (2.983)$$

$$Y = (N + h) \cos \varphi \sin \lambda \quad (2.984)$$

$$Z = [N(1 - e^2) + h] \sin \varphi \quad (2.985)$$

Where

$$N(\varphi) = \frac{a}{\sqrt{1 - e^2 \sin^2 \varphi}}, \quad (2.972)$$

N = radius of curvature in the prime vertical

2.4.5 Datum Transformations

A datum transformation transforms one coordinate system of a certain type to another coordinate system of the same type (Hofmann-Wellenhof et al, 2008).

To convert a coordinate from one datum to another, a mathematical process known as transformation is used. The transformation is often viewed from a vector perspective.

The coordinates are transformed from Cartesian ECEF XYZ values of one datum to another. If latitude, longitude and height (Φ, λ, h) are given or needed, the conversion to ECEF are done

before the vector mathematics and then the new coordinates are converted back to latitude, longitude and height (Clynch, 2006). See figure 2.12.

The following coordinate transformation methods or parameters are considered in this study.

- Three parameter transformation - $(\Delta X, \Delta Y, \Delta Z)$
- Five parameter transformation (Abridged Molodensky) - $(\Delta X, \Delta Y, \Delta Z, \Delta a, \Delta f)$
- Seven parameter transformation (Bursa-Wolf) - $(\Delta X, \Delta Y, \Delta Z, R_x, R_y, R_z, S)$
- Ten parameter transformation $(\Delta X, \Delta Y, \Delta Z, R_x, R_y, R_z, S, X_0, Y_0, Z_0)$

Figure 2.12 summarises the various ways of performing datum transformation from one datum (A) to another datum (B).

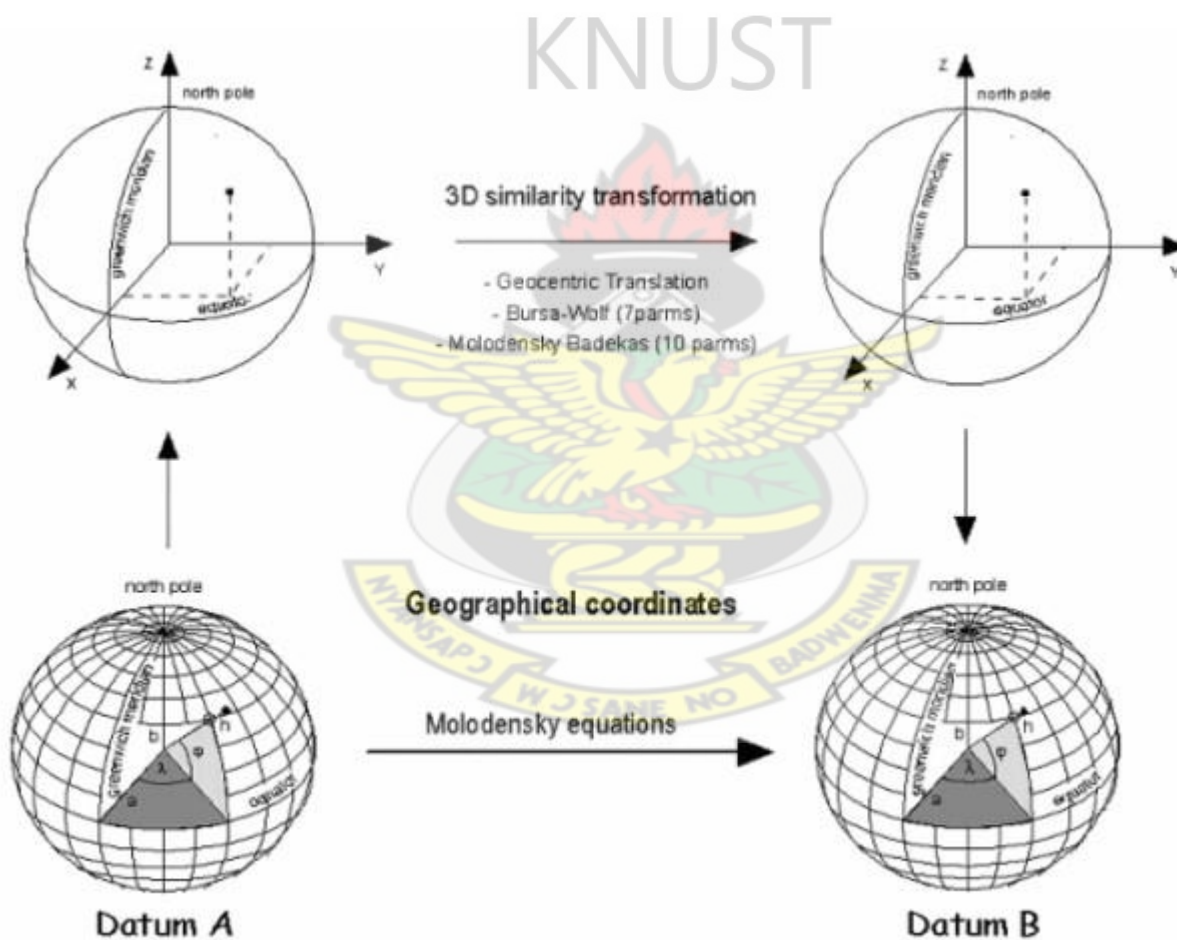


Figure 2.12: Datum Transformations (Courtesy: Ayer et al, 2008)

The application of any of these transformation models to the Cartesian coordinates of one datum (X_1, Y_1, Z_1) will always yield a new Cartesian coordinate of the other datum (X_2, Y_2, Z_2) . So depending on the level of accuracy to achieve or purpose of transformation, a particular

transformation model is applied or chosen. See (Badekas, 1969; Bursa (1962), Wolf (1963); Molodensky *et al.*, 1960 etc) for more details on the various transformation models.

Where (from above):

$\Delta X, \Delta Y, \Delta Z$ = Shifts along the x-axis, y-axis and z-axis respectively

$\Delta a, \Delta f$ = difference between the ellipsoid parameters in each system

R_X, R_Y and R_Z are the rotation parameters, ΔS is the scale factor.

X_0, Y_0, Z_0 = the average local positions of the common points or coordinates of the centroids of the Network.

Table 2.9: The published transformation parameters of Ghana

SURVEY OF GHANA

PUBLIC ANNOUNCEMENT

Geodetic Datum Transformation Parameters (Local WGS 84) And WGS 84 (UTM) Coordinates

The General Public is hereby informed that the SURVEY OF GHANA has adopted the WGS 84 (UTM - ZONE 30) Co-ordinates as from *January 2nd, 2009.*

All Land Surveyors (Official and Licensed), other Professionals and the General Public are to take note that **within the Golden Triangle*** (with vertices at Accra, Takoradi and Kumasi);

a) *All Plans (Cadastral or Approved Certified) are to be in the WGS 84 (UTM) Coordinates.*
 b) *All Maps prepared are to be in the WGS 84 (UTM) Coordinates.*

For ease of conversion from the War Office to the WGS 84 and vice versa, the following Transformation Parameters are to be used as Provisional:

Local Datum Name	Geodetic Code	Pub. Date	Transformation Parameters										Region of Use
			ΔX	ΔY	ΔZ	Rx (Rads)	Ry (Rads)	Rz (Rads)	S	X ₀	Y ₀	Z ₀	
Ghana	GHA	2008	-196.557	33.385	322.452	1.786E-7	-3.872E-8	-5.767E-8	0.9999940	6339239.290	-120750.511	686012.361	Golden Triangle Ghana
Ghana	GHA	2008	-158.635	32.174	326.783	1.786E-7	-3.872E-8	-5.767E-8	0.9999924	0	0	0	Ghana
Ghana	GHA	2008	-196.580	33.383	322.552	0	0	0	1	0	0	0	Ghana

Table 1. Transformation Parameters (War Office to WGS 84)

Reference ellipsoid		
Name	a	f
Ghana National	6378299.996	296

Table 2. Reference ellipsoid

N/B.
All enquiries should be directed to the Ag. Director of Surveys or the Regional Surveyors (in the various Regions) for prompt attention and assistance.

*List of specific Towns in the Golden Triangle is available for reference.

SGD,
Ag. Director of Surveys

CONTACTS:
 1. Telephone: 0023321 777101 / 0023321 782752/4
 Fax: 0023321765687
 Email: survey@ghana.com
 Box: CT 903 Cantonments, Accra
 2. Survey Department Offices in the Regional Capitals

09-Apr-10 06:14

2.4.6 Projected Coordinates

Normally, when carrying out GNSS surveys, the position of a point on the Earth's surface is described by the ellipsoidal coordinates of latitude and longitude (based on a reference ellipsoid) as well height (based on an ellipsoid or geoid) (see Figure 2.11). (Zogg, 2002). In surveying operations, plane rectangular or grid coordinates are needed to produce a two-dimensional surface of a map. The objective is to map a point (ϕ, λ) on the ellipsoid into a point (x, y) in a plane. (Hofmann-Wellenhof et al, 2008). Map coordinates use a 2D Cartesian system in which the two axes are known as northings and eastings. They are computed from the ellipsoidal latitude and longitude by a standard formula known as a map projection. (Ayer and Fosu, 2008). The map projection used in Ghana is the Transverse Mercator projection (TM) and that which is used worldwide, especially by the GPS system is the Universal Transverse Mercator (UTM) projection. Below in table 2.10 are the TM and UTM projection parameters on the War Office and the WGS84 ellipsoids respectively. The projection formulae for the two projections are given in appendix A

Table 2 10: Projection Parameters

<i>ELLIPSOID : WAR OFFICE</i>	<i>ELLIPSOID : WGS 84</i>
<i>PARAMETERS</i>	<i>PARAMETERS</i>
$a = 6378299.996m$ <i>Semi- major axis</i>	$a = 6378137.0m$ <i>Semi- major axis</i>
$f = 1/296$ <i>flattening</i>	$f = 1/298.257223563$ <i>flattening</i>
<i>PROJECTION PARAMETERS</i>	<i>PROJECTION PARAMETERS</i>
$\varphi_0 = [4^\circ 40']$ <i>Latitude of origin</i>	$\varphi_0 = 0$ <i>Latitude of origin</i>
$\lambda_0 = 1^\circ w$ <i>Longitude of origin</i>	$\lambda_0 = 3^\circ w$ <i>Longitude of origin</i>
$k_0 = 0.99975$ <i>scale factor</i>	$k_0 = 0.99960$ <i>scale factor</i>
$N_0 = 0.0000$ <i>false Northing</i>	$N_0 = 0.000m$ <i>false Northing</i>
$E_0 = 900000ft$ <i>false Easting</i>	$E_0 = 500000m$ <i>false Easting</i>

CHAPTER THREE - GNSS TECHNIQUE AND ALGORITHM

This Chapter presents the various algorithm, procedures and steps for computing GPS time (GPS week and seconds of week), Calculation of Satellite Position in ECEF Systems, Calculation of Receiver Position ECEF Systems, Baseline Estimation and Separation of Ambiguities, Datum Transformation of receiver position from WGS84 to War Office and vice versa and how they are executed in the Matlab programming environment.

3.1 Material

The material used in this chapter is MATLAB software.

3.2 Converting Universal Time to GPS Time

The GPS message contains information that allows a receiver to convert GPS Time into Universal Time Coordinated (UTC). To convert from Universal Time to GPS Time, the following procedure by (Hofmann-Wellenhof et al, 2008) is used. First, convert Universal Time (in Year, Month, Day, Hour, Minute, Second) into decimal hour:

$$UTC_{(dec)} = hour + \left(\frac{\text{min } ute}{60} \right) + \left(\frac{\text{sec } ond}{3600} \right) \quad (3.10)$$

Define Julian Day, JD, which is the number of days counting from 4713 B.C., January, day 1, 12:00:00. This can be computed as follow, with conditions defined in (4.3):

$$JD = \text{floor}(365.25K_y) + \text{floor}(30.6001(K_m + 1)) + \text{day} + \left(\frac{UTC_{(dec)}}{24} \right) + 1720981.5 \quad (3.11)$$

If $\text{month} \leq 2$ then $K_y = \text{year}$; $K_m = \text{month}$

If $\text{month} > 2$ then $K_y = \text{year} - 1$; $K_m = \text{month} + 12$

Where ‘floor’ is a MATLAB function in rounding down numbers. Define the coefficients K_a , K_b , K_c , K_e , K_f and K_d as follows:

$$K_a = \text{floor}(JD + 0.5) ; K_b = \text{floor}(K_a + 1537) ; K_c = \text{floor}\left(\frac{K_b - 122.1}{365.25}\right) \quad (3.12)$$

$$K_e = \text{floor}(365.25K_c) \quad ; \quad K_f = \text{floor}\left(\frac{K_b - K_e}{30.6001}\right) \quad (3.13)$$

$$K_d = \text{floor}(K_b - K_e - \text{floor}(30.6001K_f) + \text{rem}(JD + 0.5, 1)) \quad (3.14)$$

Where 'rem' is a MATLAB function that computes the remaining of a division. GPS Time in days of the week is expressed as follow:

$$t_{GPS_day_of_week} = \text{rem}(\text{floor}(JD + 0.5), 7) \quad (3.15)$$

Define GPS Standard Epoch as the Julian Day of 1980 AC, January, day 6, 00:00:00.

$$JD_{GPS_standard_epoch} = 2444244.5 \quad (3.16)$$

Define the GPS week counting from the GPS Standard Epoch:

$$t_{GPS_week} = \text{floor}\left(\frac{JD - JD_{GPS_standard_epoch}}{7}\right) \quad (3.17)$$

Finally, the GPS time in seconds of the week can be computed directly:

$$t_{GPS_second_of_week} = (\text{rem}(K_d, 1) + t_{GPS_day_of_week} + 1) \times 86400 \quad (3.18)$$

The GPS week starts on Saturday midnight (Sunday morning), and runs for 604800 seconds. The "GPS Week Rollover" occurred on the weekend of 21-22 August 1999, when the GPS week number was reset to week 0 ("week zero"). Hence if the week number is greater than 1024, subtract the integer 1024.

The MATLAB script *GPSweek.m* carries out the above algorithm. The function is executed as:

[GPS_sec_wk, GPS_wk]=GPSweek (Year, Month, Day, Hour, Minute, Seconds)

3.3 Calculation of Satellite Position in ECEF Systems

The following algorithm calculates the satellite position at the time of transmission t_r (ICD-GPS-200; IS-GPS-200; TSUI, 2005). From the ephemeris parameters listed in table (3.1), the semi major axis a , the time from ephemeris reference epoch t_{oe} , the corrected mean motion n and the mean anomaly M are calculated first as:

$$a = (\sqrt{a})^2 \quad (3.19)$$

Time elapsed since toe is computed as:

$$t = t_{tr} - t_{oe} \quad (3.20)$$

(t_r and t_{oe} are given in GPS seconds of week):

$$n = \sqrt{\frac{\mu}{a^3}} + \Delta n \quad (3.21)$$

where

$\mu = 3.986005 \times 10^{14} \text{ meters}^3 / \text{sec}^2$, Earth's gravitational constant

correction of t_r is performed as

$$t_r = t_r - 604,800 \text{ if } t > 302,400$$

$$t_r = t_r + 604,800 \text{ if } t < -302,400$$

$$M = M_0 + n * t \quad (3.22)$$

The eccentric anomaly E can be found from Equation (4.35) through iterative calculation as

$$E = M + e \sin E \quad (3.23)$$

The relativistic correction term is given as

$$\Delta t_r = Fe\sqrt{a} \sin E \quad (3.24)$$

where

$$F = \frac{-2\sqrt{u}}{c^2} = -4.442807633 \times 10^{-10} \text{ sec}/(\text{meter})^{1/2} \quad (3.25)$$

The clock correction is then performed as

$$\Delta t = a_{f_0} + a_{f_1} \times t + a_{f_2} \times t^2 + \Delta t_r - T_{GD} \quad (3.26)$$

The GPS time at time of transmission is corrected again as

$$t_k = t_{tr} - \Delta t$$

$$t = t_k - t_{oe} \quad (3.27)$$

The true anomaly is calculated from Equation (4.41) as

$$\nu = \tan^{-1} \left[\frac{\sqrt{1-e^2} \sin E}{(\cos E - e)} \right] \quad (3.28)$$

The argument of latitude is found as

$$\Phi = \nu + \omega \quad (3.29)$$

Second harmonic perturbation corrections for argument of latitude Φ , radius r and inclination i are obtained as:

$$\begin{aligned} \delta\Phi &= C_{us} \sin 2\Phi + C_{uc} \cos 2\Phi \\ \delta r &= C_{rs} \sin 2\Phi + C_{rc} \cos 2\Phi \\ \delta i &= C_{is} \sin 2\Phi + C_{ic} \cos 2\Phi \end{aligned} \quad (3.30)$$

The argument of latitude Φ , radius r and inclination i are corrected as:

$$\begin{aligned} \Phi &= \Phi + \delta\Phi \\ r &= a(1 - e \cos E) + \delta r \\ i &= i_0 + \delta i + i_{dot} * t \end{aligned} \quad (3.31)$$

and the corrected longitude of ascending node is

$$\Omega = \Omega_0 + (\Omega_{dot} - \omega_e) t - \omega_e t_{oe} \quad (3.32)$$

where

$$\omega_e = 7.2921151467 \times 10^{-5} \text{ rad/sec}, \text{ earth's rotation rate}$$

Finally coordinates of the satellite in orbital plane can be obtained from

$$\begin{aligned} x &= r \cos \Phi \\ y &= r \sin \Phi \end{aligned} \quad (3.33)$$

and ECEF coordinates are calculated as

$$\begin{aligned} X &= x \cos \Omega - y \cos i \sin \Omega \\ Y &= x \sin \Omega - y \cos i \cos \Omega \\ Z &= y \sin i \end{aligned} \quad (3.34)$$

These ECEF coordinates (XYZ) of the satellite will be used to find the receiver position. Matlab function GetSatpos.m or satposition.m is used to compute the satellite positions and this is how it is being implemented

[Satcoord, PRcorr, tGPS, satClkCorr]=GetSatpos (ObsFileName, NavFileName, Observable)

Where

Satcoord = satellite coordinates in the ECEF system

PRcorr = corrected pseudorange

SatClkCorr = satellite clock correction

tGPS = GPS Transmission time Corrected for Transit Time

3.4 Receiver Position Computation in ECEF Coordinate System

In ordinary 3D position computation three distance measurements are needed to find three unknowns x , y , z . However, in GNSS positioning the receiver clock offset is also unknown. This makes the number of unknown parameters involved with GNSS positioning to be four, which are the 3D Cartesian position parameters x , y , and z , and receiver clock offset. To determine a solution it is therefore required that at least four GNSS satellites be within view of the receiver. The pseudoranges from the satellites are used to determine the receiver position with respect to the Earth.

The steps and algorithms for calculating a receiver position are discussed in Chapter 2. The inputs are the positions of the satellites in the ECEF coordinate system and the pseudoranges.

From Equation (2.5) the code pseudorange for a satellite k and a receiver i (Hofmann-Wellenhop et.al. 2001, Fotiou & Pikridas 2002, Borre et al, 1997) can be modeled as

$$R_i^k(t) = \rho_i^k + c\delta t_i(t) - c\delta t^k(t - \tau_i^k) + \delta_{ion} + \delta_{trop} + \delta_m + \varepsilon \quad (3.35)$$

where

$\tau_i^k = t_i - t^k$ is signal traveltime

The geometric distance ρ_i^k between satellite k and receiver i from Equation (5.6) is

$$\rho_i^k = \sqrt{(X^k - X_i)^2 + (Y^k - Y_i)^2 + (Z^k - Z_i)^2} \quad (3.36)$$

where

$X^k, Y^k, Z^k =$ satellite position in an ECEF coordinate system

$(X_i, Y_i, Z_i) =$ receiver position in an ECEF coordinate system

Neglecting satellite clock offset ionospheric and tropospheric delays the pseudoranges for satellites $k = 1, 2, 3, 4$ are:

$$\begin{bmatrix} R_i^1 \\ R_i^2 \\ R_i^3 \\ R_i^4 \end{bmatrix} = \begin{bmatrix} \rho_i^1 + c\delta t_i \\ \rho_i^2 + c\delta t_i \\ \rho_i^3 + c\delta t_i \\ \rho_i^4 + c\delta t_i \end{bmatrix} \quad (3.37)$$

The geometric distance between satellite k and receiver i is then corrected for Earth rotation, defined by (Borre et al, 1997):

The matrix R_3 accounts for the rotation by the angle $\omega_e \tau_i^k$ while the signal is traveling:

$$R_3(\omega_e \tau_i^k) = \begin{bmatrix} \cos(\omega_e \tau_i^k) & \sin(\omega_e \tau_i^k) & 0 \\ -\sin(\omega_e \tau_i^k) & \cos(\omega_e \tau_i^k) & 0 \\ 0 & 0 & 1 \end{bmatrix} \quad (3.38)$$

The rotation is necessary when using vectors referenced to an Earth centered and Earth fixed system (ECEF). By method of observation equations (method of parameters), and Following the

steps in Section 2.6 in Chapter 2 equation (3) is then linearized with respect to the coordinates of the unknown point using a first order Taylor series approximation to yield

$$L = Ax \quad (3.39)$$

where

$$A = \begin{bmatrix} a_{xi}^1 & a_{yi}^1 & a_{zi}^1 & -c \\ \vdots & \vdots & \vdots & \vdots \\ a_{xi}^n & a_{yi}^n & a_{zi}^n & -c \end{bmatrix} \quad X = \begin{bmatrix} \Delta x_i \\ \Delta y_i \\ \Delta z_i \\ \delta t_i \end{bmatrix} \quad L = \begin{bmatrix} l^1 \\ l^2 \\ l^3 \\ \vdots \\ l^n \end{bmatrix} \quad (3.40)$$

$$a_{xi}^k = -\frac{x_i - x_0}{(\rho_i^k)^0}, a_{yi}^k = -\frac{y_i - y_0}{(\rho_i^k)^0}, a_{zi}^k = -\frac{z_i - z_0}{(\rho_i^k)^0} \quad (3.41)$$

$$l^k = R_i^k - (\rho_i^k)^0 - c\delta t_k$$

$$(\rho_i^k)^0 = \sqrt{(x^k - x_0)^2 + (y^k - y_0)^2 + (z^k - z_0)^2}$$

where

$(x_0, y_0, z_0) =$ preliminary coordinates of receiver initially set to zero

$$A = \begin{bmatrix} -0.7372 & -0.6452 & 0.2157 & 1.0000 \\ -0.3105 & 0.8731 & -0.3877 & 1.0000 \\ -0.9104 & -0.0858 & -0.406 & 1.0000 \\ -0.3509 & 0.3597 & 0.8720 & 1.0000 \\ -0.3851 & 0.0958 & -0.9191 & 1.0000 \\ -0.4034 & -0.2481 & 0.8761 & 1.0000 \\ -0.6050 & 0.7933 & 0.1078 & 1.0000 \\ -0.7888 & 0.3905 & -0.4843 & 1.0000 \end{bmatrix} \quad L = \begin{bmatrix} -5628.112058 \\ -4094.994035 \\ -72451.06837 \\ -35334.08197 \\ -43751.5834 \\ -35524.45769 \\ -56237.82418 \\ -67707.63986 \end{bmatrix} \quad (3.42)$$

8 by 4 8 by 1

The least-squares solution then becomes

$$X = (A^T P A)^{-1} A^T P L \quad (3.43)$$

$$X = \begin{bmatrix} 6.0386.40216 \\ -0.5117.999914 \\ 0.4265.46609 \\ -1.6080.59154 \end{bmatrix} \quad (3.44)$$

In order to find the desired position solution, this equation is used repetitively in an iterative way. A quantity is often used to determine whether the desired result is reached and this quantity can be defined as

$$\delta v = \sqrt{\Delta x_i^2 + \Delta y_i^2 + \Delta z_i^2 + \delta t_i} \quad (3.45)$$

When this value is less than a certain predetermined threshold, the iteration will stop. The solution is iterated until X is less than the threshold or a predetermined value. It should be noted that depending on a chosen threshold value, the iteration method usually can achieve the desired goal in less than 10 iterations. The final receiver coordinates become:

$$\begin{aligned} X_i &= x_0 + \Delta x_i \\ Y_i &= y_0 + \Delta y_i \\ Z_i &= z_0 + \Delta z_i \end{aligned} \quad (3.46)$$

$$\begin{bmatrix} X_i \\ Y_i \\ Z_i \end{bmatrix} = \begin{bmatrix} 6333130.541 \\ -173042.7778 \\ 736382.3983 \end{bmatrix} \quad \text{and} \quad \delta t_i = 50.998277020 \text{ sec} \quad (3.47)$$

$$GDOP = \sqrt{\text{trace}(A^T A)^{-1}} = 2.46 \quad (3.48)$$

Where trace is a Matlab function which means the sum of diagonal elements in a matrix.

It should be noted that receiver *i* represents pillar TP6 at KNUST on which GPS observation was made on July, 16 2013. The design matrix dimension is 8 by 4 meaning the number of satellites observed were 8 and there are four unknowns.

The following steps summarize the above approach:

A. Choose a nominal position and receiver clock bias $x_0, y_0, z_0, \delta t_i$ to represent the initial condition. For example, the position can be the center of the earth and the clock bias zero. In other words, all initial values are set to zero.

B. Use Equation (3.36) to calculate the pseudorange ρ_i . These ρ_i values will be different from the measured values. The difference between the measured values and the calculated values is l^k .

C. Use the calculated $(\rho_i^k)^0$ in Equation (3.41) to calculate $a_{xi}^k, a_{yi}^k, a_{zi}^k$.

D. Use Equation (3.43) to find $\Delta x_i, \Delta y_i, \Delta z_i, \delta t_i$.

E. From the absolute values of $\Delta x_i, \Delta y_i, \Delta z_i, \delta t_i$ and from Equation (3.45) calculate δv .

F. Compare δv with an arbitrarily chosen threshold; if δv is greater than the threshold, the following steps will be needed.

G. Add these values $\Delta x_i, \Delta y_i, \Delta z_i, \delta t_i$ to the initial chosen position x_0, y_0, z_0 , and the clock bias δt_i ; a new set of positions and clock bias can be obtained and they will be expressed as $x_{i1}, y_{i1}, z_{i1}, \delta t_{i1}$. These values will be used as the initial position and clock bias in the following calculations.

H. Repeat the procedure from A to G, until δv is less than the threshold. The final solution can be considered as the desired user position and clock bias.

The Matlab function `getreceiverpos` is used to implement these algorithms in computing the receiver position.

Meanpos=getreceiverpos (ObsFileName, NavFileName, Observable, NumberOfIterations, TotalEpoch)

3.5 Baseline Estimation and Separation of Ambiguities

The Aim of this section is to illustrate the computational method for computing the baseline vector from C/A code and phase observations between two stationary receivers, one as the Master or Base or Reference and the other as the Rover using double difference method.

Processing double differenced data from two receivers results in a “baseline solution.”

The estimated parameters include the vector between the two receivers, in Cartesian coordinates $(\Delta x, \Delta y, \Delta z)$ and the ambiguity parameters $N_{AB}^{i,k}$ for each set of double differences to specific satellite pairs say (i, k) .

Consider a GPS survey between stations A and B. If we call the fixed station A, then estimating the baseline vector is equivalent to estimating the coordinates of station B (x_B, y_B, z_B) .

The first step in finding receiver position is to estimate the ambiguities N_1 and N_2 . The observation equations are:

$$\begin{aligned}
 P_1 &= \rho + I - dm_1 \\
 \Phi_1 &= \rho - I + \lambda_1 N_1 - \delta m_1 \\
 P_2 &= \rho + (f_1/f_2)^2 I - dm_2 \\
 \Phi_2 &= \rho - (f_1/f_2)^2 I + \lambda_2 N_2 - \delta m_2
 \end{aligned} \tag{3.49}$$

where

$$(f_1/f_2) = 154/120$$

ρ = the satellite receiver range

I = the ionospheric group delay at the L1 frequency

The initial approach is to assume the Double Differenced Ionosphere Delay Term I is zero and the Double Difference Code Equation is now transformed into the matrix form as:

$$\underbrace{\begin{bmatrix} P_1 \\ \Phi_1 \\ P_2 \\ \Phi_2 \end{bmatrix}}_{\mathbf{b}} = \underbrace{\begin{bmatrix} 1 & 0 & 0 \\ 1 & \lambda_1 & 0 \\ 1 & 0 & 0 \\ 1 & 0 & \lambda_2 \end{bmatrix}}_{\mathbf{A}} \underbrace{\begin{bmatrix} \rho \\ N_1 \\ N_2 \end{bmatrix}}_{\mathbf{x}} - \text{noise} \tag{3.50}$$

This equation (6.2) express the relationship between the raw double differenced observables b in terms of the unknown x . The 4 by 3 Design Matrix A is defined above based on assumptions made in (6.1). The above is a system of 4 equations with 3 unknowns: the ideal pseudorange and the two ambiguities on L1 and L2. Least square method is used in solving x :

$$x = \left(\begin{array}{c} \underbrace{A^T W A}_{3 \text{ by } 3} \end{array} \right)^{-1} \underbrace{A^T W b}_{3 \text{ by } 1} \quad (3.51)$$

The weight matrix W is defined as follow:

$$W = \begin{bmatrix} 1/\sigma_{P_1}^2 & 0 & 0 & 0 \\ 0 & 1/\sigma_{\Phi_1}^2 & 0 & 0 \\ 0 & 0 & 1/\sigma_{P_2}^2 & 0 \\ 0 & 0 & 0 & 1/\sigma_{\Phi_2}^2 \end{bmatrix} \quad (3.52)$$

Where σ is the standard deviation: the subscripts P_1, P_2, Φ_1, Φ_2 represents respectively the Pseudorange on L1 and L2, Phase Distance on L1 and L2. Reasonable values of the corresponding standard deviations are defined as follow in meters:

$$\begin{aligned} \sigma_{P_1} &= \sigma_{P_2} = 0.3 \\ \sigma_{\Phi_1} &= \sigma_{\Phi_2} = 0.005 \end{aligned} \quad (3.53)$$

The least squares solution consists of two reals n_1 and n_2 from which we have to recover two integers N_1 and N_2 . Here Goad method of ambiguity resolution with use of a Kalman filter is use. The implementation of the method is based on the example in (Borre et al 1997, Petrovskyy et al, 2007).

The estimated difference $n_1 - n_2$ is rounded to the nearest integer and named K_1 . The rounded value of $60n_1 - 77n_2$ we call K_2 . The best integer estimates for N_1 and N_2 are then found as the solution

$$\begin{aligned} \hat{N}_2 &= (60K_1 - K_2)/17 \\ \hat{N}_1 &= \hat{N}_2 + K_1 \end{aligned} \quad (3.54)$$

The system equation is a steady model $\mathcal{X}_{k|k-1} = \mathcal{X}_{k-1|k-1}$ so the covariance prediction is

$$\sum_{k|k-1} = \sum_{k-1|k-1} + \sum_{\varepsilon,k} \quad (3.55)$$

where the transitional covariance matrix $\Sigma_{\varepsilon,k}$ is diagonal

$$\Sigma_{\varepsilon,k} = \begin{bmatrix} 10000 & 0 & 0 \\ 0 & 0 & 0 \\ 0 & 0 & 0 \end{bmatrix} \quad (3.56)$$

This matrix will create some chance to change ρ in x from epoch to epoch. Covariance update and Gain matrix are as follows:

$$\Sigma_{k|k} = \left(A \Sigma_{k|k-1} A^T + W \right)^{-1} \quad (3.57)$$

The state update is computed according to the following equation

$$x_{k|k} = x_{k|k-1} + K_k (b_k - A x_{k|k-1}) \quad (3.58)$$

The corrected covariance matrix prepared for the next epoch

$$\Sigma_{k|k} = (I - K_k A) \Sigma_{k|k-1} \quad (3.59)$$

The process starts from initial values

$$\Sigma_{0|0} = \begin{bmatrix} 10 & 0 & 0 \\ 0 & 10 & 0 \\ 0 & 0 & 10 \end{bmatrix} \quad (3.60)$$

$$x_{1|0} = (A^T A)^{-1} b_0$$

The true ambiguities are found from the combinations based on the set of equations 3.54

$$\begin{aligned} K_1 &= \text{round}(x_{k|k}(2,1) - x_{k|k}(3,1)) \\ K_2 &= \text{round}(60 * b_k(2,1) / \lambda_1 - 77 * b_k(4,1) / \lambda_2) \end{aligned} \quad (3.61)$$

$$\begin{aligned} \text{true}N_2 &= \text{round}((60 * K_1 - K_2) / 17) \\ \text{true}N_1 &= \text{round}(\text{true}N_2 + K_1) \end{aligned} \quad (3.62)$$

When K_1 is filtered to the correct value, equation (3.62) will produce the true ambiguities, since the error in K_2 will be reduced by division by 17, and removed completely by rounding. Furthermore, to ensure the removal of the error in K_2 , it can be averaged over epochs. The more epochs are processed, the more correctly K_1 is filtered, and consequently, the more reliable are the resolved ambiguities.

Now after resolving the ambiguities, the final step is the baseline estimation.

First, let the first guess of Rover position X_j be the same as Master position X_i *only in the* 1st iteration:

$$X_j = X_i = X_{j, \text{this iteration}} = X_{j, \text{previous iteration}} \quad (3.63)$$

From the first epoch, we define the double frequency (i.e. L1 and L2 code) Design Matrix A and Constant Noise Vector b ; Rover Position Updating Vector x_j :

$$A = \begin{bmatrix} J \\ J \end{bmatrix}_{\text{this iteration}} ; x_j = \begin{bmatrix} dx_j \\ dy_j \\ dz_j \end{bmatrix} \equiv \begin{bmatrix} x_{j, \text{previous iteration}} - x_{j, \text{this iteration}} \\ y_{j, \text{previous iteration}} - y_{j, \text{this iteration}} \\ z_{j, \text{previous iteration}} - z_{j, \text{this iteration}} \end{bmatrix} ; b = \begin{bmatrix} C_{1,ij}^{kl} \\ C_{2,ij}^{kl} \end{bmatrix} \quad (3.64)$$

where J is the Jacobian Matrix, define as follow $C_{1,ij}^{kl}$ and $C_{2,ij}^{kl}$ are the Constant Noise Vector for L1 and L2 code respectively:

$$J \equiv \begin{bmatrix} u_i^l - u_i^k \end{bmatrix} = \begin{bmatrix} \frac{(x^l - x_i) - (x^k - x_j)}{\rho_i^k} & \frac{(y^l - y_i) - (y^k - y_j)}{\rho_i^k} & \frac{(z^l - z_i) - (z^k - z_j)}{\rho_i^k} \end{bmatrix} \quad (3.65)$$

The original satellite coordinates are corrected for Earth rotation by $\omega_e \tau_i^k$.

where

$\omega_e = 7.2921151467 \times 10^{-5} \text{ rad/sec}$, earth's rotation rate

$\tau_i^k = \rho_i^k / c$

$$\begin{bmatrix} X^k \\ Y^k \\ Z^k \end{bmatrix}_{NEW} = \begin{bmatrix} \cos(\omega_e \tau_i^k) & \sin(\omega_e \tau_i^k) & 0 \\ -\sin(\omega_e \tau_i^k) & \cos(\omega_e \tau_i^k) & 0 \\ 0 & 0 & 1 \end{bmatrix} \begin{bmatrix} X^k \\ Y^k \\ Z^k \end{bmatrix} \quad (3.66)$$

$$C_{q,ij}^{kl} = \Phi_{q,ij}^{kl} - \lambda_q N_{q,ij}^{kl} - (\rho_i^k)^0 + (\rho_i^l)^0 + (\rho_j^k)^0 - (\rho_j^l)^0 \quad (3.67)$$

$$C_{1,ij}^{kl} = [\Phi_{1,ij}^{kl} - T_{ij}^{kl} - \lambda_1 N_{1,ij}^{kl} - \rho_{ij}^{kl}] \quad (3.68)$$

$$C_{2,ij}^{kl} = [\Phi_{2,ij}^{kl} - T_{ij}^{kl} - \lambda_2 N_{2,ij}^{kl} - \rho_{ij}^{kl}] \quad (3.69)$$

The index $q = 1, 2$ corresponds to observations on frequencies $L1$ and $L2$. There is an equation for each rover receiver $j = TP6$ and satellite l , except the reference station $i = \text{KNUST N1}$ and satellite $k = 26$.

The least-squares solution of the complete system $Ax = b$ yields the position vector.

$$A = \begin{bmatrix} 0.158126709906973 & 0.854387444299954 & 0.010391656071983 \\ -0.326909699032277 & 0.558437763918909 & 0.347657895683072 \\ 0.128794309047893 & -0.456262616741665 & 0.316095617937950 \\ 1.076311809630047 & -0.199811491423139 & 0.098245268948668 \\ 0.758874193520302 & 1.045781030149912 & 0.097654754629285 \\ -0.124783013214679 & 1.047537852416381 & 0.928367041405299 \end{bmatrix} \quad (3.70)$$

6 by 3

$$b = \begin{bmatrix} 0.154049005359411 \\ 0.302481837570667 \\ -0.607413969933987 \\ 0.516133606433868 \\ -0.567049462348223 \\ 0.056685995310545 \end{bmatrix} \quad (3.71)$$

6 by 1

Covariance matrix for double difference observables (C)

$$C = \begin{bmatrix} 0.4285 & -0.0714 & -0.0714 & -0.0714 & -0.0714 & -0.0714 \\ -0.0714 & 0.4285 & -0.0714 & -0.0714 & -0.0714 & -0.0714 \\ -0.0714 & -0.0714 & 0.4285 & -0.0714 & -0.0714 & -0.0714 \\ -0.0714 & -0.0714 & -0.0714 & 0.4286 & -0.0714 & -0.0714 \\ -0.0714 & -0.0714 & -0.0714 & -0.0714 & 0.4286 & -0.0714 \\ -0.0714 & -0.0714 & -0.0714 & -0.0714 & -0.0714 & 0.4286 \end{bmatrix} \quad (3.72)$$

6 by 6

$$X = \begin{bmatrix} -0.948236877906794E^{-9} \\ 0.016473256786442E^{-9} \\ 0.996259970353908E^{-9} \end{bmatrix} ; \begin{bmatrix} X_i \\ Y_i \\ Z_i \end{bmatrix} = \begin{bmatrix} 6333131.026 \\ -173042.314 \\ 736358.328 \end{bmatrix} ; \begin{bmatrix} \Delta X \\ \Delta Y \\ \Delta Z \end{bmatrix} = \begin{bmatrix} 1.358 \\ 1.691 \\ -5.516 \end{bmatrix} \quad (3.50)$$

In summary, the baseline computation is achieved in the following steps:

Step 1 - The positions of the satellites: The satellite positions are to be computed in Earth-fixed x, y, z coordinates, from the ephemerides that are transmitted in Keplerian coordinates using the RINEX navigation data files (N- files). This implemented by the Matlab M-file satposition.m or GetSatpos.m

Step 2 - Preliminary position of the receiver: Here the initial position of the receiver is computed based on the pseudorange data from each satellite using information from RINEX observation files (O-files).The Matlab M-file getreceiverpos.m is used to this effect.

Step 3 - Estimation of ambiguities and the baseline vector: Here the ambiguities $N_{1,ij}^{kl}$ and $N_{2,ij}^{kl}$ for double differenced observations are resolved and the subsequent estimation of the baseline vector $(\Delta x, \Delta y, \Delta z)$ between the two receivers, the base and the rover.

The Matlab M-file geBaseline.m is used to implement these algorithms in estimating the baseline components and the receiver (rover) position. Its usage is shown below:

OUTPUT

INPUT

[Roverpos, BaselineV]=getBaseline (BasePos, ObsFileName, NavFileName, NumberOfIterations)

Where

BasePos=Base receiver position in ECEF (X, Y, Z) frame.

ObsFileName=Rinex Observation files

NavFileName=Rinex Navigation files

Roverpos= Rover receiver position in ECEF (X, Y, Z) frame.

BaselineV= Baseline vectors $(\Delta X, \Delta Y, \Delta Z)$ between base and rover receivers

3.6 Transformation of Receiver Position

After the rover receiver position (X_r, Y_r, Z_r) in Cartesian coordinate system is found in section 3.5, it is important to convert those positions in the ECEF system into the geodetic coordinate system or other system as desired by the user, because the user position on the surface of the earth is given either in the 3D Geodetic coordinate system (ϕ, λ, h) or 2D Cartesian coordinate system (N, E) and finally to the user desired datum or coordinate frame, in this study for instance, from the WGS 84 datum to the War Office datum since the Rover first position system is in the WGS 84 coordinate system. This section therefore seeks to outline the computational procedures of the various methods of datum transformation of the user position or coordinate from WGS 84 ellipsoid to War office ellipsoid and vice versa using the published transformation parameters and conversions from Geographic (ϕ, λ) to plane (N, E) coordinates and vice versa on both ellipsoids.

3.6.1 Parameter Transformation from WGS 84 – War Office

The 3, 7 and 10 parameter Transformation models are given below:

Three Parameter Model

$$\begin{bmatrix} X_2 \\ Y_2 \\ Z_2 \end{bmatrix}_{NEW} = \begin{bmatrix} \Delta X \\ \Delta Y \\ \Delta Z \end{bmatrix} + \begin{bmatrix} X_1 \\ Y_1 \\ Z_1 \end{bmatrix}_{Original}$$

Seven Parameter Model

$$\begin{bmatrix} X_2 \\ Y_2 \\ Z_2 \end{bmatrix} = \begin{bmatrix} \Delta X \\ \Delta Y \\ \Delta Z \end{bmatrix} + (1 + \Delta S) \begin{bmatrix} 1 & R_z & -R_y \\ -R_z & 1 & R_x \\ R_y & -R_x & 1 \end{bmatrix} \begin{bmatrix} X_1 \\ Y_1 \\ Z_1 \end{bmatrix}$$

Ten Parameter Model

$$\begin{bmatrix} X_2 \\ Y_2 \\ Z_2 \end{bmatrix} = \begin{bmatrix} \Delta X \\ \Delta Y \\ \Delta Z \end{bmatrix} + \begin{bmatrix} X_0 \\ Y_0 \\ Z_0 \end{bmatrix} \begin{bmatrix} (1 + \Delta S) & R_z & -R_y \\ -R_z & (1 + \Delta S) & R_x \\ R_y & -R_x & (1 + \Delta S) \end{bmatrix} \begin{bmatrix} X_1 - X_0 \\ Y_1 - Y_0 \\ Z_1 - Z_0 \end{bmatrix}$$

Where;

X_1, Y_1, Z_1 = Cartesian coordinates of a point in WGS 84 Datum

X_2, Y_2, Z_2 = Cartesian coordinates of the same point in the War Office Datum

The five parameter transformation model or formulae are given in appendix 1.

The published transformation parameters from War Office to WGS 84 are given in table 2.9 of section 2.4.5 of chapter two. After the datum transformation and the new ECEF coordinates in the War Office sort, they are now converted to geographic coordinates on the same ellipsoid using conversion formulae as describe in sub-section 2.4.4.1 of chapter two. The transformation processes are illustrated in figure 2.21 of sub-section 2.4.5 of chapter two.

The Matlab M-file xyz2wo.m is used to implement these transformations.

[Lat, long]=xyz2wo (X₁, Y₁, Z₁, parameter, Enterparameters)

Where

X_1, Y_1, Z_1 = Cartesian coordinates of a point in WGS 84 Datum as explain above

Parameter=3, 5, 7 and 10 for 3, 5, 7, 10 parameter transformation to be performed.

Enterparameters= the transformation parameters to be used. Either published or user-defined.

Lat, long=Latitude and Longitude coordinates in the War Office (WO) ellipsoid.

The reverse datum transformation is also considered.

The Matlab M-file wo2wgs.m is used to implement these transformations.

[Lat long]=wo2wgs (latitude, longitude, parameter, Enterparameters)

3.6.7 Geographic Coordinates to National Grid on War Office ellipsoid

The geographic coordinates after datum transformation, are now projected to the National Grid coordinates (N, E) using the TM projection. The projection parameters and formulae are given in table 2.91 of sub-section 2.4.6 of chapter two and appendix A respectively.

The Matlab M-files wo2ng.m and ng2wo.m performs these conversions

[N, E]=wo2ng (latitude, longitude, SemiMajorAxis, inverseFlattening)

[Lat, long]=ng2wo (N, E, input_unit, SemiMajorAxis, inverseFlattening)

3.6.6 Geographic Coordinates to UTM on WGS84 ellipsoid

The geographic coordinates in the WGS84 ellipsoid can also be projected to the plane (N, E) coordinates using the UTM projection. The projection parameters and formulae are given in table 2.91 of sub-section 2.4.6 of chapter two and appendix A respectively.

The Matlab M-files wgs2utm.m and utm2wgs.m performs these conversions

[N, E, zone]=wgs2utm (latitude, longitude, SemiMajorAxis, inverse Flattening)

[Lat, long]=utm2wgs (N, E, input_unit, ZONE, SemiMajorAxis, inverseFlattening)

Conclusion: This chapter described the conventional GNSS techniques and algorithm, used to determine satellite and receiver positions as well as the estimation of Baseline vectors and ambiguity resolutions. Datum transformation and map projection computational procedure are also outlined.

CHAPTER FOUR - SOFTWARE DEVELOPMENT AND TESTING

This chapter highlights on how the GNSS Suite was developed in the Matlab Programming Language environment and tested. Also in this chapter, presents the detailed methodology of testing the GNSS package of the Suite from GPS data collection conducted by making field observation to processing the GPS data collected using the developed GNSS Suite, Sokkia Spectrum Survey (SSS) and the TOPCON software. The results obtained from those applications are tabulated. The equipment used, the technique employed and the study area for the data collection is also not left out in this chapter. In addition, the datum transformation and the geodetic computations (Direct and Inverse) packages of the suite are also run and tested in this chapter.

4.1 Software Development

This section seeks to outline the materials and the methodology that was used to develop the GNSS Suite. The Development of the software or Suite was in two phases:

- ✓ The Development or writing of M-file functions
- ✓ The Designing of the Graphical User Interface (GUI)

4.1.1 Materials Used

The material used in developing the suite which includes, the designing of the Graphical User Interface (GUI) and the development of the codes (M-Files) to run the various applications was the MATLAB 8.0.0.783 (R2012b) programming language. The statistical capabilities and the ability to tackle large matrices involved in scientific and engineering calculations especially in GNSS position computations triggered its use in this research. The current versions of MATLAB includes the GUI which makes it easier for users to create GUI by using drag and drop method. The interface for creating the GUI is shown in figure 4.1 below.

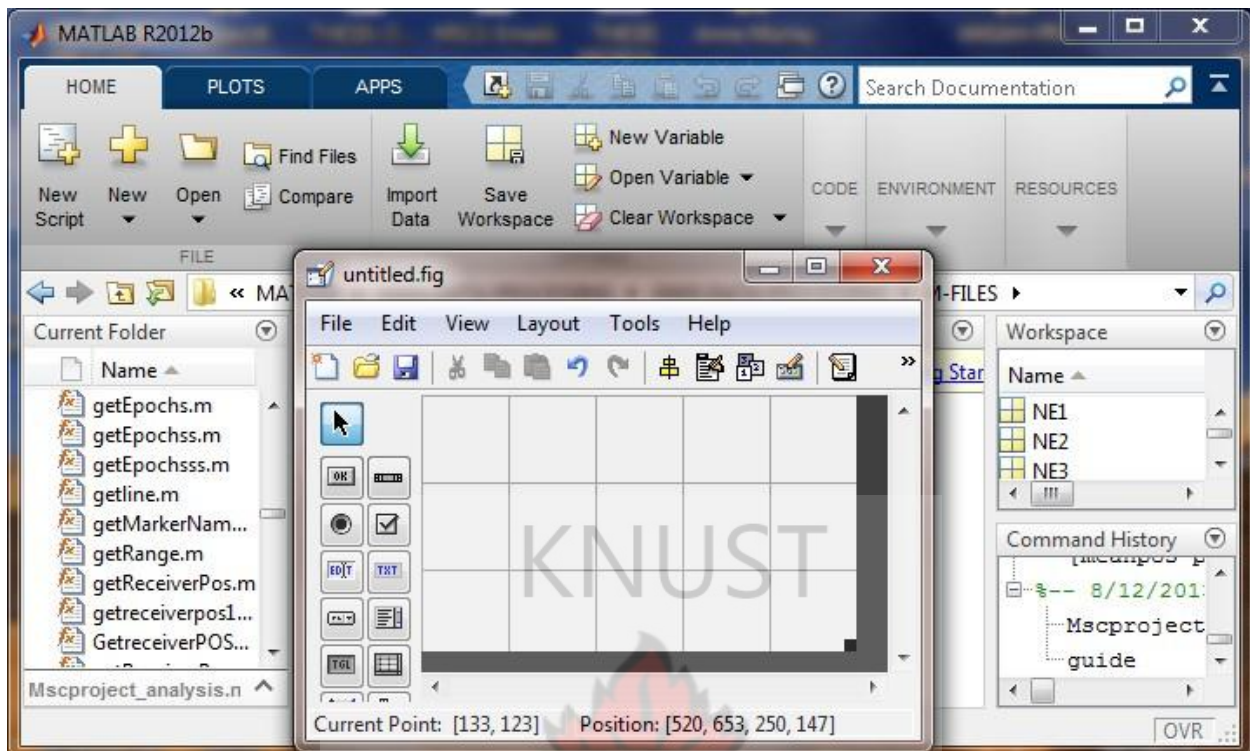


Figure 4.1: Interface for the creation of GUI in MATLAB

The MATLAB codes are written in the M-file Editor which is automatically generated when the GUI is saved. It can also be generated manually without the GUI. The MATLAB M-file Editor which is where the codes are entered is also shown in figure 4.2 below.

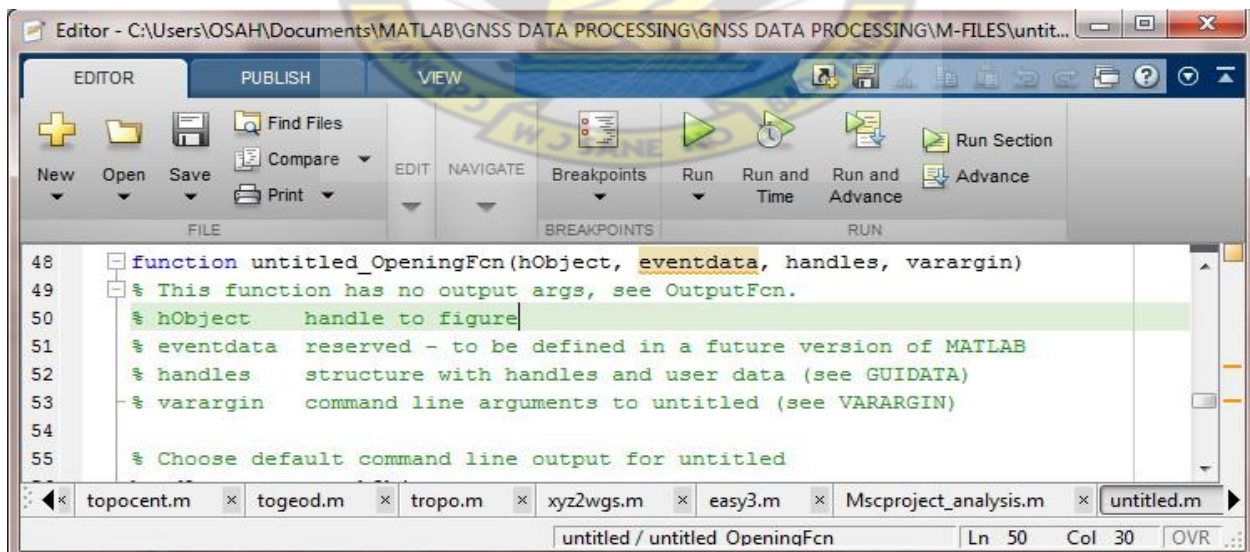
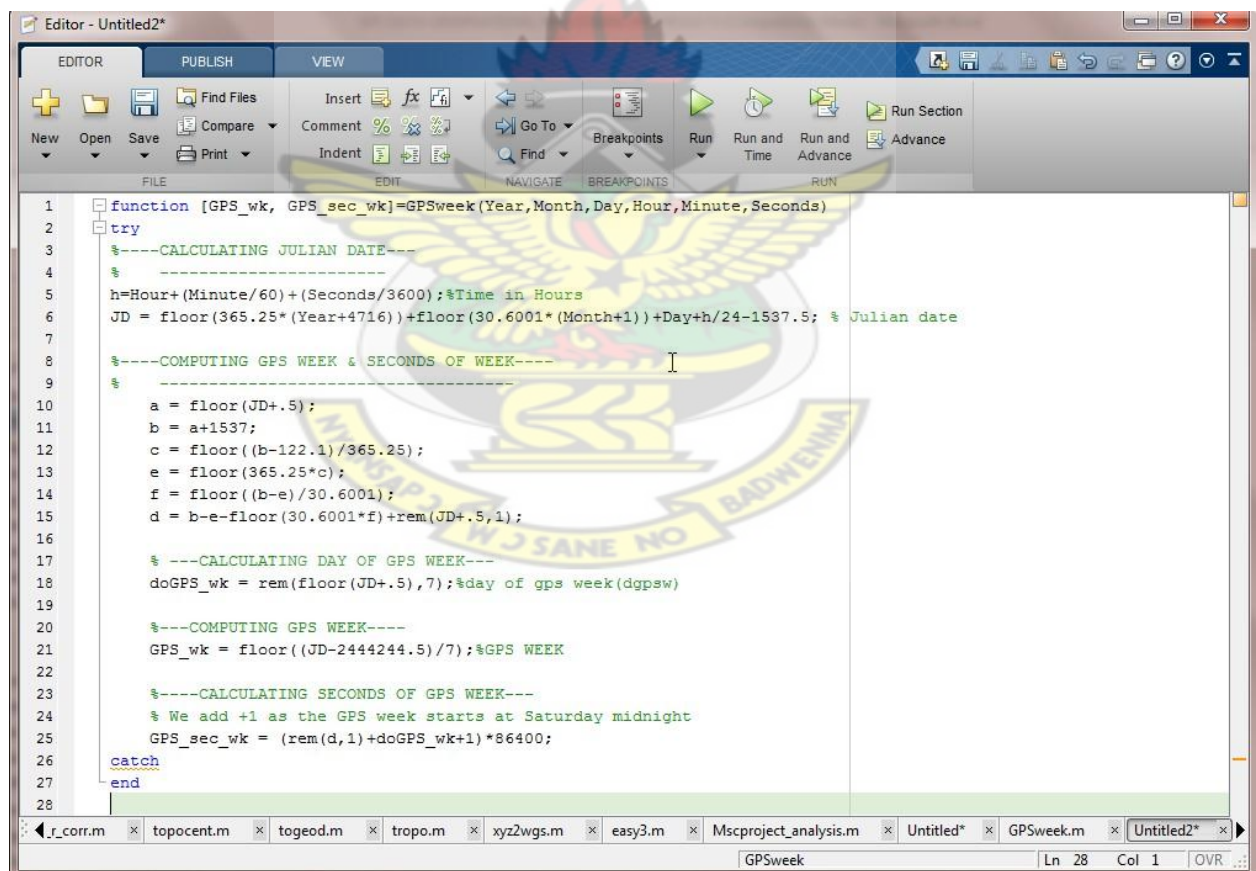


Figure 4.2: MATLAB M-file Editor

In developing GNSS Suite and other applications using Matlab, the following steps were taken into consideration:

- The mathematical formulae involved in the GNSS techniques, datum transformation and geodetic computations as far as this research is concern, were identified and gathered.

These formulae or algorithms as outlined in Chapter three and appendix A, were implemented in the MATLAB programming language by creating M-file functions for each formulae or algorithm in the M-file Editor as separate from the GUI. From the MATLAB Editor Menu as shown in figure 4.2 above, click on New and select function. This opens a Blank Editor where the codes are written and save as the name of the function.m, eg GPSweek.m. Where GPSweek is the function's name and the .m is the extension. Figure 4.3 below shows how the GPSweek function was written in a Blank M-file Editor.



```
1 function [GPS_wk, GPS_sec_wk]=GPSweek(Year,Month,Day,Hour,Minute,Seconds)
2 try
3 %---CALCULATING JULIAN DATE---
4 %
5 h=Hour+(Minute/60)+(Seconds/3600);%Time in Hours
6 JD = floor(365.25*(Year+4716))+floor(30.6001*(Month+1))+Day+h/24-1537.5; % Julian date
7
8 %---COMPUTING GPS WEEK & SECONDS OF WEEK---
9 %
10 a = floor(JD+.5);
11 b = a+1537;
12 c = floor((b-122.1)/365.25);
13 e = floor(365.25*c);
14 f = floor((b-e)/30.6001);
15 d = b-e-floor(30.6001*f)+rem(JD+.5,1);
16
17 % ---CALCULATING DAY OF GPS WEEK---
18 doGPS_wk = rem(floor(JD+.5),7);%day of gps week(dgpsw)
19
20 %---COMPUTING GPS WEEK---
21 GPS_wk = floor((JD-2444244.5)/7);%GPS WEEK
22
23 %---CALCULATING SECONDS OF GPS WEEK---
24 % We add +1 as the GPS week starts at Saturday midnight
25 GPS_sec_wk = (rem(d,1)+doGPS_wk+1)*86400;
26 catch
27 end
28
```

Figure 4.3: GPSweek M-file

- The graphical user interface was created using the GUIDE window of MATLAB. This was done as follows:
 - ✓ In the MATLAB command window: `>>guide`
 - ✓ This opens GUIDE quick start. Select Blank GUI...
 - ✓ File > Preferences > GUIDE > Show names component palette.
 - ✓ View > Property Inspector
 - ✓ Click and drag to resize gridded layout area to desired size, or use Position property in Property Inspector to set an exact size.
 - ✓ Tools > Application Options > Resize behaviour = Proportional.
 - ✓ Add components
 - ✓ Use Static Text component for labels
 - ✓ Align components using the Align tool bar button.
 - ✓ Label components using string property.
 - ✓ Label figure using Name property.
 - ✓ For Popup Menu, String property gets one line per menu entry.
 - ✓ Tag components, Tag property. E.g. "button_exit"
 - ✓ Save GUI using Tools > Run. Will save both a .fig figure file and a .m M-file under the chosen name. The designed form is saved with a .fig extension.
 - ✓ After designing the interface, the codes for running the program are developed as follows:
 - ✓ Place code that should run when the application starts in the opening function which is called `guiname_OpeningFcn ()`. Place code after comment that begins `% varargin...`
 - ✓ Place codes for buttons and other components in the appropriate callback function stubs that are at the end of the .m file.

The flow chart diagram in figure 4.4 below shows the methods used in the design of the suite.

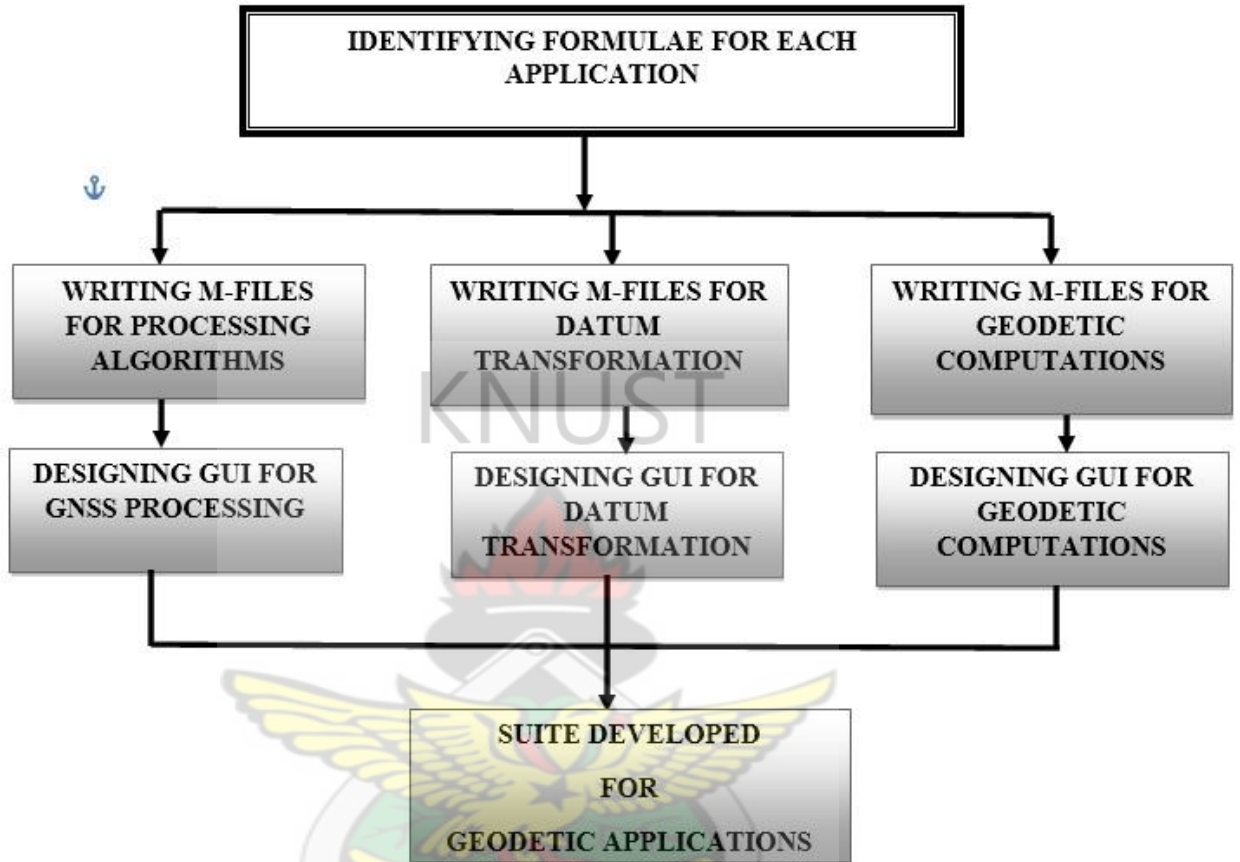


Figure 4.4: Flow Chart Diagram for Designing Suite

4.2 Software Testing of GPS Data Processing

In this section, the GNSS post-processing package of the developed suite is tested with other processing software as mentioned above in this chapter on GPS data collected over four survey pillars. The detailed processing methodology and data collection technique are elaborated in the following sub-sections.

4.2.1 Data Collection

In order to test the post-processing package of the GNSS suite developed, GPS data was collected by field observations on already established survey pillars. The study area for the data collection was KNUST and some part of Ayeduase. Before the field observations, a

reconnaissance survey of the area was carried out where a total of five survey pillars N1, TP6, SGA P130/ 13 /2, SGA P130/ 13 /1 and GCG A29 /49/ 90 were selected and were believed to be more stable and free from disturbance as well as being away from structures and tall trees which could obstruct the satellite signals. The locations of the pillars were at the N Block (N1 and TP6) of the College of Engineering, the administration roundabout (SGA P130/ 13 /2), Library (SGA P130 /13 /1) all of KNUST and the Ayeduase mango road (GCG A29 /49/ 90). The diagram of survey is shown below (see figure 4.1). After the reconnaissance survey, a differential GNSS (DGNSS) technique was employed in the field observational procedure where N1 was used as the base or reference station and TP6, SGA P130/ 13 /2, SGA P130/ 13 /1 and GCG A29 /49/ 90 as the rover stations. The Sokkia Radian IS Dual frequency GPS receivers were used as the equipment for this exercise. One of the GPS receivers was set over N1 and the other roving around TP6, SGA P130/ 13 /2, SGA P130/ 13 /1 and GCG A29 /49/ 90 making position measurements. The occupational time for each rover station was about 15 to 20 minutes long with 10-seconds epoch interval in static mode. 4 satellites were .at least tracked throughout the surveyed time. This was to ensure that enough and quality data was collected for fixed solution during the post-processing. Table 4.1 shows the field booking.

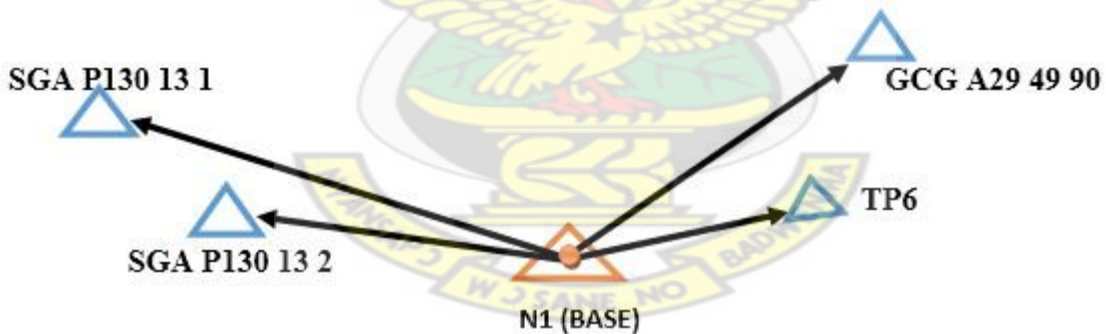


Figure 4.5: Diagram of Survey showing Baselines

Table 4.1: Occupational Times

Sessions	Date	Start Time	End Time	Pillars Observed
01	16 / 07 / 2013	09 : 05 : 20 am	12 : 17 : 40 pm	N1
02	16 / 07 / 2013	09 : 11 : 30 am	09 : 30 : 50 am	TP6
03	16 / 07 / 2013	10 : 16 : 40 am	10 : 31 : 00 am	SGA P130/13/2
04	16 / 07 / 2013	10 : 59 : 50 am	11 : 13 : 00 am	SGA P130 /13/ 1
05	16 / 07 / 2013	11 : 59 : 30 am	12 : 13 : 10 pm	GCG A29/49/90

4.2 Data Processing

The observed data was then processed using the Sokkia spectrum survey software the TOPCON software and the GNSS suite developed. This was to help validate or test the post-processing package of the suite.

4.2.1 Data Processing using SSS v3.2

The Spectrum Survey software is a comprehensive, automated suite of programs for GPS surveying including post-processing and support real-time measurements. It was developed by POINT, Inc. of Olathe, Kansas - U.S.A. The software processes L1/L2 data and reports the processed project results output in text format. The data processing was done throughout the following step:

1. The Spectrum Survey started up and Create new project was selected after the welcome to Spectrum Survey dialog was opened.
2. After creating new project, the import data files from disk was selected from the project startup dialog.
2. The Data File Manager dialog was open and all imported files were selected using the select all button.
3. Baseline and network adjustment was processed with the following settings: a cut-off angle of 15°, ephemeris, broadcast; data type, code and phase L1.

4. After the processing run was completed the results were displayed automatically in text format.

4.2.2 Data Processing using TOPCON Software

The TOPCON Software is a comprehensive, automated suite of programs for GPS surveying including post-processing and support real-time measurements. The software accept RINEX data file. The following steps demonstrate the method that was applied to process GPS data:

1. The RINEX data file was imported and all points appeared on the screen after selecting all and open button clicked.
2. To completion the data processing, the RINEX file is converted to TOPSURV file by selecting convert file on the file in the main Toolbar.
3. Finally, the data was processed, by selecting process in the main tools bar, where a menu bar was display. Then compute coordinate was clicked to complete the processing.

4.2.2 Data Processing using GNSS Suite Developed

The Suite developed was tested by processing the field data obtained through DGNSS technique of surveying. The suite uses RINEX format as data input. For this reason the spectrum survey was used to convert the raw GPS data to RINEX format. Baseline from the base to rovers was processed using the suite with the following setting: a cut-off angle of 15°, ephemeris, broadcast; data type, code and phase. The Suite has a graphical user interface that is user-friendly and interactive. The user has the choice of selecting the type of transformation parameters (3, 5, 7, and 10) to be used for the baseline processing. The RINEX file can also be imported either from a set of mixed files or folders. The steps taken to test the Suite is as follows:

1. From the Project settings window, 'MSC PROJECT' was entered as project name. Location where results were to be saved was browsed to using the Browse button. The default coordinate system is the WGS 84. This was change to Transverse Mercator(TM) by clicking the drop-down list. The seven Transformation parameters was chosen and other settings were performed by clicking on the 'Settings' button. The 'OK' button was clicked when everything was done (see figure 4.6 below).



Figure 4.6: Project Settings

2. After clicking the 'OK' button from the Project Settings window, the Import window was opened where the option to import rinex data from either files or folders was displayed. (See figure 4.7). Here, 'Import RINEX Data From Folders' was selected where another system window was opened to browse for the rinex data to be imported.



Figure 4.7: Import Rinex Option

- Finally after importing the RINEX data, another window was opened where the imported rinex files (O-files and N-files) and other information were displayed in table format. The base or reference receiver coordinates based on the selected coordinate system were entered (see figure 4.8). The 'OK' button was finally clicked to process the GPS data. The processing result is displayed automatically in a text file (which opens by default).

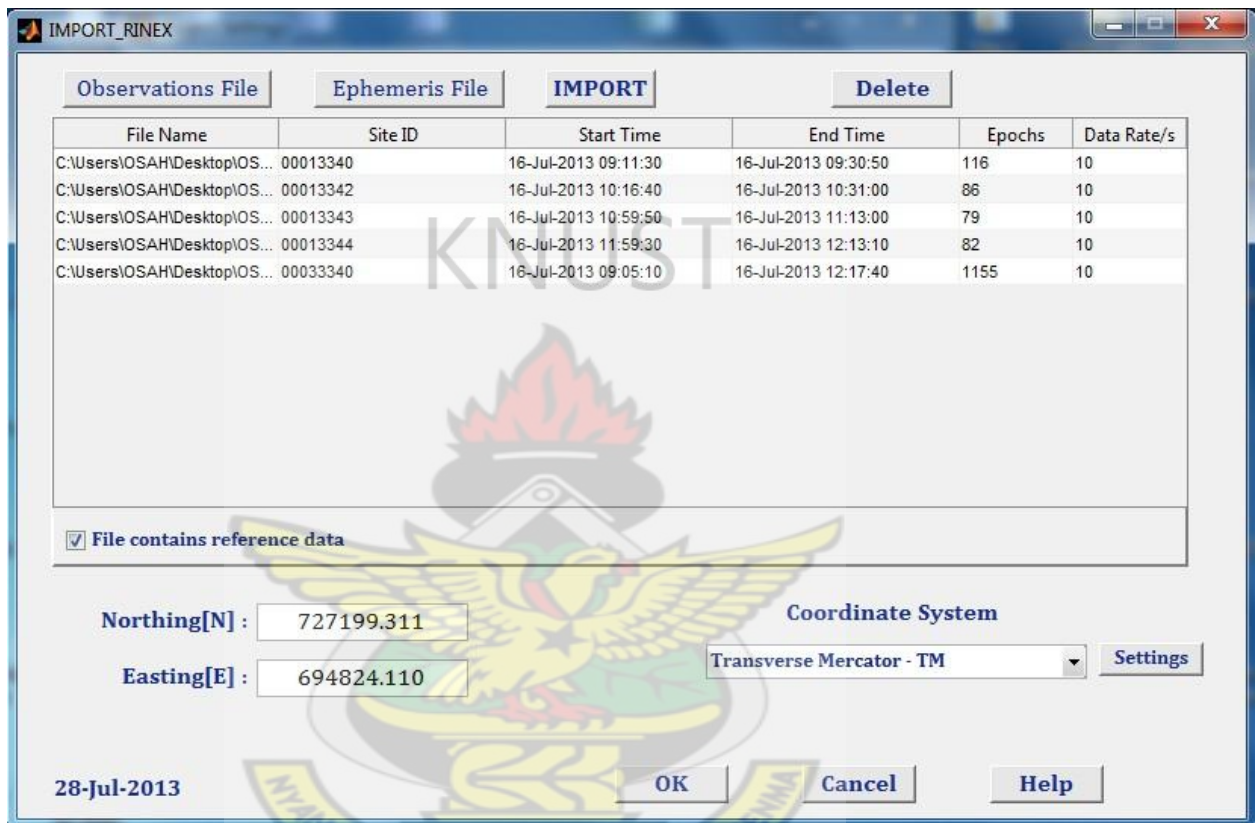


Figure 4.8: Import Rinex

4.3 Software Testing of Datum Transformation

The datum transformation package of the suite was also tested, using coordinates of three existing points within the Golden Triangle common to both the WGS 84 and War Office ellipsoids. These are presented in table 4.2, 4.3 and table 4.4 below. The testing procedure of the application is illustrated in figure 4.9 below in a form of a flow chart. The package is also shown in figure 4.91.

Table 4.2: Test point coordinates on WGS84

Golden triangle WGS84 Coordinates							
Points	Latitudes(N)			Longitudes(W)			Ellipsoidal heights
CFP 109	5	27	36.32569	0	25	24.81766	78.2744
CFP 200	5	37	32.87415	0	33	33.54116	304.9379
CFP 225	5	27	18.31243	1	30	3.96614	275.1437

Table 4.3: Test point coordinates on Ghana War office ellipsoid

Golden triangle War office Coordinates							
Points	Latitudes(N)			Longitudes(W)			Ellipsoidal heights
CFP 109	5	27	26.29465	0	25	25.84579	
CFP 200	5	37	22.8541	0	33	34.55078	
CFP 225	5	27	8.187017	1	30	4.874719	

Table 4.4: Projected Northings and Eastings for test points on Ghana TM

Existing National Grid Coordinates		
Points	Northings(ft)	Eastings (ft)
CFP 109	286868.63	1109433.05
CFP 200	346933.94	1060041.45
CFP 225	285019.85	717756.06

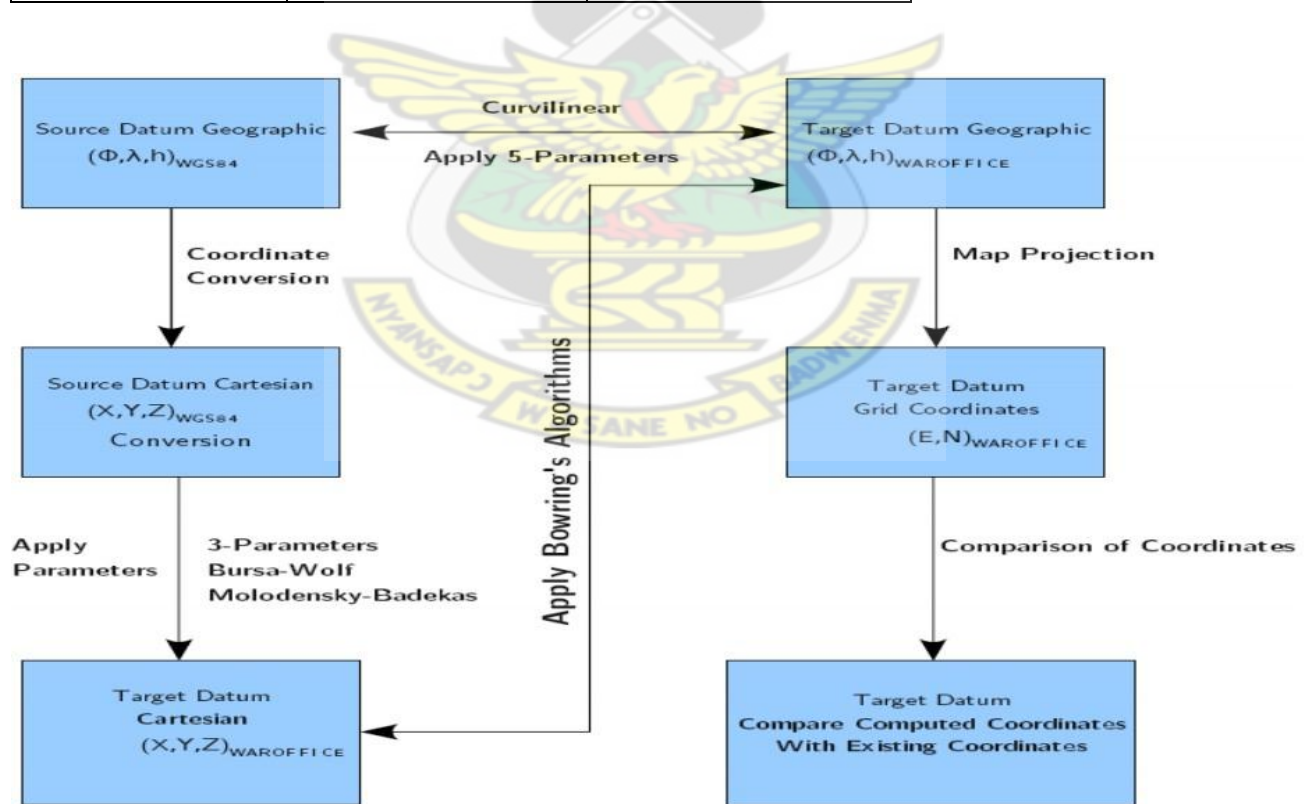


Figure 4.9: Flow chart for the testing procedure.

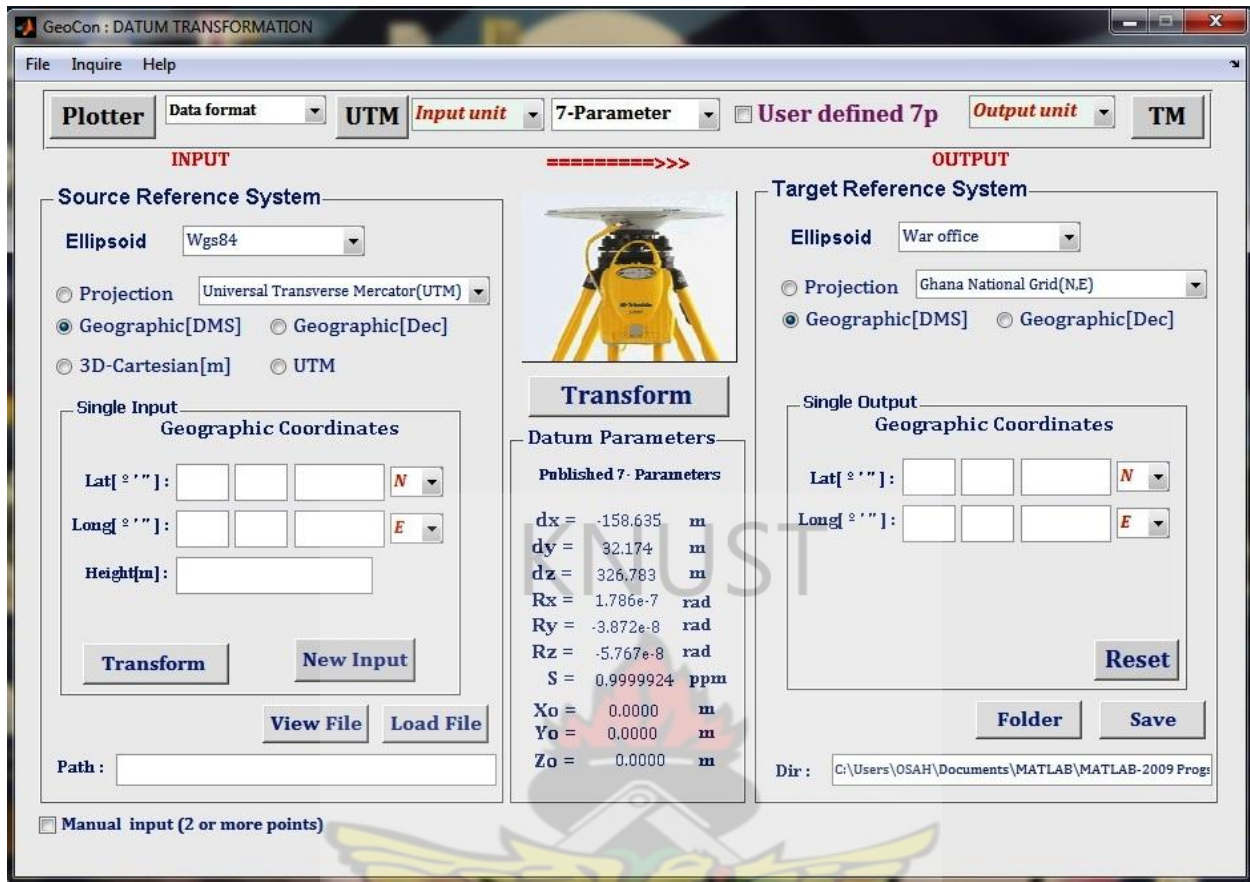


Figure 4.10: Datum Transformation

The application runs on a separate graphical user interface (see fig. 4.10) and performs any form of datum transformation or coordinate conversion between the WGS 84 and War Office ellipsoids using the existing published transformation parameters (3,5,7,and 10) of Ghana or user-defined transformation and ellipsoid parameters. In this research, the 7 parameter transformation was used. The application is user friendly and easy to use. It has the load file button to load file from any directory. Data can also be manually entered in a table using the manual input checkbox or using the single input section for single entries or inputs (fig. 4.10). After all other information are provided from the suite, the 'Transform' button is finally clicked or pressed to perform user's action.

4.4 Software Testing of Geodetic Computations

The Geodetic Computations package of the suite was also tested, both Direct and Inverse, using coordinates of existing points. Though results were obtained, but there were no checks on the results since there were no existing data particularly azimuth and geodetic distance to be compared with. This application also runs on a separate graphical user interface (see fig. 4.11) and performs both Direct and Inverse geodetic computations using geodetic methods such as, Gauss Mid Latitude , Clarke's , Bowring's and Vincenty's formulae on any ellipsoid, where the user is required to provide the ellipsoid parameters (semi major axis and inverse flattening) in text boxes named 'Semi-Major Radius(a)' and 'Inverse Flattening(1/f)' by selecting 'User Defined' from the drop down named 'Select Ellipsoid' or by selecting some default ellipsoids such as, WGS 84 ,War Office, Clarke 1880, Everest 1830,Bessel 1841, GRS 80, Airy 1830, etc from the same drop down where their parameters are also displayed in the same text boxes (see fig. 4.11below).



Figure 4.11: Direct & Inverse Geodetic Computations

CHAPTER FIVE - RESULT AND ANALYSIS

This Chapter presents the results after,

- ❖ Processing the GPS data with the various processing suites,
 - ❖ Datum Transformation,
- and the analysis on the results obtained.

5.1 RESULTS

5.1.1 Data Processing

The GPS code pseudorange and carrier phase data were processed in double differenced mode by the Spectrum Survey software, the TOPCON software and the developed GNSS suite. The positions obtained from the GPS processed reports were in the ECEF coordinates WGS84 reference frame later transformed onto the Transverse Mercator (TM) mapping system which is the National Grid coordinates. The results after processing are tabulated in tables 5.1-5.6 below respectively for purposes of analysis. Each table contains the Northings and Eastings, baseline results as well as ECEF coordinates (X, Y, Z) and the baseline vectors (ΔX , ΔY , ΔZ) in

Table 5.1: Baseline results from SSS processing

BASELINE	Distance	3D Cartesian			BASELINE VECTORS		
		X	Y	Z	ΔX	ΔY	ΔZ
N1-TP6	105.88	6333132.374	-173040.628	736353.009	-0.098	31.035	8.853
N1-SGA P130 13 2	2013.68	6333086.580	-173671.288	736467.715	-45.825	-599.459	123.532
N1-SGA P130 13 1	2487.18	6333094.964	-173818.277	736470.121	-37.508	-746.614	125.965
N1-GCG A29 49 90	2684.18	6333098.161	-172451.085	736876.185	-34.311	620.578	532.02

Table 5.2: Baseline results from TOPCON processing

BASELINE	Distance	3D Cartesian			BASELINE VECTORS		
		X	Y	Z	ΔX	ΔY	ΔZ
N1-TP6	105.88	6333127.892	-173047.009	736379.726	-0.099	31.034	8.852
N1-SGA P130 13 2	2013.68	6333082.153	-173677.497	736494.390	-45.838	-599.454	123.516
N1-SGA P130 13 1	2487.18	6333090.495	-173824.653	736496.838	-37.496	-746.611	125.964
N1-GCG A29 49 90	2684.18	6333093.674	-172457.464	736902.900	-34.316	620.578	532.025

Table 5.3: Baseline results from developed GNSS suite processing

BASELINE	Distance	3D Cartesian			BASELINE VECTORS		
		X	Y	Z	ΔX	ΔY	ΔZ
N1-TP6	105.88	6333130.132	-173042.309	736356.179	-2.34	29.354	12.023
N1-SGA P130 13 2	2013.68	6333082.231	-173669.985	736464.534	-50.241	-598.322	120.378
N1-SGA P130 13 1	2487.18	6333090.998	-173817.47	736473.008	-41.474	-745.807	128.852
N1-GCG A29 49 90	2684.18	6333089.548	-172448.612	736874.329	-42.924	623.051	530.173

Table 5.4: Baseline results in TM Mapping System (SSS vs. Suite)

PILLAR	TM (Spectrum)		TM (GNSS suite)		Difference	
	N (ft)	E (ft)	N (ft)	E (ft)	ΔN	ΔE
TP6	727228.398	694925.892	727230.429	694923.202	2.031	-2.690
SGA P130 13 2	727615.318	692854.399	727611.084	692852.662	-4.234	-1.737
SGA P130 13 1	727618.979	692373.211	727616.293	692375.984	-2.686	2.7730
GCG A29 49 90	728949.793	696857.783	728953.075	696852.435	3.282	-5.348

Table 5.5: Baseline results in TM Mapping System (TOPCON vs. Suite)

PILLAR	TM (TOPCON)		TM (GNSS suite)		Difference	
	N (ft)	E (ft)	N (ft)	E (ft)	ΔN	ΔE
TP6	727228.393	694925.888	727230.429	694923.202	2.036	-2.686
SGA P130 13 2	727615.187	692854.974	727611.084	692852.662	-4.103	-2.312
SGA P130 13 1	727619.005	692373.231	727616.293	692375.984	-2.712	2.753
GCG A29 49 90	728949.751	696857.805	728953.075	696852.435	3.324	-5.37

Table 5.6: Baseline results in TM Mapping System (SSS vs. TOPCON)

PILLAR	TM (Spectrum)		TM (GNSS suite)		Difference	
	N (ft)	E (ft)	N (ft)	E (ft)	ΔN	ΔE
TP6	727228.398	694925.892	727228.393	694925.888	-0.005	-0.004
SGA P130 13 2	727615.318	692854.399	727615.187	692854.974	-0.131	0.575
SGA P130 13 1	727618.979	692373.211	727619.005	692373.231	0.026	0.02
GCG A29 49 90	728949.793	696857.783	728949.751	696857.805	-0.042	0.022

5.1.2 Datum Transformation

The testing of the Datum Transformation application was done in two ways. First, by transforming the WGS84 ellipsoid coordinates to the war Office ellipsoid coordinates and Projected Northings and Eastings coordinates on Ghana TM. The results are tabulated in table 5.7 and 5.8 below. Second, by projecting the existing War Office ellipsoid coordinate in table 4.3 of sub-section 4.3 of chapter 4 to Northings and Eastings coordinates on Ghana TM. The results are tabulated in table 5.9 below.

Table 5.7: Transformed coordinates on Ghana War office ellipsoid

War office Coordinates						
Points	Latitudes(N)			Longitudes(W)		
CFP 109	5	27	26.257	0	25	25.84
CFP 200	5	37	22.824	0	33	34.552
CFP 225	5	27	8.241	1	30	4.891

Table 5.8: Transformed National Grid Coordinates

Existing National Grid Coordinates		
Points	Northings	Eastings
CFP 109	286867.852	1109433.629
CFP 200	346932.899	1060041.36
CFP 225	285019.314	717755.386

Table 5.9: Projected National Grid Coordinates

Existing National Grid Coordinates		
Points	Northings	Eastings
CFP 109	286868.63	1109433.05
CFP 200	346933.94	1060041.45
CFP 225	285019.85	717756.06

5.2 ANALYSIS

5.2.1 Data Processing Results

In this sub-section, variation of computed positions in the ECEF frame over time, positions as processed by the spectrum survey, the TOPCON software and the GNSS suite developed are analyzed. The analysis is achieved by comparing the processing results tabulated above in sub-section 5.1.1 of this chapter by the three processing applications and also with the original positions of some of the pillars which were observed as discussed in sub-section 4.2.1 of chapter four.

5.2.1 Positions over Time

Positions were computed epoch by epoch till the final epoch reached during the processing with the GNSS Suite developed. Positions are enhanced as the number of epochs increases relative to the first epoch. This means that the accuracy of receiver position is improved if the number of epochs increases. Figure 5.1 below shows the Variation in Coordinates (XYZ) of one of the observed pillars, Relative to the First Epoch.

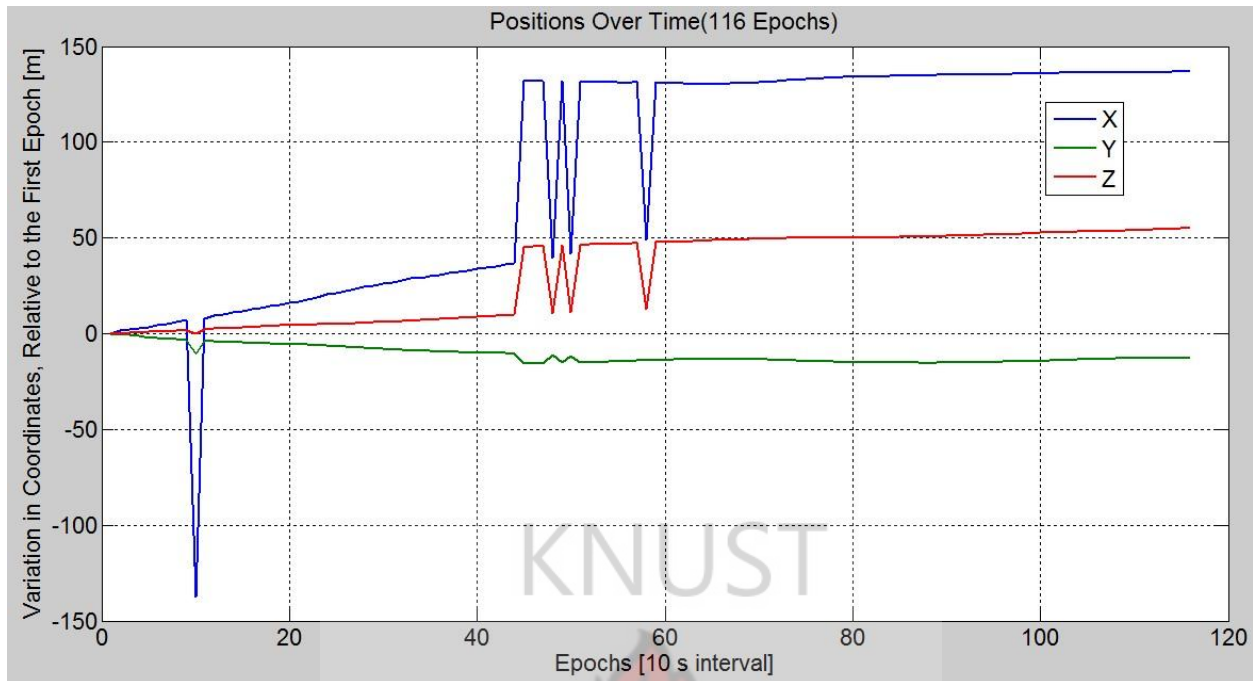


Figure 5.1: Positions of Pillars over Time

It is clear from figure 5.1 above that the position of the point was improved when the number of epochs increases till such a time when the differences or changes was negligible. The rinex file from which the position was computed from, contains a total of 116 epochs at 10 seconds interval.

5.2.2 Comparison of Processed Results

This sub-section presents the comparison of processed results of the GNSS suite developed with that of Spectrum Survey, the TOPCON software and the original coordinates of pillars TP6, SGA P130/ 13 /2, and GCG A29 /49/ 90. In addition, results obtained from Spectrum Survey and the TOPCON software are also compared and with the original coordinates of TP6, SGA P130/ 13 /2, and GCG A29 /49/ 90.

5.2.2.1 GNSS Suite vs. Spectrum Survey

In order to ascertain the computational accuracy of the developed GNSS suite, GPS survey was conducted on four (4) survey pillars or controls. These pillars were processed with the developed GNSS suite and the Sokkia Spectrum Survey. The processing results are tabulated in tables 5.1, 5.3 and 5.4. The deviations or differences in the northing and easting national grid coordinates

are also computed in table 5.4. From the results in Table 5.4 and Figure 5.2, the maximum deviations on the four (4) controls are [4.234ft] and [5.348ft] for Northings and Eastings respectively, and minimum deviations of [2.031ft] and [1.737ft]. Taking absolute values of the differences in columns 6 and 7 of Table 5.4, a mean deviation of 3.05825ft and 3.137ft, and standard errors of $\pm 0.936\text{ft}$ and $\pm 1.547\text{ft}$ for Northings and Eastings were deduced. Standard deviation σ is computed according to the following formula

$$\sigma = \sqrt{\frac{1}{n-1} \sum_{i=1}^n (x_i - \bar{x})^2} \quad ; \quad \text{where} \quad \bar{x} = \frac{1}{n} \sum_{i=1}^n x_i \quad (5.1)$$

Therefore the positional accuracy GNSS suite as compared with the Sokkia Spectrum Survey is $3.05825\text{ft} \pm 0.936\text{ft}$ and $3.137\text{ft} \pm 1.547\text{ft}$ for Northings and Eastings coordinates respectively.

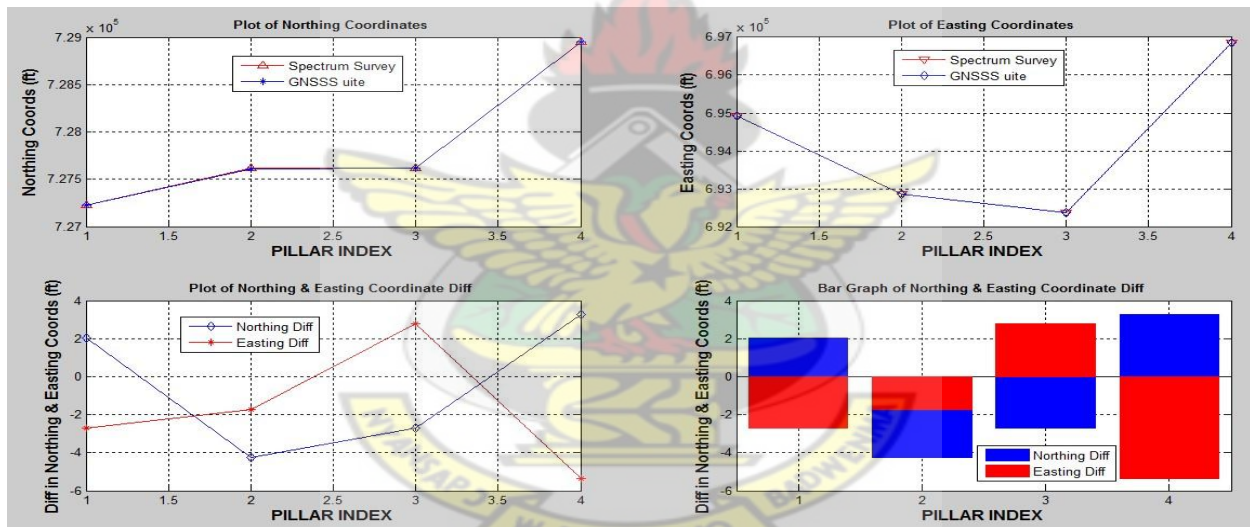


Figure 5.2: Plot Showing the Coordinates (N, E) & Differences (ΔN , ΔE) -Suite vs. SSS

5.2.2.2 GNSS Suite vs. TOPCON Software

In order to further ascertain the computational accuracy of the developed GNSS suite, the same GPS data was processed with the TOPCON software. The processing results are tabulated in tables 5.2, and 5.5. The deviations or differences in the northing and easting national grid coordinates are also computed in table 5.5. From the results in Table 5.5 and Figure 5.3, the maximum deviations on the four (4) controls are [4.103ft or 1.510m] and [5.37ft or 1.637m] for Northings and Eastings respectively, and minimum deviations of [2.036ft or 0.6206m] and

[2.312ft or 0.7047m] . Taking absolute values of the differences in columns 6 and 7 of Table 5.5, a mean deviation of [3.04375ft or 0.9277m] and [3.28025ft or 0.999m], and standard errors of [± 0.8806 ft or ± 0.2684 m] and [± 1.4066 ft or ± 0.4287 m] for Northings and Eastings were deduced. Standard deviation σ is computed according to equation 5.1.

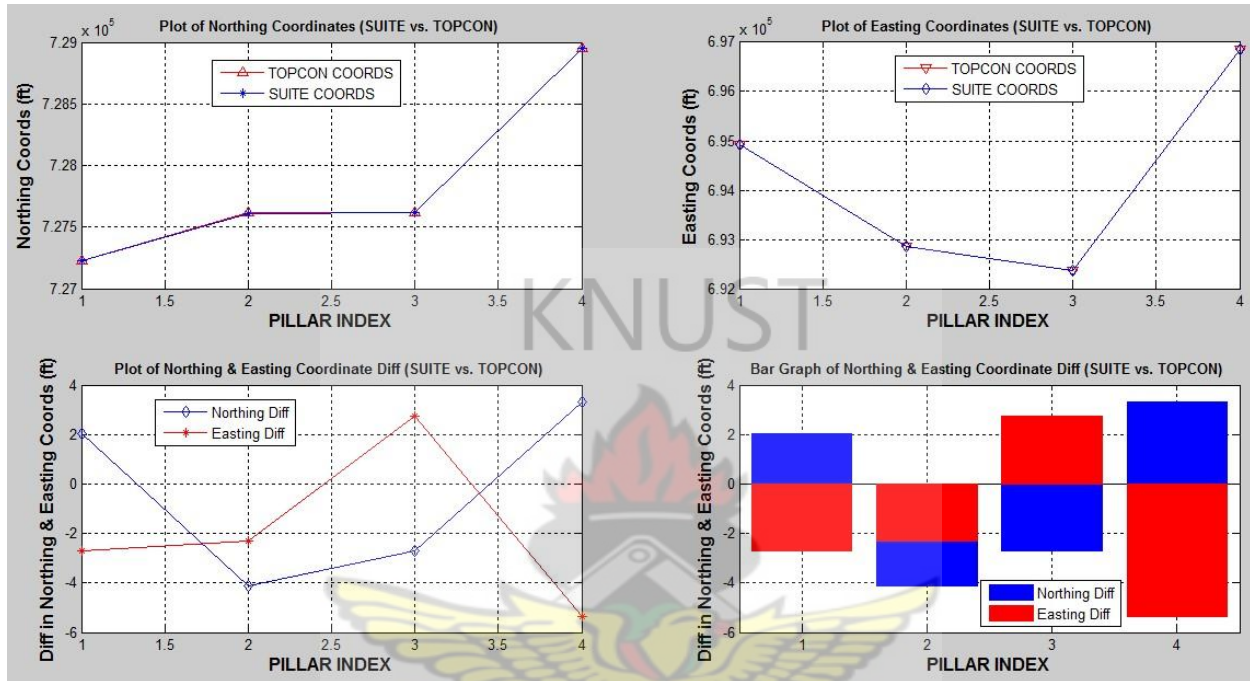


Figure 5.3: Plot Showing the Coordinates (N, E) & Differences (ΔN , ΔE)-Suite vs. Topcon

5.2.2.3 SSS vs. TOPCON Software

The results obtained after processing with these two software and deviation or difference in the northing and easting national grid coordinates are tabulated in table 5.6. From the results in Table 5.6 and Figure 5.4, the maximum deviations on the four (4) controls are [0.131ft] and [0.575ft] for Northings and Eastings respectively, and minimum deviations of [0.005ft] and [0.004ft]. Taking absolute values of the differences in columns 6 and 7 of Table 5.6, a mean deviation of 0.051ft and 0.15525ft, and standard errors of ± 0.05544 ft and ± 0.27994 ft for Northings and Eastings were deduced. Standard deviation σ is computed according to equation 5.1.

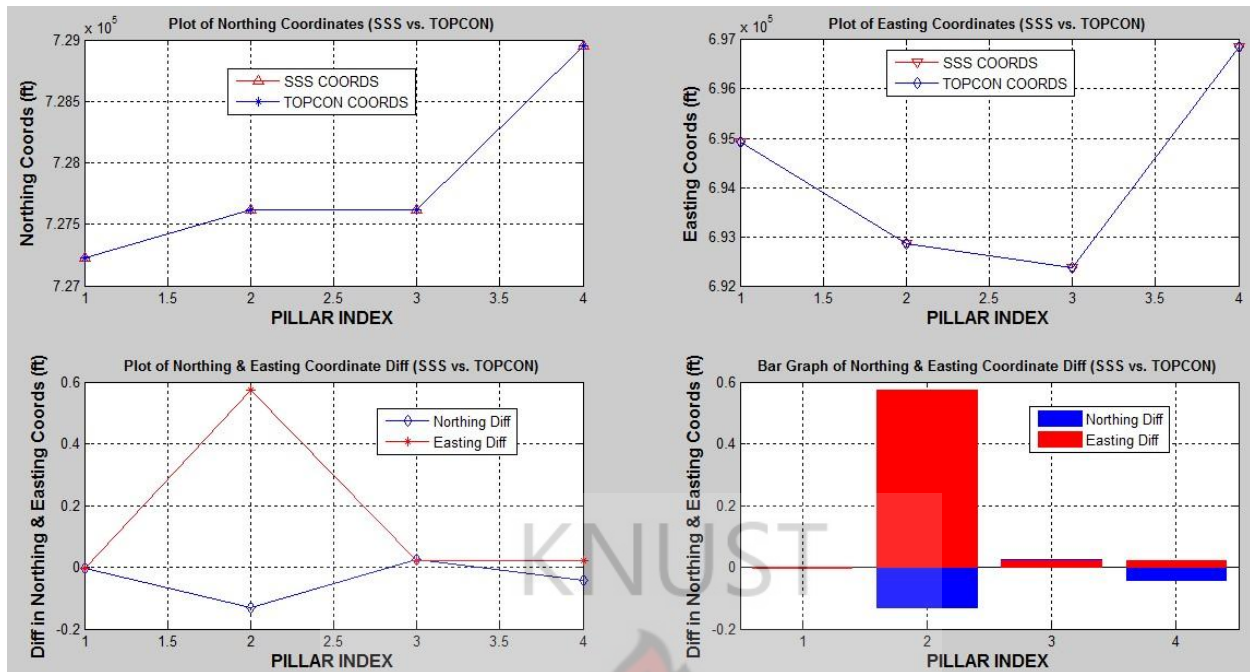


Figure 5.4: Plot Showing the Coordinates (N, E) & Differences (ΔN , ΔE): SSS vs. Topcon

5.2.2.4 GNSS Suite vs. Original Coordinates

In order to further ascertain or compare the processing accuracy between the processing results of GNSS Suite developed and that of the Sokkia Spectrum Survey and TOPCON software, the original coordinates of three (3) of the control points or pillars TP6, SGA P130/ 13 /2, and GCG A29 /49/ 90 were obtained from the Department of Geomatic Engineering KNUST and Survey and Mapping Division of Ghana Ashanti Region-Kumasi. Those coordinates were assumed to be error-free. In table 5.91 the deviation or difference in northing and easting coordinates of the GNSS Suite processing result and that of the original coordinates of TP6, SGA P130/ 13 /2, and GCG A29 /49/ 90 are computed. From the results in Table 5.10 and Figure 5.5, the maximum deviations on the three (3) controls are [4.031ft] and [5.421ft] for Northings and Eastings respectively, and minimum deviations of [2.579ft] and [2.254ft]. Taking absolute values of the differences in columns 6 and 7 of Table 5.10, a mean deviation of 3.426ft and 3.378ft, and standard errors of ± 0.755 ft and ± 1.773 ft for Northings and Eastings were also deduced. Therefore the positional accuracy of the GNSS suite as compared to the original coordinates is $3.426\text{ft} \pm 0.755\text{ft}$ and $3.378\text{ft} \pm 1.773\text{ft}$ for Northings and Eastings coordinates respectively.

Table 5.10: Comparison of GNSS suite Processed Coordinates & Original coordinates.

PILLAR	Original		GNSS suite		Difference	
	N (ft)	E (ft)	N (ft)	E (ft)	ΔN	ΔE
TP6	727227.85	694925.66	727230.429	694923.202	-6.421	-5.458
SGA P130 13 2	727615.115	692854.916	727611.084	692852.662	-3.031	-2.254
GCG A29 49 90	728949.408	696857.856	728953.075	696852.435	-2.333	-5.421

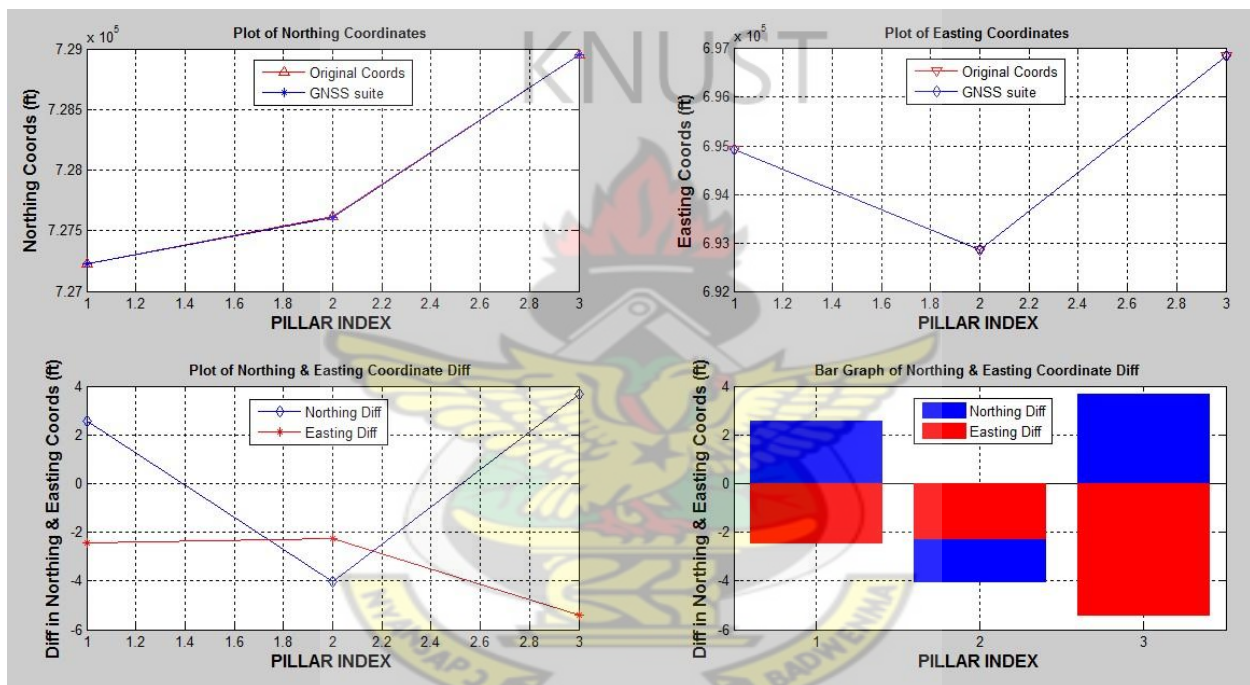


Figure 5.5: Plot Showing the Original & Suite processed Coordinates (N, E) & Differences (ΔN , ΔE)

5.2.2.5 SSS vs. Original Coordinates

Similarly, the processed results by the Sokkia Spectrum Survey software was also compared to the original coordinates of the three (3) control points or pillars TP6, SGA P130/ 13 /2, and GCG A29 /49/ 90. The deviation or difference in northing and easting coordinates of the Spectrum Survey processing result and that of the original coordinates of TP6, SGA P130/ 13 /2, and GCG A29 /49/ 90 are tabulated in table 5.11. From the results in Table 5.11 and Figure 5.6, the maximum deviations on the three (3) controls are [0.548 ft] and [0.517 ft] for Northings and

Eastings respectively, and minimum deviations of [0.203 ft] and [0.073 ft]. Taking absolute values of the differences in columns 6 and 7 of Table 5.11, a mean deviation of 0.379ft and 0.274ft, and standard errors of ± 0.173 ft and ± 0.225 ft for Northings and Eastings were also deduced. Therefore the positional accuracy of the SSS as compared to the original coordinates is $0.379\text{ft} \pm 0.173\text{ft}$ and $0.274\text{ft} \pm 0.225\text{ft}$ for Northings and Eastings coordinates respectively.

Table 5.11: Comparison of Spectrum Processed Coordinates & Original coordinates.

PILLAR	Original		Spectrum		Difference	
	N (ft)	E (ft)	N (ft)	E (ft)	ΔN	ΔE
TP6	727227.85	694925.66	727228.398	694925.892	0.548	0.232
SGA P130 13 2	727615.115	692854.916	727615.318	692854.399	0.203	-0.517
GCG A29 49 90	728949.408	696857.856	728949.793	696857.783	0.385	-0.073

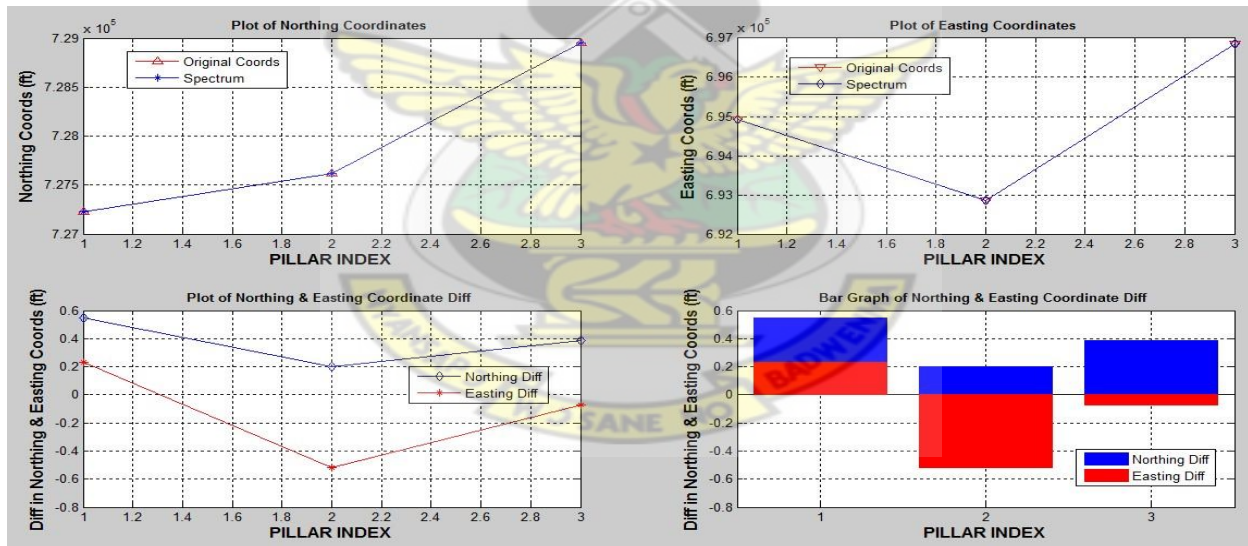


Figure 5.6: Plot Showing the Original & Spectrum processed Coordinates (N, E) & Differences (ΔN , ΔE)

5.2.2.6 TOPCON Software vs. Original Coordinates

Again, the processed results by the TOPCON software was also compared to the original coordinates of the three (3) control points or pillars TP6, SGA P130/ 13 /2, and GCG A29 /49/ 90. The deviation or difference in northing and easting coordinates of the TOPCON processing

result and that of the original coordinates of TP6, SGA P130/ 13 /2, and GCG A29 /49/ 90 are tabulated in table 5.93. From the results in Table 5.12 and Figure 5.7, the maximum deviations on the three (3) controls are [0.543 ft] and [0.228ft] for Northings and Eastings respectively, and minimum deviations of [0.072ft] and [0.051ft]. Taking absolute values of the differences in columns 6 and 7 of Table 5.12, a mean deviation of 0.319ft and 0.112ft, and standard errors of ± 0.236 ft and ± 0.10 ft for Northings and Eastings were also deduced. Therefore the positional accuracy of the TOPCON software as compared to the original coordinates is $0.319\text{ft} \pm 0.236\text{ft}$ and $0.112\text{ft} \pm 0.10\text{ft}$ for Northings and Eastings coordinates respectively.

Table 5.12: Comparison of TOPCON Processed Coordinates & Original coordinates.

PILLAR	Original		TOPCON		Difference	
	N (ft)	E (ft)	N (ft)	E (ft)	ΔN	ΔE
TP6	727227.85	694925.66	727228.393	694925.888	0.543	0.228
SGA P130 13 2	727615.115	692854.916	727615.187	692854.974	0.072	0.058
GCG A29 49 90	728949.408	696857.856	728949.751	696857.805	0.343	-0.0512

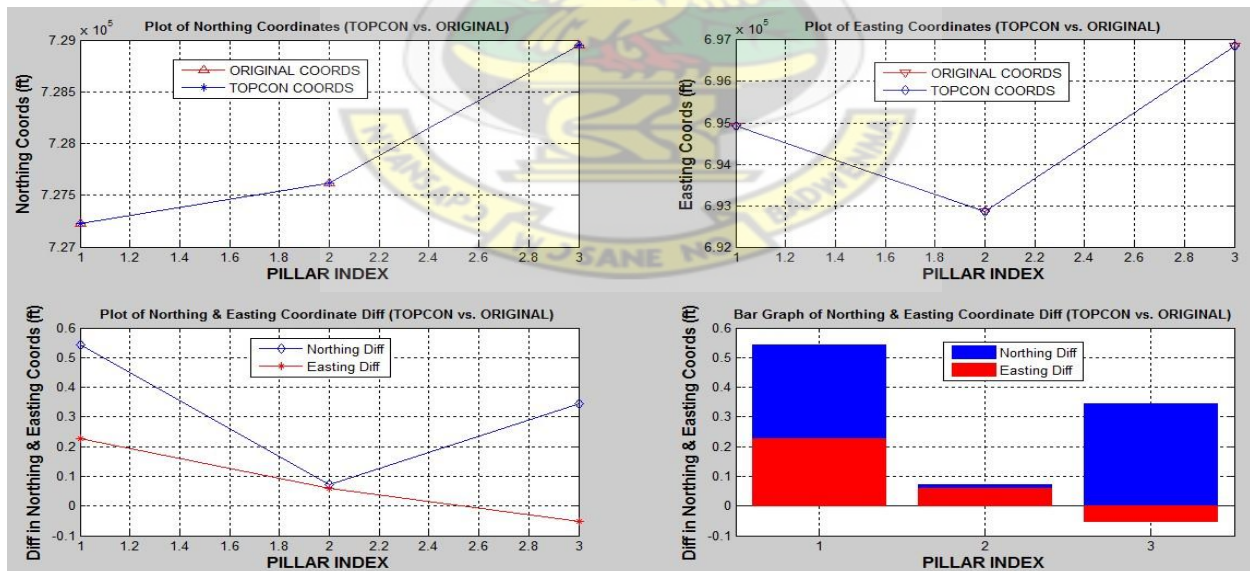


Figure 5.7: Plot Showing the Original & TOPCON processed Coordinates (N, E) & Differences (ΔN , ΔE)

Concluding Remarks: For the purpose of validating the suite, GPS data collected during field observations was processed using the suite and two other software as discussed above in chapter 4 and the results tabulated and analyzed as detailed in this chapter. From the various comparisons made during the analysis, it was shown that the deviation or difference in northing and easting coordinates of the GNSS suite processing results and that of the other software and the original coordinates was averagely about [4.122ft or 1.256m] and [5.38ft or 1.640m] as the maximum deviations for Northings and Eastings respectively, and [2.215ft or 0.675m] and [2.101ft or 0.640m] as the minimum deviations for Northings and Eastings respectively. The deviations might have been resulted from:

- ❖ Cycle slips not detected and repaired during the ambiguity resolution of carrier phase observations.
- ❖ Ionospheric delay assumed to be zero for short baseline.
- ❖ The use Ordinary least-squares principle in the estimation of the receiver preliminary or initial position.

5.2.1 Datum Transformation Results

This sub-section presents the analysis on the results obtained after the datum transformation. This is achieved by comparing the Transformed and projected results tabulated above in sub-section 5.1.2 with the existing coordinates of points within the Golden Triangle.

5.2.1.1 Transformed vs. Existing War Office Geographic Coordinates (ϕ , λ)

The existing and transformed War Office geographic coordinates are tabulated in table 4.2 of sub-section 4.3 of chapter 4 and 5.7 of sub-section 5.2.1 of chapter 5 respectively. The deviation or differences in latitude and longitude coordinates are given in table 5.13 below. From the results in Table 5.13, the maximum deviations on the three (3) points are [0.054"] and [0.016"] for latitudes and longitudes respectively, and minimum deviations of [0.030"] and [0.001"]. Taking absolute values of the differences in Table 5.13, a mean deviation of 0.041" and 0.008", and standard errors of ± 0.012 " and ± 0.008 " for latitudes and longitudes were also deduced.

Table 5.13 Geographic coordinate difference

Points	Difference	
	$\Delta\phi''$	$\Delta\lambda''$
CFP 109	-0.03765	-0.00579
CFP 200	-0.0301	0.00122
CFP 225	0.053983	0.016281

5.2.1.2 Transformed vs. existing National Grid Coordinates (N, E)

The WGS84 projected coordinates on the Ghana TM and the existing National Grid coordinates are tabulated together in table 5.14 with the difference in northing and easting coordinates.

Table 5.14: Transformed and existing National Grid Coordinates

Points	Existing Coordinates		Datum Transformation		Difference	
	Northings	Eastings	Northings	Eastings	ΔN	ΔE
CFP 109	286868.63	1109433.05	286867.852	1109433.629	-0.778	0.579
CFP 200	346933.94	1060041.45	346932.899	1060041.36	-1.041	-0.09
CFP 225	285019.85	717756.06	285019.314	717755.386	-0.536	-0.674

From the results in Table 5.14, the maximum deviations on the three (3) points are [1.041ft] and [0.674ft] for Northings and Eastings respectively, and minimum deviations of [0.536ft] and [0.09ft]. Taking absolute values of the differences in columns 6 and 7 of Table 5.14, a mean deviation of 0.785ft and 0.448ft, and standard errors of ± 0.253 ft and ± 0.313 ft for Northings and Eastings were also deduced. Therefore the transformational accuracy of the suite as compared to the existing coordinates is $0.785\text{ft} \pm 0.253\text{ft}$ and $0.448\text{ft} \pm 0.313\text{ft}$ for Northings and Eastings coordinates respectively.

5.2.1.2 Projected vs. existing National Grid Coordinates (N, E)

In order to further ascertain how best the suite can project War Office coordinates of latitude and longitude to Grid coordinates on the Ghana TM, the existing War Office coordinates of the three points within the Golden Triangle were projected using the suite to the National Grid coordinates on the Ghana TM. The results obtained and the existing National Grid coordinates are tabulated together in table 5.15 with the differences in northing and easting coordinates for the purpose of analysis.

Table 5.15: Projected and existing National Grid Coordinates

Points	Existing Coordinates		Projection		Difference	
	Northings	Eastings	Northings	Eastings	ΔN	ΔE
CFP 109	286868.63	1109433.05	286868.63	1109433.05	0.00	0.00
CFP 200	346933.94	1060041.45	346933.94	1060041.45	0.00	0.00
CFP 225	285019.85	717756.06	285019.85	717756.06	0.00	0.00

From the results in Table 5.15, it is clear that the projected coordinates computed by the suite and the existing National Grid Coordinates are the same and showed no difference or deviation in the Northings and Eastings coordinates.

Concluding Remarks: For the purpose of validating the Datum Transformation package of the GNSS suite, coordinates of existing controls or points within the Golden Triangle common to both the WGS 84 and War Office ellipsoids were transformed and projected using the Datum Transformation package of the developed GNSS suite as discussed above in chapter 4 and the results tabulated and analyzed as detailed in this chapter. From the various comparisons made during the analysis, it was shown that the deviation or difference in northing and easting and latitude and longitude coordinates of the GNSS suite transformation results and that of the existing coordinates were [1.041ft max and 0.09ft min] and [0.674ft max and 0.536ft min], [0.054" max and 0.030" min] and [0.016" max and 0.001" min] respectively. Projection from the War Office coordinates to National Grid coordinates showed no difference.

CHAPTER SIX-CONCLUSIONS AND RECOMMENDATION

The task was to develop GNSS Suite for geodetic applications such as GNSS data post-processing, datum transformation, direct and inverse geodetic computations etc and to test or validate the suite developed by making field observations for data collection for post-processing using the suite and any other commercial software. The Sokkia Spectrum Survey version 3.2 and the TOPCON software were used in that regard.

6.1 Conclusions

In this study, a GNSS Suite, 'GeoSuite', written in the Matlab programming language has been developed for Geodetic Applications such as

- ❖ GNSS data post-processing,
- ❖ Datum transformation,
- ❖ Direct and Inverse geodetic computations

The Suite has a graphical user interface that is user-friendly, interactive and easy to use. The post-processing application of the Suite uses GPS code pseudorange and carrier phase in double differenced mode where baseline vectors are computed. The Rinex file format is the source of data input for this application program. The application has a positional accuracy of $3.426\text{ft} \pm 0.755\text{ft}$ and $3.378\text{ft} \pm 1.773\text{ft}$ for Northings and Eastings coordinates which can be improved. From the results and analysis made, it was evident that the TOPCON software gave more accurate results followed by the Sokkia Spectrum Survey.

The issue of datum transformation is based on the WGS 84 and the War Office ellipsoids or user-defined ellipsoid. The application runs on a separate graphical user interface and performs any form of transformation between the aforementioned ellipsoids using the existing published or user-defined transformation parameters. This means that users can transform coordinates from WGS84 [geographic (ϕ , λ , h), 3D Cartesian(X, Y, Z) and UTM (N, E)] to War Office [geographic (ϕ , λ) and National Grid (N, E)] and vice versa. Coordinate conversions can also be achieved on each of the ellipsoids.

Again, from the analysis made on datum transformation, it was clear that the results obtained from the datum transformation were very good. This indicate that the datum transformation

application or package of the suite can be used for any form of transformation on the WGS 84 and the War Office ellipsoids or user-defined ellipsoid.

The source codes for this study are systematically written for easy understanding and are freely made available which can be modified and redistributed and also develop new processing applications.

By referring to the results obtained and the analysis made, the following conclusions can be drawn:

1. The same GPS data can be successfully processed using the developed suite for survey work that do not require much higher accuracy.
2. Few processing steps or procedures were involved to acquire positional results.
3. Data import with suite was fast and reliable.
4. Datum Transformation between the WGS84 ellipsoid, the War Office ellipsoid and other ellipsoids particularly Africa can be performed.
5. Software can easily be adapted for other countries particularly Africa since datum transformation parameters can easily be provided by user for processing or transformation.

6.2 Recommendations

Based on the theoretical studies on the GNSS processing algorithms and test results obtained in this research, the following recommendations are made for future research work to improve on the accuracy of this research.

- ✓ Determination of cycle slips to repair the ambiguity resolution of carrier phase observations.
- ✓ Improvement of the ambiguity resolution method by using other methods like the LAMBDA Method.
- ✓ Improvement on receiver preliminary or initial position estimation using the Bancroft method or Grid Point Method.
- ✓ Modeling of the Ionospheric delay (zero was used in this research for short baseline)

- ✓ Use of different models for tropospheric delay such as the Hopfield model. (This research used the Saastamoinen model)
- ✓ Implementation of transformation parameters for other African countries.

KNUST



REFERENCES

- Abidin, H. Z., 2003. GPS Positioning and Surveying.
- Afrifa. A. A., 2008. Developing a Differential GPS (DGPS) Service in Ghana.
- Angrisano, A., Gaglione, S., Gioia, C., Robustelli, U., and Vultaggio, M., 2011. Algorithms for GNSS Positioning in Difficult Scenario.
- ARINC Engineering Services. Navstar GPS Space Segment/Navigation User Interfaces. Interface specification IS-GPS-200, Rev. D (Public Release Version), Available at: <http://www.navcen.uscg.gov/gps/geninfo/IS-GPS-200D.pdf>, 7 December 2004 (accessed May 6, 2013).
- Ashtech Inc., 2001. Reliance Field Asset Management Tools, Magellan Corporation, Santa Clara, CA.
- Ayer, J. and Fosu, C., 2008, Map Coordinate Referencing and the Use of GPS Datasets in Ghana, *Journal of Science and Technology*, Vol. 28, No. 1
- Ayer, J. and Tiannah, T., 2007. Datum Transformations by iterative Solution of the abridging inverse Molodensky formulae.
- Badekas, J., 1969. Investigations related to the establishment of a world geodetic system, Report 124, Department of Geodetic Science, Ohio State University, Columbus.
- Bâki İz, H., 2010. Satellite and Physical Geodesy.
- Blewitt, G., 1997. Basics of the GPS Technique: Observation Equations, Department of Geomatics, University of Newcastle.
- Borre, K and Strang, G., 1997. Linear Algebra, Geodesy, and GPS.
- Bowring, B. R., 1985. The accuracy of geodetic latitude and Height equations. *Survey Review*, 28(218):202-206.
- Bursa, M., 1962. The theory for the determination of the non-parallelism of the minor axis of the reference ellipsoid and the inertial polar axis of the Earth, and the planes of the initial
- Calais, E., 2008. Satellite Orbits, Purdue University- EAS Department, Civil 3273 – ecalais@purdue.edu

Carl, C., 1997. Principles of GPS.

Chan, C.N., 2008. Advance NAVSTAR-GPS Positioning Techniques for UAVs.

Chao-heh C., 1998. Calculations for Positioning with the Global Navigation Satellite System, MSc Thesis, College of Engineering and Technology Ohio University.

Clynch, J. R., 2006. Datums - Map Coordinate Reference Frames: Part 2 – Datum Transformation.

Clynch, J. R., 2006. Time Systems and Dates: Universal Time, GPS Time, Julian Dates.

Curiel, A.S., 2000. Orbital Motion

Dana, P. H., 1997. Global Positioning System (GPS) Time Dissemination for Real-Time Applications.

El-Rabbany, A., 2002. Introduction to GPS: the Global Positioning System.

Fotiou, A. and Pikridas, C., 2002. The Global Positioning System – GPS. Lecture Notes, Aristotle University of Thessaloniki, Greece.

Gurtner, W. and Estey, L., 2008. RINEX: The Receiver Independent Exchange Format Version 3.00.

Gyamfi, Y. P., 2011. History of GNSS, ppt.

Hofmann-Wellenhof B., Lichtenegger H., and Collins J. 2001. Global Positioning System: Theory and Practice, (5th Edition). New York: Springer Verlag Wien.

Hofmann-Wellenhof, B., Lichtenegger, H. and Wasle, E., 2008. GNSS – Global Navigation Satellite Systems

<http://maia.usno.navy.mil/conventions.html>, July 1996 (accessed June 15, 2013).

ICD-GPS-200, October, 1993.

Jensen, A. B.O., 2008. GNSS Satellite Orbits: Lecture notes for 30550.

- Kaplan, E. D. and Hegarty C. J., 2006. Understanding GPS: principles and applications (2nd Edition).
- Leick, A. 2004. GPS Satellite Surveying (3rd Edition), John Wiley & Sons, Inc., New Jersey
- McCarthy, D. D., 1996. Iers conventions. IERS Technical Note 21, International Earth Rotation and Reference Systems Service, Available at:
- Molodensky, M.S., Eremeev, V.F. and Yurkina, M.I. 1960. Methods for study of the external gravitational field and figure of the Earth. Trudy CNIIGAiK.
- Nagi, Z. M. and Munzir B. E., 2011. Software Testing of GPS Data Processing, Department of Surveying Engineering, SUST.
- Petrovskyy, V., Tretyak, V., 2007. Precise GPS Position and Attitude.
- Rizos, C., 1997. Principles and Practice of GPS Surveying, Monograph 17, School of Geomatic Engineering, The University of New South Wales, 555pp.
- Satirapod, C., 2002. Improving the GPS Data Processing Algorithm for Precise Static
- Seeber, G., 1993. Satellite Geodesy: Foundations, Methods & Applications, Walter de Gruyter, Berlin New York, 531pp.
- Sickle, J. V., 2001. GPS for Land Surveyors (2nd Edition). Taylor & Francis Group.
- Spilker Jr., J.J., 1978. GPS signal structure and performance characteristics, *Navigation*, Journal of The (U.S.) Institute of Navigation, 25(2), 121-146.
- TSUI, J. B.Y., 2005. Fundamentals of Global Positioning System Receivers: A Software Approach, (2nd Edition).
- Warren D. L. M. and Raquet J. F., 2003. Broadcast vs. Precise GPS, ephemerides: a historical perspective.
- Wing-ye C., 2006. Introduction to RINEX, GPS Raw Data (ppt)
- Wolf, H., 1963. Geometric connection and re-orientation of three-dimensional triangulation nets. *Bulletin Géodésique* vol. **68**:165-169.
- Xu, G., 2007. GPS Theory, Algorithms and Applications (2nd Edition).
- Zogg, J. M., 2002. GPS Basics: Introduction to the system Application overview.

APPENDICES

Appendix A: Projection Formulae

1. Transverse Mercator projection Formulae

Transverse Mercator mapping from Ellipsoid to the plane

$$t = \tan \phi$$

$$\omega = \lambda - \lambda_0 \quad \nu = \frac{a}{\sqrt{1 - e^2 \sin^2 \phi}} \quad \rho = \frac{a(1 - e^2)}{(1 - e^2 \sin^2 \phi)^{3/2}} \quad \psi = \frac{\nu}{\rho}$$

$$f = \frac{a - b}{a} = \textit{flattening} \quad e^2 = 2f - f^2 = \textit{eccentricity squared}$$

$$m = a(A_0 \phi - A_2 \sin 2\phi + A_4 \sin 4\phi - A_6 \sin 6\phi)$$

$$m_0 = a(A_0 \phi_0 - A_2 \sin 2\phi_0 + A_4 \sin 4\phi_0 - A_6 \sin 6\phi_0)$$

Where

$$A_0 = 1 - \left(\frac{e^2}{4}\right) - \left(\frac{3e^4}{64}\right) - \left(\frac{5e^6}{256}\right) \quad A_2 = \frac{3}{8} \left(e^2 + \frac{e^4}{4} + \frac{15e^6}{128}\right) \quad A_4 = \frac{15}{256} \left(e^4 + \frac{3e^6}{4}\right) \quad A_6 = \frac{35e^6}{3072}$$

Easting Coordinate of point (E)

$$E = E' - E_0$$

$$E' = k_0 \nu \omega \cos \phi (1 + \textit{Term1} + \textit{Term2} + \textit{Term3})$$

$$\textit{Term1} = \frac{\omega^2}{6} \cos^2 \phi (\psi - t^2)$$

$$\textit{Term2} = \frac{\omega^4}{120} \cos^4 \phi [4\psi^3 (1 - 6t^2) + \psi^2 (1 + 8t^2) - \psi 2t^2 + t^4]$$

$$\textit{Term3} = \frac{\omega^6}{5040} \cos^6 \phi (61 - 479t^2 - t^6)$$

Northing Coordinate of point (N)

$$N = N' + N_0$$

$$N' = k_0(m - m_0 + Term1 + Term2 + Term3 + Term4)$$

$$Term1 = \frac{\omega^2}{2} \nu \sin \phi \cos \phi$$

$$Term2 = \frac{\omega^4}{24} \nu \sin \phi \cos^3 \phi (4\psi^2 + \psi - t^2)$$

$$Term3 = \frac{\omega^6}{720} \nu \sin \phi \cos^5 \phi [8\psi^4(11 - 24t^2) - 28\psi^3(1 - 6t^2) + \psi^2(1 - 32t^2) - \psi(2t^2) + t^4]$$

$$Term4 = \frac{\omega^8}{40320} \nu \sin \phi \cos^7 \phi (1385 - 3111t^2 + 543t^4 - t^6)$$

Transverse Mercator Inverse Mapping from Plane to Ellipsoid

$$\phi' = \sigma + \left(\frac{3n}{2} - \frac{27n^3}{32} \right) \sin 2\sigma + \left(\frac{21n^2}{16} - \frac{55n^4}{32} \right) \sin 4\sigma + \left(\frac{151n^3}{96} \right) \sin 6\sigma + \left(\frac{1097n^4}{512} \right) \sin 8\sigma$$

$$n = \frac{a-b}{a+b} \quad G = a(1-n)(1-n^2) \left(1 + \frac{9n^2}{4} + \frac{225n^4}{64} \right) \left(\frac{\pi}{180} \right)$$

$$\sigma = \frac{m' \pi}{180G} \quad m' = m_0 + \frac{N'}{k_0} \quad N' = N - N_0$$

$$t = \tan \phi' \quad ; \quad x = \frac{E'}{k_0 \nu} \quad ; \quad y = \frac{(E')^2}{k_0^2 \rho \nu} \quad ; \quad E' = E - E_0$$

LONGITUDE OF POINT (λ)

$$\lambda = \lambda_0 + Term1 - Term2 + Term3 - Term4$$

$$Term1 = x \sec \phi' \quad ; \quad Term2 = \frac{x^3 \sec \phi'}{6} (\psi + 2t^2)$$

$$Term3 = \frac{x^5 \sec \phi'}{120} [-4\psi^3(1 - 6t^2) + \psi^2(9 - 68t^2) + 72\psi t^2 + 24t^4]$$

$$Term4 = \frac{x^7 \sec \phi'}{5040} (61 + 662t^2 + 1320t^4 + 720t^6)$$

LATITUDE OF POINT(ϕ)

$$\phi = \phi' - \text{Term1} + \text{Term2} - \text{Term3} + \text{Term4}$$

$$\text{Term1} = \left(\frac{t}{k_0 \rho} \right) \left(\frac{E' x}{2} \right) ; \text{Term2} = \left(\frac{t}{k_0 \rho} \right) \left(\frac{E' x^3}{24} \right) \left[-4\psi^2 + 9\psi(1-t^2) + 12t^2 \right]$$

$$\text{Term3} = \left(\frac{t}{k_0 \rho} \right) \left(\frac{E' x^5}{720} \right) \left[8\psi^4(11-24t^2) - 12\psi^3(21-71t^2) + 15\psi^2(15-98t^2+15t^4) \right. \\ \left. + 180\psi(5t^2-3t^4) + 360t^4 \right]$$

$$\text{Term4} = \left(\frac{t}{k_0 \rho} \right) \left(\frac{E' x^7}{40320} \right) \left[1385 + 3633t^2 + 4095t^4 + 1575t^6 \right]$$

2. Universal Transverse Mercator projection Formulae

Universal Transverse Mercator mapping from Ellipsoid to the plane

$$\text{Easting, } E = FE + k_0 \nu \left[A + (1-T+C)A^3/6 + (5-18T+T^2+72C-58e^2)A^5/120 \right]$$

$$\text{Northing, } N = FN + k_0 \left\{ M - M_0 + \nu \tan \phi \left[A^2/2 + (5-T+9C+4C^2)A^2/24 + \right. \right. \\ \left. \left. (61-58T+T^2+600C-330e^2)A^6/720 \right] \right\}$$

Where

$$T = \tan^2 \phi$$

$$C = \frac{e^2 \cos^2 \phi}{1-e^2}$$

$$A = (\lambda - \lambda_0) \cos \phi, \text{ with } \lambda \text{ and } \lambda_0 \text{ in radians}$$

$$\nu = \frac{a}{(1-e^2 \sin^2 \phi)^{\frac{1}{2}}}$$

$$M = a \left[\left(1 - e^2/2 - 3e^2/64 - 5e^6/256 - \dots \right) \phi - \left(3e^2/8 + 3e^4/32 + 45e^6/1024 + \dots \right) \sin 2\phi \right. \\ \left. + \left(15e^4/256 + 45e^6/1024 + \dots \right) \sin 4\phi - \left(35e^6/3072 + \dots \right) \sin 6\phi + \dots \right]$$

$$\lambda_0 = [ZW] - \left[\lambda_1 + \frac{W}{2} \right]$$

$$Z = INT((\lambda + \lambda_1 + W)/W) \text{ with } \lambda, \lambda_1 \text{ and } W \text{ in degrees. If } \lambda < 0, \lambda = (\lambda + 360) \text{ degrees}$$

Universal Transverse Mercator Inverse Mapping from Plane to Ellipsoid

$$\phi = \phi_1 - (\nu_1 \tan \phi_1 / \rho_1) \left[D^2/2 - (5 + 3T_1 + 10C_1 - 4C_1^2 - 9e'^2) D^4/24 \right. \\ \left. + (61 + 90T_1 + 298C_1 + 45T_1^2 - 252e'^2 - 3C_1^2) D^2/720 \right]$$

$$\lambda = \lambda_0 + \frac{[D - (1 + 2T_1 + C_1) D^3/6 + (5 - 2C_1 + 28T_1 - 3C_1^2 + 8e'^2 + 24T_1^2) D^5/120]}{\cos \phi_1}$$

$$\nu_1 = \frac{a}{(1 - e^2 \sin^2 \phi_1)^{\frac{1}{2}}}, \quad \rho_1 = \frac{a(1 - e^2)}{(1 - e^2 \sin^2 \phi_1)^{\frac{3}{2}}}$$

ϕ_1 is the latitude of the point on the central meridian which has the same Northing as the point whose coordinates are sought, and is found from?

$$\phi_1 = \mu_1 + (3e_1/2 - 27e_1^3/32 + \dots) \sin 2\mu_1 + (21e_1^2/16 - 55e_1^4/32 + \dots) \sin 4\mu_1 \\ + (151e_1^3/96 + \dots) \sin 6\mu_1 + (1097e_1^4/512 - \dots) \sin 8\mu_1 + \dots$$

Where

$$e_1 = \frac{1 - (1 - e^2)^{\frac{1}{2}}}{1 + (1 - e^2)^{\frac{1}{2}}}; \quad \mu_1 = \frac{M_1}{a(1 - e^2/4 - 3e^4/64 - 5e^6/256 - \dots)}; \quad M_1 = M_0 + \frac{(N - FN)}{k_0}$$

$$T_1 = \tan^2 \phi_1; \quad C_1 = e'^2 \cos^2 \phi_1; \quad e'^2 = \frac{e^2}{(1 - e^2)}; \quad D = \frac{E - FE}{\nu_1 k_0}$$

Appendix B: List of MATLAB M-Files

This section summarizes all the relevant MATLAB M-files used in this research.

CreatePro.m	M-file for creating project
LoadRinexData1.m	M-file for Loading Rinex data from folders
LoadRinexData2.m	M-file for Loading Rinex data from files
ReadNavheader.m	M-file for reading rinex navigation header
ReadObsheader.m	M-file for reading rinex observation header
ReadRinexNav.m	M-file for reading rinex navigation data section
ReadRinexObsData.m	M-file for reading rinex observation data section
GPSweek.m	M-file for calculating GPS Time.
satellitepos.m	M-file for calculating satellite position
getReceiverPos.m	M-file for calculating receiver preliminary position
getReceiverPos_Baseline.m	M-file for calculating baseline vectors and receiver position
xyz2geo.m	M-file for converting 3D Cartesian coordinates to geographic
geo2xyz.m	M-file for converting geographic coordinates to 3D Cartesian
wgs2wo.m	M-file for datum transformation from WGS84 to War Office
wgs2ng.m	M-file for datum transformation from WGS84 to National Grid
wgs2utm.m	M-file for projecting WGS84 coordinates to UTM (2D plane)
utm2wgs	M-file for converting UTM coordinate to WGS 84 (φ , λ)
utm2wo	M-file for datum transformation from UTM to War Office (φ , λ)
wo2ng.m	M-file for projecting geographic to national grid coordinates
wo2ng.m	M-file for projecting geographic to national grid coordinates

Appendix C: Glossary of GNSS Terminology

Glossary of GNSS Terminology

Global Navigation Satellite System (GNSS): is a generic term used to describe all forms of satellite based navigation systems that provide global coverage and signals for navigation, positioning, surveillance and timing information for ground, marine, aviation and space applications.

Satellite Constellation: In GPS, the collection of orbiting satellites, located in 6 orbital planes elevated 55 degrees to the equator at an altitude of 20,200 kilometers (10,900 nautical miles), with three or four satellites per orbit for a total of 24 (21 functioning, 3 operational backups).

RINEX (Receiver Independent Exchange): An ASCII data file format based on a set of standard definitions for GNSS time, phase, and range observables to promote the free exchange of GPS data and facilitate the use of data from any GPS receiver with any software package.

Clock Bias: The difference between a clock's indicated time and true universal time.

Clock Offset: Difference in the time reading between two clocks.

Ephemeris – *almanac*: The description of the satellite orbits and clock correction parameters variable over time used for positioning and baseline computations. The ephemeris may be broadcast (projected ahead into time and subject to selective availability) or precise (post-fitted).

Epoch: A specific instant in time. GPS carrier phase measurements are made at a given frequency (e.g. every 30 seconds) or epoch rate.

Epoch Date: The date, usually expressed in decimal years, for which published coordinates and data are valid.

GPS week: Incremental number of weeks, starting at 0 hour UTC on the date January 6, 1980. April 6, 1997 is the first day of GPS week 900.

Pseudorange: A range (distance) measurement based on the correlation of a satellite-transmitted code and a receiver's internally generated code that has not been corrected for clock synchronization errors between the satellite and receiver's clocks.

Post-Processing: A technique of differential correction where data from rover receivers are corrected for numerous sources of error

Code-Correlation: The method by which a satellite-receiver range is determined by comparing the time difference between the satellite's and receiver's copies of a unique code.

Cycle Slip: A discontinuity, or skip, in the counting of carrier sine waves between the satellites and receiver

Ambiguity: The uncertainty in the measurement of the number of wave cycles of the GPS carrier between the satellite and the receiver.

Carrier Phase Positioning: GPS measurements based on measuring the number of wavelengths of the L1 or L2 GPS carrier signal between a satellite and receiver.

Differential Correction: A technique used to improve the accuracy of a radio navigation system by determining position error at a known location and applying that determined error-correction value to the data of a user of the same system at another, unknown position.

Mask angle - cut-off angle: The point above the observer's horizon below which satellite signals are no longer tracked and/or processed. 10° to 25° is typical.

PRN - Pseudo-random noise, a sequence of digital 1's and 0's which appears to be randomly distributed like noise, but can be exactly reproduced. Each NAVSTAR satellite has its own unique C/A and P pseudo-random-noise codes and are often referred to by their PRN number.

Phase difference processing - relative positioning Computation of the relative difference in position between two points by the process of differencing simultaneous reconstructed carrier phase measurements at both sites. The technique allows cancellation of all errors which are common to both observers, such as clock errors, orbit errors, and propagation delays. This cancellation effect provides for determination of the relative position with much greater precision than that to which a single position (pseudorange solution) can be determined.

Accuracy: The degree of conformance between the measured position and its true position. GPS accuracy is usually given as a statistical measure of system error. Not to be confused with precision.

Dual-Frequency Receiver: A receiver capable of simultaneously receiving both the L1 and L2 frequencies transmitted by the GPS satellites. Such receivers have the advantage of being able to compensate for most ionospheric refraction.

Base: refers to a GNSS receiver stationed over a known, accurately surveyed point, used to apply differential corrections to Rover receivers.

Rover: GNSS receivers used to determine the positions of unknown points. Data from rover receivers are generally differentially corrected with data collected by base receivers.

KNUST

